

# **Petrographic and Geochemical Characterization of Ore-bearing Intrusions of the Noril'sk type, Siberia; With Discussion of Their Origin**

Gerald K. CZAMANSKE\*, Tatyana E. ZEN'KO\*\*, Valeri A. FEDORENKO\*\*,  
Lewis C. CALK\*, James R. BUDAHN\*\*\*, John H. BULLOCK Jr.\*\*\*, Terry L.  
FRIES\*, Bi-Shia W. KING\*, and David F. SIEMS\*\*\*

\*U. S. Geological Survey, 345 Middlefield Road, Menlo Park, California,  
94025, USA

\*\*Central Research Institute of Geological Prospecting for Base and Precious  
Metals (TsNIGRI), Varshavskoye Shosse 129B, Moscow, 113545, Russia

\*\*\*U. S. Geological Survey, Denver Federal Center, Denver, Colorado,  
80225, USA

**Abstract:** Because of extensive drilling on 25- to 100-m centers during delineation of orebodies, the economically important, Noril'sk-type, ore-bearing intrusions could be the most well defined in the world. However, this is not the case and, instead, they are little known to Western geologists. We present a combined petrographic, geochemical, and mineral-chemical description of these intrusions which relies heavily on detailed study of four sections, but draws from a broad base of Russian data.

The ore-bearing intrusions represent one small component of a major episode of mafic magmatic activity at ~250 Ma that included formation of one of Earth's most extensive flood-basalt provinces and emplacement of a wide range of sub-volcanic, mafic intrusions. This system delivered mafic magmas of different geochemical and isotopic compositions, and enormous amounts of immiscible sulfide melt enriched in Cu, Ni, and PGE.

The Noril'sk I, Talnakh, and Kharaelakh ore-bearing intrusions have generally comparable external morphology and internal stratigraphy; they are relatively thin (<350 m) and elongate. Commonly those parts of the intrusions that are thicker than 30-50 m contain a lithologic sequence in which three distinct groups of rocks can be recognized, but these are not typical, layered mafic intrusions.

At the base of each intrusion is a fine-grained, contact facies several meters thick, which has the MgO content of basalt and contains sulfide only as a late introduction. An overlying taxitic unit and an olivine-enriched, picritic unit complete the lower group of rocks; contacts between these three units are gradational, but the upper contact of the picritic unit is abrupt. The taxitic unit (8-18 wt% MgO) is heterogeneous; grain size and proportions of minerals within it are highly variable. The picritic unit (18-29 wt% MgO) contains 40-80 modal percent of fine-grained, resorbed olivine grains (Fo •81.5), thought to have been carried into the chamber from a deep staging chamber in the Earth's crust. Chromium contents commonly are 3000-4000 ppm in the upper part of the picritic unit, decrease to 300-500 ppm in the middle and lower parts of the unit, and are at basaltic levels of 100-200 ppm in taxitic and contact-facies rocks. The entire thickness of the picritic and taxitic units contains disseminated ore over much of the area of each intrusion. These ores are unusual, largely consisting of relatively undeformed globules 0.5-2 cm across in picritic gabbrodolerite and more xenomorphic masses as much as 3-4 cm across in taxitic gabbrodolerite.

Massive orebodies as thick as 45 m formed when pools of sulfide melt were emplaced into the lowermost parts of the intrusions and metasedimentary footwall rocks just beneath the thickest parts of the intrusions. Massive orebodies are associated with disseminated ore, but sulfide concentrations in disseminated ores never increase downward and pass into massive ore. Ratios among Cu, Ni, and PGE show that the sulfide melts were greatly enriched by scavenging metals from massive amounts of mafic, silicate melt. The total sulfide content of the Kharaelakh intrusion is estimated as 7 wt%.

The mid-sections of the intrusions are composed of a thick sequence of rocks containing 47.2 to 50.8 wt% SiO<sub>2</sub> and 6 to 14 wt% MgO (occasionally 16 wt%) in which olivine crystallized *in situ* and commonly partly surrounds earlier-formed, plagioclase laths. These rocks typically contain <0.10 wt% S and have Ni, Cu, and PGE contents comparable to those found in most basaltic lavas of the region; olivine within them has not been depleted in Ni. Upward in this mid-section of the intrusion, the modal concentration of this olivine gradually decreases and the habit of clinopyroxene changes from oikocrystic to subprismatic. The upper parts of the intrusions can be divided into three units of relatively coarse-grained, quartz-bearing rocks that contain 3.9 to 7.3 wt% MgO (1.2-1.7 in hybrid rocks) and as little as 2-20 ppm Cr, in comparison with concentrations of 100-800 ppm Cr in the mid-section. Rocks of this upper sequence are interpreted to represent crystallization from a discrete liquid layer, enriched in volatiles, that formed by differentiation and melt extraction from the underlying units as they crystallized. Often, the uppermost unit in the intrusions is leucocratic gabbro, rich in large, early-formed, tabular plagioclase grains and interpreted to represent one of the earliest crystallized units in the intrusions.

There are numerous complications to this generalized stratigraphy, especially with respect to the upper parts of the intrusions. Leucocratic gabbro is poorly represented in the Talnakh intrusion and the overall proportions of the coarse-grained, upper sequence are highly variable. It is common to find the various members of the upper sequence to be repeated in section. It is also common to find interfingering between the coarse-grained, lowermost unit of the quartz-bearing sequence and the uppermost, olivine-poor rocks of the mid-section.

Whereas ratios among incompatible elements indicate that all units of the intrusions were ultimately derived by processing of similar, mantle-derived melts, construction of the intrusions appears to have been a complex process that involved sequential emplacement of several distinct, but related, magmas from a deep, crustal chamber. The later sections of this report discuss models for emplacement of the intrusions, their most enigmatic aspects, and the factual constraints that must be addressed by any credible model for their construction.

## INTRODUCTION

The Noril'sk I, Talnakh, and Kharaelakh intrusions of the Noril'sk district host one of the outstanding metal concentrations in the world; contained Cu-Ni resources are comparable to the deposits at Sudbury, Ontario and the platinum-group element (PGE) resource is second only to that of the Bushveld Complex. Our opportunity to cooperatively sample and study this district in Siberian Russia arose in 1990 through a memorandum of understanding between the U.S. Geological Survey and the former Ministry of Geology of the U.S.S.R. The world-class significance of these deposits and the possibility that understanding their geologic context, including construction of a credible "ore-deposit model," will lead to discovery of similar deposits elsewhere, inspired extensive studies of the ores, the mafic-intrusions which host them, and associated flood basalts. Comprehensive geochemical and isotopic data have been obtained for the

Siberian flood basalts (78 samples), the Noril'sk I intrusion (borehole NP-29, 22 samples), the Kharaelakh intrusion (borehole KZ-1879, 28 samples), the Talnakh intrusion (KZ-1713 and KZ-1799, 54 samples), the Lower Talnakh intrusion (borehole SG-28, 17 samples), and ores from the Noril'sk I, Kharaelakh, and Talnakh intrusions (43 samples). Data sets have been published by CZAMANSKE et al. (1992, 1994), WOODEN et al. (1992, 1993), WALKER et al. (1994) and HORAN et al. (in press), who present details of sampling and analytical techniques.

Significant obstacles to Western (and, to some extent, Russian) understanding of the ore-bearing intrusions have been (1) poor appreciation of the petrography of the major rock types; (2) limited availability of systematic analytical data; and (3) substantial disagreement among Russian writers about the existence and characteristics of a "typical" section through these intrusions. Our detailed study of four boreholes and careful re-examination of an additional twenty-eight boreholes clearly show that there is far more variation in intrusion sections than would be assumed from the "standard" sections described by GODLEVSKY (1959) and KOROVYAKOV et al. (1963). Moreover, the uppermost units of the intrusions are not well described in these and subsequent reports.

This contribution is a true team effort. Over the past 20 years, TATYANA ZEN'KO has had the opportunity to become familiar with vast amounts of classified information obtained during drilling of the Talnakh ore junction from the 1960s to the 1980s. A great debt is owed V. F. KRAVTSOV of NKGRE, as well as V. A. LUL'KO and L. M. SHADRIN of NKGRE for carefully documenting and systematizing this information. Re-examination of core from tens of boreholes by TATYANA ZEN'KO, collection and logging of critical core by VALERI FEDORENKO, the contribution of the best obtainable analyses from the USGS laboratories, and continuing integration and synthesis of field and laboratory data have added to this invaluable base of knowledge. This contribution should add significantly to Western appreciation of the Noril'sk-type, ore-bearing intrusions as a special "class," and contribute to a more enlightened search for comparable intrusions and ores elsewhere. We hope that it also can be an important element in better understanding these intrusions, both in terms of their petrologic evolution as silicate-magma bodies and as hosts to the fabulously enriched and abundant, sulfide ores.

## OVERVIEW

The Noril'sk region (Fig. 1) lies at the extreme northwest corner of the Siberian platform and is characterized by the thickest (>3500 m) volcanic-rock sequence of the Late Permian-Early Triassic, Siberian flood-basalt province (~251 Ma; CAMPBELL et al., 1992; DALRYMPLE et al., 1995; KAMO et al., in prep.). This province is perhaps the world's largest, with relatively continuous exposures of basalt covering an area of at least  $3.4 \times 10^5 \text{ km}^2$  and an estimated volume of  $2\text{-}3 \times 10^6 \text{ km}^3$ . The basalts overlie a ca. 5000-m thickness of Paleozoic sedimentary rocks, ca. 4000 m of Late Proterozoic sedimentary and volcanic rocks, and a Proterozoic basement of granitoids, granitic gneisses, schists, and

amphibolites whose age is estimated at 0.9-2.3 Ga (WOODEN et al., 1993, unpublished data). Detailed information about the volcanic sequence at Noril'sk and its geochemical and isotopic characteristics were presented by LIGHTFOOT et al. (1990, 1993, 1994), WOODEN et al. (1993), FEDORENKO (1994a), and HAWKESWORTH et al. (1995). This sequence has been subdivided into three assemblages (Fig. 2; FEDORENKO, 1981; WOODEN et al., 1993; FEDORENKO, 1994a). The Early assemblage is high-Ti and evolved from trachybasalt through basalt to picrite; it can be as much as 500 m thick, and includes the Ivakinsky (Iv), Syverminsky (Sv), and Gudchikhinsky (Gd) suites. The Middle assemblage starts with the Khakanchansky (Hk) tuff suite, but is largely composed of several overlying lava units; it may reach 500 to 650 m in thickness. The Tuklonsky suite (Tk), the lowermost of these, belongs to a low-Ti magma type with high Th/U ratios; it is composed of basalts and picrites. Overlying are the Lower and Middle Nadezhdinsky basaltic subsuites (Nd<sub>1</sub> and Nd<sub>2</sub>), thought to have formed after crustal contamination (6.5%) and Pl + Cpx + Ol fractionation (38%) of Tuklonsky basaltic magma (FEDORENKO, 1994a). The Nd<sub>1</sub> subsuite shows strong evidence of sulfide extraction and the Nd<sub>2</sub> lavas also probably underwent some sulfide extraction (NALDRETT et al., 1992; BRÜGGMANN et al., 1993; LIGHTFOOT et al., 1994; FEDORENKO, 1994a; HAWKESWORTH et al., 1995). The Upper Nadezhdinsky (Nd<sub>3</sub>) and Lower Morongovsky (Mr<sub>1</sub>) subsuites complete the the Middle assemblage. They may have formed after mixing of 34% of the Nd<sub>2</sub> magma and 66% of new mantle-derived magma that belonged to the same type as that which formed the Late-assemblage lavas (FEDORENKO, 1994a).

A tuff ~100-m thick lies between the Middle and Late assemblages. Late-assemblage lavas have a thickness of 2000-2300 m and include the Upper Morongovsky (Mr<sub>2</sub>) subsuite and the Mokulaevsky (Mk), Kharaelakhsky (Hr), Kumginsky (Km), and Samoedsky (Sm) suites. They are composed mainly of low-Ti basalts with low Th/U ratios, and show little compositional variation (WOODEN et al., 1993; HAWKESWORTH et al., 1995). However, two distinctive units of high-Ti lava appear sporadically in the upper assemblage -- the Kaltaminsky ankaramites and the Ikonsky andesitobasalts (FEDORENKO, 1981, 1994a; DISTLER and KUNILOV, eds., 1994; HAWKESWORTH et al., 1995).

The entire 3500-m-thick volcanic sequence is thought to have formed in about 1 m. y. (LIND et al., in press) just at the Permian-Triassic boundary. Geological peculiarities of Noril'sk-region magmatism that are important for understanding the tectonic environment of this period have been summarized by FEDORENKO (1991, 1994a) and DISTLER and KUNILOV, eds. (1994). Lavas, tuffs, and intrusions are estimated to compose, respectively, 84%, 9.5%, and 6.5% of the total volume of the magmatic rocks in the Noril'sk area (FEDORENKO, 1994a). Most of this magma was erupted quietly on the surface and formed lava flows, some portions lacked sufficient energy to reach the surface and formed intrusions, whereas other portions erupted explosively and formed tuffs, including agglomeratic tuffs. Thus, tectonic conditions were quite variable during the period of magmatic activity.

More than 200 lava flows and about 30 tuff layers are present in the volcanic sequence of the Noril'sk area; the thickness of individual flows varies from 1 to 100 m (avg 15 m). An upper amygdaloidal zone, which averages 36% of flow thickness, is well developed in almost every flow. The flows commonly occur as "packets," several tens to a few hundreds of meters thick, composed of a single rock type. Packets can be mapped for tens, to several hundreds of kilometers, within which individual flows commonly wedge out rapidly and replace one another. Tuff layers often cover similar areas, with thicknesses of tens of centimeters to 50-100 m, which may increase to 200-400 m close to explosive centers. Remarkably, the Khakanchansky tuff is preserved with a thickness of 18 to 22 m over an area of  $\sim 30,000 \text{ km}^2$ . Some tuffs with thicknesses of 1-5 m are preserved over similar areas. Tuffs were non-lithified when overlying lavas were erupted; their preservation shows that flood-basalt lavas did not cause significant mechanical or thermal erosion.

Available paleontological and geochemical data indicate that the tuff layers up to middle of the Morongovsky suite accumulated in shallow-water lakes or marine lagoons (FEDORENKO, 1991). The tuffs and lavas of the upper part of the volcanic sequence were formed under subaerial conditions. Accumulation of the entire sequence was accompanied by nearly ideally balanced subsidence, with the preservation of flat relief, close to sea level. The extremely high rate of this balanced subsidence (3500 m/1 m.y.) may be explained most readily if formation of volcanic depressions was due to draining of underlying, intermediate magma chambers in the Earth's crust.

At present, the volcanic sequence fills the vast Tunguska syncline, located to the SE of Noril'sk, and smaller depressions located in the Noril'sk area (Fig. 1). Paleo-reconstruction, however, shows that these structures are post-volcanic. Originally the lavas covered in the entire Noril'sk region, at least to the east of the Yenisei River (Fig. 1; FEDORENKO, 1991). At the time of volcanism, the structural pattern was significantly different from that of today. The lavas of the Early, Middle, and Late assemblages filled different paleodepressions that were unrelated to one another (FEDORENKO, 1991, 1994a; NALDRETT et al., 1992; WOODEN et al., 1993). This considerable structural rearrangement, with preservation of low relief, strongly suggests that lavas of the three assemblages were related to separate, intermediate magma chambers. Studies of lava distribution (e.g., FEDORENKO, 1991, 1994a) suggest that these chambers were subhorizontal (sill-like), thin (probably several hundred meters), but very extensive (some hundreds of kilometers across).

A few dikes are known in the region that may have been feeders for the Late-assemblage lavas, but it is impossible to relate the great volume of these lavas to these few dikes. Feeders for the Early- and Middle-assemblage lavas have not been found, despite extensive search. This is surprising because in the Maymecha-Kotuy region (500 km NE of Noril'sk) each lava type has definite feeder systems, represented by wide (several kilometers) and extensive (some tens of kilometers) belts of numerous thin and short dikes of various orientations

(FEDORENKO, unpublished data, 1991-1994). Apparently, eruption of lava in the Maymecha-Kotuy region was associated with significant extension. Perhaps such feeder dikes were thinner in the Noril'sk region and the fissures were closed by tectonic readjustment after eruption. Study of the thicknesses of lava packets and lateral changes in the chemistry of the picritic basalts led FEDORENKO (1991) to conclude that feeders were located in a few elongate zones near present-day fault zones. Most mafic intrusions also are located close to these zones, of which the Noril'sk-Kharaelakh fault zone is by far the most important (Figs. 1 and 3). The outstanding importance of the Noril'sk-Kharaelakh fault zone to the formation of the ore-bearing intrusions has been emphasized many times (e.g., MASLOV, 1963; GENKIN et al., 1981; DUZHIKOV et al., 1992; NALDRETT et al., 1992; ZEN'KO and CZAMANSKE, 1994a).

The most recent discussion of the mafic intrusions of the Noril'sk region was prepared by V. A. FEDORENKO and published in DISTLER and KUNILOV, eds. (1994), on the basis of earlier interpretations (FEDORENKO et al., 1984, unpublished) and new chemical data (NALDRETT et al., 1992; CZAMANSKE, et al. 1994, unpublished; HAWKESWORTH et al., 1995). Fifteen types of intrusion have been recognized in the region; each has specific geochemical and isotopic signatures and can be related to distinct episodes of magmatic activity. Some of these intrusion types are comagmatic to lava suites, others are post-volcanic (Fig. 2). Considered as a group, the intrusion types have a compositional range similar to that of the lavas, from high-Ti trachydolerite to low-Ti picrite. Rare, mica lamprophyres and a stock of granodiorite that is significantly younger (~223 Ma; DALRYMPLE et al., 1995) are the only exceptions.

Most intrusions are concordant with bedding. Vertical sections through both tholeiitic and subalkalic to mafic-alkalic intrusions may show little variation in petrographic characteristics and chemical composition. These undifferentiated intrusions are usually sills, and range in thickness from several to 100 m, occasionally to 150-200 m; where thickness increases, they resemble laccoliths. Individual sills extend for several tens of kilometers. Sills that are compositionally uniform often occur close to each other in the host-rock sequence; such "packets" of sills may extend more than 150 km. Intrusions for which the average, weighted MgO content is more than 8 to 10 wt% are distinctly layered and contain picritic rocks. Differentiated (layered) intrusions that are concordant with bedding are typically elongate in plan, often arcuate; they may be 20 km long, with thicknesses to 180 m (rarely to 350 or 400 m). Almost all concordant intrusions are located in the upper part of the sedimentary section, and are especially abundant in rocks of the Tungussskaya series (Fig. 4). They usually compose 15-30% (sometimes 50-80%) of the upper kilometer of the sedimentary section, and are common as much as 2 km below the base of the lava sequence. They are never found in deep Paleozoic strata during oil exploration. Only a few thin sills are found in the volcanic sequence, where they extend along tuff layers or the amygdaloidal zones of lava flows. Discordant bodies and dikes are far less common than concordant bodies. They usually dip at high angles (70°-90°) and have diverse strikes in relation to tectonic

structures; their thickness ranges from several to tens of meters. Some types of post-volcanic intrusions occur as complex, multi-level groups of sills and discordant bodies.

Six of the 15 intrusion types are comagmatic with specific lava suites (Fig. 2). They provide excellent examples of spatial relations between intrusive and extrusive comagmatism in a flood-basalt province. Four of these six intrusion types are distributed over the same areas as their extrusive analogs, but there is not a single documented case where a lava flow can be connected with a comagmatic sill, either directly or through dikes. Two intrusion types are widely distributed in areas where comagmatic lavas are absent or poorly developed, but related tuffs are well developed. Thus, there is no evidence that sills served as conduits for lava flows. On the other hand, no feeders have been recognized for any of the 15 intrusion types.

Five of the 15 intrusion types are of mafic-ultramafic composition and include differentiated (layered) bodies. One of these five (the Fokinsky type, comagmatic with the Gudchikhinsky lavas) is predominately picritic, wherever it has been studied. The four other types are represented over large areas by relatively thin (from several to a few tens of meters) doleritic sills, with ultramafic rocks appearing only in limited areas where the intrusions become far thicker. This has been taken as evidence of separate introduction of basaltic and picritic magmas for each of these four types. Within each type, the mafic and ultramafic rocks have comparable geochemical and isotopic characteristics and are considered to have come from the same source, but large distinctions between the intrusion types indicate that the source of the basaltic and picritic magmas was distinct for each type.

Intrusions of the Fokinsky type are sulfide free, whereas the other four mafic-ultramafic types contain sulfide mineralization. Only the Noril'sk type is associated with abundant sulfide that is notably enriched in Cu, Ni, and PGE. Intrusions of the Lower Talnakh type contain weak, but rather widespread mineralization that is poor in PGE. The Ruinny and Kulgakhtakhsky types carry only minor sulfide disseminations, that are rather rich in PGE, but not so enriched as those found in the Noril'sk-type intrusions (see DISTLER and KUNILOV, eds., 1994).

KOROVYAKOV et al. (1963) and IVANKIN et al. (1971) showed that the Noril'sk-type, ore-bearing intrusions are directly related to a variety of intrusive bodies that show various degrees of differentiation and mineralization, ranging to undifferentiated sulfide-free, dolerite sills. Recently, V. A. FEDORENKO (see DISTLER and KUNILOV, eds., 1994) systematized and included all of these intrusions under the Noril'sk type, which he subdivided as follows: (1) Ore-bearing intrusions (the Talnakhsky subtype of the Noril'sk type), differentiated from picritic gabbrodolerite to magnetite gabbro and leucogabbro and containing economic, disseminated and massive sulfide ores. There are only three such intrusions known: the Kharaelakh and Talnakh intrusions of the Talnakh ore junction and Noril'sk I intrusion of the Noril'sk ore junction (Fig. 3). (2) Weakly-



mineralized intrusions of the Chernogorsky and Dvugorbinsky subtypes. Chernogorsky-subtype intrusions have almost no distinction from the ore-bearing intrusions in their internal construction, but contain only sub-economic, sulfide disseminations. Chernogorka, Noril'sk II, Tangaralakh, Imangda, and some other intrusions in the broader Noril'sk region belong to this subtype (for names and locations, see NALDRETT et al., 1992). The Dvugorbinsky subtype (Upper and Lower Dvugorbaya, Burkan, and several other intrusions) are predominately mafic in composition; they include only lenses of ultramafic rocks and very poor sulfide disseminations. (3) Leucogabbro sills (the Kruglogorsky subtype; first studied in detail by LIKHACHEV, 1965), composed of leucogabbro in their upper to middle parts and mafic gabbrodolerite with rare lenses of picritic-like rocks and poor sulfide mineralization in the lower part. Often fine-grained dolerite with sparse small plagioclase phenocrysts is present along both the upper and lower endocontacts. (4) Dolerite sills (the Makusovsky subtype), a good example being the sill complex present in the NW part of the Talnakh ore junction, between the Kharaelakh and Tangaralakh intrusions (NALDRETT et al., 1992). Every borehole in that area cuts 4 to 6 sills that range in thickness from 3 to 22 m. These sills have an average MgO content of 7.88 wt% and compositions close to those of the monotonous, Late-assemblage basalts, although K<sub>2</sub>O contents (avg 0.83 wt%) are about twice as high. Exploration drilling revealed that lenses and short sills of similar composition, but varying in texture from microdolerites to relatively coarse-grained rocks, may be well developed around the ore-bearing intrusions, especially at the continuations of the three frontal parts of the Kharaelakh intrusion. Dozens of such bodies (nicknamed "tildochkas" by exploration geologists), with thicknesses of tens of centimeters to several meters, extend from one to a few hundred meters from the intrusion. All ore-bearing and weakly-mineralized intrusions have similar elongate shapes in map plan and similar thickness of 100-350 m, despite large differences in overall composition. Leucogabbroic and doleritic sills are isometric in plan and have thicknesses of several to 50 m. Rarely the weakly-mineralized, leucogabbroic, and doleritic, Noril'sk-type intrusions are found as dike-like bodies.

The Noril'sk-type, ore-bearing intrusions are found in close spatial connection with Lower Talnakh-type, differentiated intrusions; i.e., the Lower Talnakh and Lower Noril'sk intrusions are generally found a few 10s to 100s of meters beneath the Noril'sk-type intrusions (e.g., Fig. 5B). These weakly-mineralized intrusions were emplaced nearly contemporaneously with the ore-bearing intrusions (DALRYMPLE et al., 1995), but thickened parts of them appear to have influenced emplacement of the ore-bearing intrusions and the north end of the NE branch of the Talnakh intrusion cuts the Lower Talnakh intrusion (Fig. 5B; a, 1986, 1989, 1992; ZEN'KO and CZAMANSKE, 1994a, 1994b). In spite of their spatial and temporal connection, the Noril'sk and Lower Talnakh-type intrusions have profound isotopic and geochemical distinctions (e.g., NALDRETT et al., 1992; CZAMANSKE et al., 1994; HAWKESWORTH et al., 1995). For example, picritic rocks in the Noril'sk-type intrusions contain as much as 30 times more Cr than those in the Lower Talnakh type intrusions and their olivine contains 0.18 to

0.33 versus 0.06 to 0.13 wt% Ni (at Fo<sub>78-82</sub>); they have initial <sup>87</sup>Sr/<sup>86</sup>Sr ratios of 0.7051 to 0.7065 versus 0.7075 to 0.7086 and Os values of +4 to +9 versus +46 to +71. The isotopic data show that the magmas that formed the Lower Talnakh-type intrusions were contaminated at depth by crustal rocks. In summary, rocks of the Lower Talnakh-type intrusions have some similarities with, yet significant distinctions from, the Nd<sub>3</sub>-Mr<sub>1</sub> lavas. Rocks of the Noril'sk-type intrusions are compositionally similar to the Mr<sub>2</sub>-Mk lavas, as first noted by NALDRETT et al. (1992). FEDORENKO (1994a, 1994b) suggested that formation of the Lower Talnakh- and Noril'sk-type magmas took place at the end of Middle-assembly volcanism, after eruption of the Nd<sub>3</sub>-Mr<sub>1</sub> lavas. Magma is thought to have remained in the intermediate chamber and undergone additional, crustal contamination to produce the magmas parental to the Lower Talnakh-type intrusions. Formation of the Noril'sk-type magma occurred after replenishment of this chamber with a new portion of mantle-derived magma, of the Mr<sub>2</sub> geochemical type. Emplacement of both the Lower Talnakh- and Noril'sk-type intrusions is thought to have taken place at the time of formation of the thick tuff layer between Mr<sub>1</sub> and Mr<sub>2</sub> volcanic subsuites, after about 30% of the flood-basalt sequence had accumulated.

Rocks of the Noril'sk-type intrusions are almost indistinguishable from the Mr<sub>2</sub>-Mk basalts in ratios of incompatible trace elements: Gd/Yb = 1.33-1.72 versus 1.37-1.75; Ta/La = 0.026-0.041 versus 0.033-0.040; and Th/U = 1.7-3.4 versus 2.1-3.1. However, they have a wider range of slightly higher K and Rb contents, as well as higher initial <sup>87</sup>Sr/<sup>86</sup>Sr ratios. These and other characteristics allow clear distinction of the Noril'sk-type intrusions from all other magmatic formations in the region.

FEDORENKO's new classification has been adopted in this report, although we have not made extensive use of the specific names for his subtypes. Previously, most geologists have reserved the term "Noril'sk type" for the three ore-bearing intrusions and a few other intrusions that have similar, well-developed layering (e.g., Chernogorka and Imangda); these are the so-called "fully-differentiated" intrusions of GENKIN et al. (1981). ZEN'KO and CZAMANSKE (1994a) referred only to the three, ore-bearing intrusions when they wrote of the "Noril'sk type," and used "Zubovsky type" to refer to the weakly-mineralized intrusions; they considered the Kruglogorsky-type sills to represent apophyses to the ore-bearing intrusions. In this report, the words "Noril'sk-type, ore-bearing" or simply "ore-bearing" are used to refer specifically to the three, economically important intrusions. Although the name "Kruglogorsky type" also is used here for these sill-like bodies described by ZEN'KO and CZAMANSKE (1994a), their conclusion that these bodies are apophyses to the much thicker, main bodies of the ore-bearing intrusions is questioned, as LIKHACHEV (1965) and FEDORENKO propose that they represent earlier-formed sills.

The ore-bearing, and related, weakly-mineralized, leucogabbroic, and doleritic intrusions, here considered as belonging to the Noril'sk type, are found

together in only a few limited areas in the Noril'sk region, where they have a tight spatial connection. The term "ore junction" widely used in Russian literature, and introduced into the Western literature by NALDRETT et al. (1992), specifically applies to the areas occupied by these ore-bearing, intrusive complexes. Various geologists recognize 5 to 7 ore junctions and potential ore junctions in the broader Noril'sk region, but only two of them are currently established as being of economic importance, the Talnakh and Noril'sk ore junctions, in which Lower Talnakh-type intrusions are also found. These two ore junctions lie, respectively at the northern end of the Noril'sk depression and the southern end of the Kharaelakh depression, where these basins are cut by the Noril'sk-Kharaelakh fault zone (Fig. 1).

The Kharaelakh, Talnakh, and Noril'sk I intrusions occupy successively higher positions in sedimentary strata within 650 m of the contact between Tunguskaya series, continental (Middle Carboniferous-Upper Permian) and the flood-basalt sequence (Fig. 4). The Kharaelakh intrusion lies in Lower to Middle Devonian, marine sedimentary rocks and the Talnakh intrusion in Middle Carboniferous to Lower Permian sedimentary rocks. The Noril'sk I intrusion of the Noril'sk ore junction lies closest to the Tunguskaya series/basalt contact; it cuts the lower three of the eleven suites of the volcanic sequence at its north end and the lower six suites to the south. Feeders for the Noril'sk-type intrusions apparently followed zones of weakness related to the NNE-striking, Noril'sk-Kharaelakh fault zone (Figs. 1 and 3), interpreted to have been only a flexure zone at the time of intrusion emplacement (DISTLER and KUNILOV, eds., 1994).

The Kharaelakh and Talnakh intrusions of the Talnakh ore junction and the Noril'sk I intrusion of the Noril'sk ore junction each consist of a "main body," 220 to 350-m thick, that thins abruptly to 20-30 m along its flanks and is partly surrounded by more or less extensive, flanking sills. The Talnakh intrusion is divided into NE and SW branches by the Noril'sk-Kharaelakh fault, and the Kharaelakh intrusion consists of three, subequal branches. Outlines of these intrusions as typically drawn (e.g., Figs. 3 and 5A) represent only the thickened "main body" of each intrusion, which has been termed "fully-differentiated" because it displays a broad petrographic and compositional (4-29 wt% MgO) range of rock types (Fig. 6). The main body of each intrusion is situated in the lowest stratigraphic position and contains the picritic rocks and magmatic sulfide ores. Drilling on 25 to 100-m intervals has shown that at the margins of the main bodies, the intrusions consistently rise to higher stratigraphic positions and decrease sharply in thickness; at their ends they split in section or in plan. Host-rock lithology appears to have had a significant influence on morphological relations along the flanks and frontal parts of the intrusions, such that flanking relations are more abrupt in more poorly laminated rocks (ZEN'KO and CZAMANSKE, 1994a). The main bodies of the intrusions may be flanked by one or two weakly-mineralized, less-differentiated sills (the Kruglogorsky type). Such sills extend 6.5-15 km from the Kharaelakh intrusion and spread over an area of more than 80 km<sup>2</sup> (ZEN'KO, 1986, 1989; ZEN'KO and CZAMANSKE, 1994a, 1994b). They are far less developed surrounding the Talnakh intrusion and

appear to be nearly absent surrounding the Noril'sk I intrusion; they are absent where the side of an ore-bearing intrusion lies against the Noril'sk-Kharaelakh fault zone.

The close-spaced drilling has established a puzzling feature of the Noril'sk and Lower Talnakh-type intrusions, which is explicitly expressed in Russian as "insertion of the intrusions." This expression is meant to convey the fact that the main bodies of these intrusions appear to largely occupy space that was previously occupied by strata of the host-rock sequence; i.e., part of the sedimentary section appears to be missing. This relation is quite dissimilar to that typical for undifferentiated, doleritic sills in the area, which appear to have spread apart the host-rock sequence, with little loss of section. At the same time, evidence of significant *in situ* contamination of the Noril'sk- and Lower Talnakh-type intrusions is generally absent, with the possible exception of their upper contacts.

The Noril'sk-type, ore-bearing intrusions not only have rather similar morphological characteristics, but are composed of rock types of essentially identical textures and compositions. The lithologic sequence of ultramafic rocks overlain by progressively less mafic rocks in the middle 80-90 percent of vertical sections through the main bodies of the ore-bearing intrusions is generally consistent with fractional crystallization (Fig. 6). Russian petrologists have long considered that the magmas which formed the ore-bearing intrusions carried substantial amounts of olivine, immiscible sulfide melt, and plagioclase from a deeper chamber; they have made a sharp distinction between this intratelluric or "first-generation" olivine and plagioclase, and the "second-generation" olivine and plagioclase which crystallized *in situ*.

Within the main bodies of these intrusions, the intratelluric olivine is concentrated in picritic rocks, and the disseminated sulfide in picritic and taxitic units that overlie the quench-textured, lower contact rocks. The thickest, middle part of each main body is a sequence of olivine-bearing rocks, rich in plagioclase and augite, composed entirely of minerals that crystallized *in situ*. Upward in this sequence, concentrations of second-generation olivine regularly decrease, and augite habit evolves from oikocrystic to subprismatic, as augite concentrations increase. Appearing with irregular thickness and distribution above this thick sequence are: (1) a relatively coarse-grained group of quartz-bearing rocks that may have crystallized from a residual-liquid layer after crystallization of the lower and middle parts of the sequence and (2) leucocratic gabbro, an early-formed, rock unit with a large component of first-generation, tabular plagioclase.

Abrupt transitions between some rock types, anomalous variations in some major- and minor-element concentrations, and numerous exceptions to the complete lithologic sequence of Figure 6 suggest that several distinct magma types were emplaced into an expanding sill, and that the intrusions cannot be understood solely in terms of *in situ* fractional crystallization and differentiation of either a single input of crystal-free magma or of a single input of magma that carried intratelluric olivine, plagioclase, and sulfide melt. Assuming that magmas

of dissimilar bulk composition were emplaced, the very coherent data for incompatible trace elements and their ratios (e.g., Fig. 17) indicate that these magmas were derived by processing of similar parental magmas in an intermediate staging chamber(s). The existence of such chambers is clearly indicated by geochemical and isotopic studies of the flood-basalt sequence (e.g., WOODEN et al., 1993).

Sulfur, Cu, and Ni contents are comparable to Mr<sub>2</sub>-Mk basalt in the middle parts of the ore-bearing intrusions and in the basal contact gabbrodolerite (e.g., Fig. 17, Appendixes 1 and 2; CZAMANSKE et al., 1994), but disseminated, Cu-Ni-PGE ore with globular and xenomorphic texture is found in picritic and taxitic gabbrodolerite over nearly the entire areal extent of these rocks within the ore-bearing intrusions. Massive orebodies as much as 1 by 4 km in plan and 45-m thick (Fig. 3A; CZAMANSKE et al., 1992) occur as sub-conformable lenses lying (1) in metasedimentary rocks, with their upper contacts within 7 m of the footwall of the intrusions or (2) in the lowermost parts of the intrusions (e.g., LIKHACHEV, 1994; KUNILOV, 1994; TORGASHIN, 1994; DISTLER and KUNILOV, eds., 1994). The total amount of sulfide associated with the intrusions has been estimated at 0.2 wt% for Noril'sk I, 3 wt% for the Talnakh, and 7 wt% for the Kharaelakh intrusion (ZEN'KO, 1994; ZEN'KO and CZAMANSKE, 1994b). On the basis of experimental data for the solubilities of S and PGE in mafic melts, NALDRETT et al. (1992) estimated that the amount of sulfide in the main bodies of the Talnakh and Kharaelakh intrusions is about 50 times, and the PGE contents of the ores 300 to 1,800 times more than could have been dissolved in the volumes of silicate magma found there. There is no indication that massive-sulfide orebodies accumulated by gravitational settling of immiscible sulfide liquid from the immediately overlying parts of the intrusions. These facts, together with the fact that massive ore may be transgressive to rocks of the intrusions and is often emplaced in metasedimentary rocks several meters beneath the intrusions, have led many to believe that a sulfide ore magma from a deep accumulation chamber was emplaced as a final, distinct event. Clearly, vast amounts of sulfide melt were extensively mobile after emplacement and consolidation of the host intrusion, but this might be expected because of the lower solidification temperatures and low viscosity of such melts.

Whereas the primary motivation for this report is to provide a clear representation of the morphology, petrography, mineralogy, and geochemistry of the Noril'sk-type, ore-bearing intrusions, understanding the processes which led to their formation is an essential part of understanding the origin of the mineralization associated with them. From an economic perspective, the most remarkable aspects of the intrusions are: (1) association with far more magmatic sulfide than could have been carried in solution by the volumes of mafic magma that crystallized to form them; (2) PGE concentrations which require that the sulfide component reacted with many times more mafic magma than is represented by the main bodies of the intrusions; (3) globular ore textures in picritic gabbrodolerite which imply unusual processes; and (4) massive ores which were decoupled from disseminated ores and mobilized, often to positions

in the metasedimentary rocks of the footwall. From a broader perspective, those puzzling attributes of the ore-bearing intrusions whose explanation would have the most significant impact are: (1) the "insertion" of the intrusions (i.e., sedimentary strata appear to be missing where the intrusions have been emplaced); (2) their exceptionally thick metamorphic/metasomatic haloes in metasedimentary host strata; (3) the isotopically-heavy sulfur in the ores ( $\delta^{34}\text{S} = +9$  to  $+11$ ); and (4) the absence of any recognized feeders.

## **PETROGRAPHIC AND GEOCHEMICAL CHARACTERISTICS**

Much has been published on the petrography and mineralogy of the ore-bearing intrusions of the Noril'sk and Talnakh ore junctions, including major works by GODLEVSKY (1959), KOROVIYAKOV et al. (1963), ZOLOTUKHIN et al. (1975), RYABOV and ZOLOTUKHIN (1977), and GENKIN et al. (1981). However, these unique intrusions are very poorly known to Western petrologists and there has been no previous attempt to (1) tightly correlate petrographic characteristics with rock chemistry or (2) develop geochemical profiles for individual, representative boreholes. Thin sections and data from the four boreholes that we sampled in detail, coupled with study of drill core and thin sections from tens of boreholes by TATYANA ZEN'KO provide a firm basis for the descriptive part of the report. It is on this basis that we present Tables 1 and 2 as key elements to better understanding the petrographic characteristics of these intrusions.

The first column of Table 1 includes rock names, as well as those examples from the four studied boreholes that fit both (1) the definitive mineralogic, modal, and textural characteristics of columns two and three and (2) the definitive chemical parameters of Table 3. Approximately 20 percent of our analyzed samples are not listed in column one because they fail to meet one or the other of these criteria; these samples include both contaminated rocks from near intrusion contacts and transitional-facies rocks from within the intrusions. Indeed, whereas the rock types of Table 1 would be acknowledged as the most significant by most Russian students of these intrusions (e.g., LIKHACHEV, 1994), we have eliminated from discussion several rock types that we ourselves initially included. Principal among the rock types not discussed in Table 1 are: upper taxitic gabbrodolerite; picritic-taxite-like gabbrodolerite; and olivine-taxite-like gabbrodolerite. Upper taxitic gabbrodolerite is of restricted extent in the intrusions and is not represented in the cores we studied in detail. We defer discussion of this rather poorly understood unit to DUZHIKOV et al. (1992) and SLUZHENIKIN et al. (1994). Transitional rocks that might have been called picritic-taxite-like or olivine-taxite-like gabbrodolerite by some Russian workers are included here with picritic and taxitic gabbrodolerite, respectively. The name "gabbrodolerite," firmly entrenched in the literature of Noril'sk, will not be generally recognized or understood by Western petrologists. This report continues that name, which was established because these subvolcanic intrusions contain rocks that are too coarse-grained to be properly called "dolerites." The term "gabbrodolerite" will be clarified by this report, in which textural, modal, and compositional information about these rocks is presented.

Figure 7, which allows them to be considered the context of the familiar IUGS terminology (STRECKEISEN, 1973), shows that the ore-bearing intrusions are composed of rocks that trend completely across the triangular diagram for gabbroic rocks, from leuco-gabbroite to mela-olivine gabbroite, with relatively constant modal proportions of clinopyroxene.

The second column of Table 1 is in a "shorthand" used by TATYANA ZEN'KO and may appear overwhelming until the footnotes are studied carefully. In fact, this form of presentation is an extremely concise way to show the mineralogical make-up and modal mineral proportions for each rock type and, especially, to allow mineralogic comparison between the various rock types. Petrologic interpretations and the second column of Table 1 rely heavily on the classification scheme for the morphological types and generations of the main rock-forming minerals listed in Table 2. Aside from subtleties of mineral shape and size, many of which may be seen in the photomicrographs of Figures 8, 9, 10, and 11, the most significant points to be taken from Table 2 are that olivine and plagioclase are considered products of both intratelluric and *in situ* crystallization, whereas all augite is thought to have crystallized *in situ*, with its habit dependent on whether it was a liquidus or intercumulus phase. The Noril'sk- and Lower Talnakh-type intrusions of the ore junctions are not the only intrusion types that contain grains of first-generation olivine (Ol<sub>1</sub>) and plagioclase (Pl<sub>1</sub>); however, Ol<sub>1</sub> and Pl<sub>1</sub> grains found in these intrusion types are of similar, almost unique composition. They are more forsteritic and anorthitic than coexisting second-generation grains of these minerals, and than Ol<sub>1</sub> and Pl<sub>1</sub> grains in most other intrusion types of the Noril'sk region (RYABOV, 1992). Grains of Ol<sub>1</sub> are idiomorphic or resorbed (rounded or oval; 0.5 to 3 mm in diameter) and contain no inclusions of other minerals. Second-generation olivine (Ol<sub>2</sub>), considered to have crystallized *in situ*, occurs as either (1) clutch or paw-like (1 to 5 mm), oikocrystic (0.5 to 1 mm), or xenomorphic (0.3 to 0.5 mm) grains that contain, or are penetrated by small laths of plagioclase or (2) small to very small (0.01 to 0.04 mm) rounded and idiomorphic grains. Grains of Pl<sub>1</sub> are untwinned and show no zoning. Large grains of Pl<sub>1</sub> (0.5 to 1 cm long), with either idiomorphic shapes or corroded margins, often form cores that compose the greater parts of zoned, tabular-prismatic to xenomorphic grains of second-generation plagioclase (Pl<sub>2</sub>; lengths > 0.6 to 0.8 mm, width:length > 1:3). Small grains of Pl<sub>1</sub> with corroded margins may be included in various zones of other large, zoned grains of Pl<sub>2</sub>. All grains of Pl<sub>2</sub>, whether small laths or cored with large grains of Pl<sub>1</sub>, are found as zoned laths (width:length < 1:3) with abundant twins. For each grouping of rock types in Table 1, there is a listing of typical grain sizes for Ol<sub>1</sub>, Ol<sub>2</sub>, (Pl<sub>1</sub> + Pl<sub>2</sub>), and Au below the shorthand, as discussed in the footnote; these values for grain size provide refinement, for specific rock types, to the general ranges of grain size listed in Table 2. The third column of Table 1 lists those petrographic features that best distinguish individual, or related, rock types. In addition to the examples provided by Figures 8, 9, 10, and 11, we have endeavored to assist the reader by using the terminology of

MACKENZIE et al. (1982) in the third column, with reference to their photomicrographs.

In the following paragraphs we briefly discuss each rock type, and integrate petrographic (Table 1) and geochemical (Table 3) characteristics with a modest amount of petrological reasoning. This discussion is partly based on major-element and trace-element analyses of more than 100 samples from four boreholes through the three ore-bearing intrusions of the Noril'sk and Talnakh ore junctions -- the Noril'sk I (NP-29), Talnakh (KZ-1713 and KZ-1799), and Kharaelakh (KZ-1879) intrusions. Analyses for boreholes NP-29 and KZ-1879 were presented by CZAMANSKE et al. (1994), whereas comprehensive analyses for our samples of boreholes KZ-1713 and KZ-1799 are presented in Appendixes 1 and 2. Virtually all samples from these intrusions are characterized by incompatible-trace-element and isotopic ratios that show only small, regular or irregular variation: i.e., Ta/La = 0.026-0.041; Th/U = 1.67-3.38; La/Sm = 1.86-2.95; La/Yb = 2.58-4.30; Gd/Yb = 1.33-1.72; ( $^{87}\text{Sr}/^{86}\text{Sr}$ )<sub>i</sub> = 0.7052-0.7061; and ( $^{206}\text{Pb}/^{204}\text{Pb}$ )<sub>i</sub> = 17.8-18.3. Deviation from these characteristics in a few samples from near intrusion contacts is taken as clear evidence of *in situ* contamination.

Tabulation and discussion of major-element data in this report are on the basis of normalization of the major oxides to 100 wt% anhydrous, after subtracting CaO equivalent to CaCO<sub>3</sub> (on the basis of the CO<sub>2</sub> determinations) and estimating the amount of Fe combined with S; this estimate was based on the composition of disseminated ore in picritic gabbrodolerite from the Noril'sk I intrusion (sample 90MC10, CZAMANSKE et al., 1992). All Fe is given as FeO, as is appropriate for mafic igneous rocks and because extensive alteration and sulfide mineralization render determinations of Fe<sup>2+</sup>/Fe<sup>3+</sup> meaningless for whole-rock chemistry. Our intent in making these corrections is to be able to consider the lithologic sequence within the intrusions strictly in terms of silicate-magma chemistry.

Leucocratic gabbro -- Leucogabbro is an important rock type in understanding emplacement of the ore-bearing intrusions, as first established by LIKHACHEV (1965). It may form an upper unit 10 to 20 m thick (e.g., Fig. 6), but is often far thinner and may occur only as rare lenses, or be absent; it is usually present in the Kharaelakh and Noril'sk I intrusions, but rare in the two branches of the Talnakh intrusion (e.g., Fig. 18). It also may constitute as much as 40 vol% of the Kruglogorsky-type sills that extend outward from the ore-bearing intrusions (LIKHACHEV, 1965; ZEN'KO, 1986, 1989; ZEN'KO and CZAMANSKE, 1994a). In the main bodies of the intrusions, leucogabbro lies along the roof, above olivine-bearing gabbrodolerite or prismatic gabbro; it is not known to lie above quartz diorite or magnetite gabbro. Only upper contact gabbrodolerite or upper taxitic gabbrodolerite are occasionally found above leucogabbro. Where olivine-bearing gabbrodolerite and the residual sequence are absent, leucogabbro may lie above olivine gabbrodolerite (e.g., in borehole KZ-1879). Leucogabbro often includes fragments of metamorphosed roof rocks, from



millimeters to a few meters across. On the other hand, leucogabbro may occur as fragments of varying size in upper taxitic gabbrodolerite, where that unit is present, or in the olivine-bearing to olivine gabbrodolerite sequence. We analyzed a relatively fresh, 20-cm fragment (xenolith) of typical leucogabbro found in olivine gabbrodolerite of the Kharaelakh intrusion about 50 m below the leucogabbro layer at the roof of the intrusion, which was its presumed source (sample KZ-1818-1757.1, Fig. 8A; note that in all cases, the last digits of sample numbers represent depth in the borehole, in meters). Leucogabbro typically occupies the upper to middle part of Kruglogorsky-type sills, where it is underlain by olivine gabbrodolerite (sometimes taxitic-like) and is often overlain by fine-grained dolerite, that may contain plagioclase phenocrysts.

The major-element characteristics of leucogabbro reflect abundance of highly zoned, tabular plagioclase (mainly of the first generation, An<sub>45-100</sub>), which commonly exceeds 75 modal%; Al<sub>2</sub>O<sub>3</sub> content is high, 20-24 wt%, and FeO<sup>T</sup> content is low, 5-7 wt%. [Here and below, compositions of plagioclase are based on unpublished electron-microprobe analyses by T. E. ZEN'KO and A. P. LIKHACHEV of samples from borehole KZ-1821 (Fig. 3A) through the Kharaelakh intrusion, and estimates published by LIKHACHEV (1994)]. Exceptional enrichment of PGE in an irregularly distributed, rather minor sulfide fraction is characteristic of leucogabbro (e.g., Table 4). Our analysis of sample KZ-1818-1757.1 shows that this sample has the PGE enrichment typical of leucogabbro, even though the olivine gabbrodolerite in which the fragment was found is characterized by basaltic, PGE contents (e.g., Table 4). Thus, PGE enrichment is a primary (syngenetic) characteristic of leucogabbro. Notable in Figure 8A is the relatively coarse, average grain size of the rock, the considerable range in plagioclase grain size, and the presence of several percent of olivine.

Quartz diorite, magnetite gabbro, prismatic gabbro -- This group of rocks, which we call the "residual sequence," ranges from 0 to 100 m thick (commonly 6-20 m) and may be in sharp or interfingering contact with underlying units. Rocks of this sequence contain large, prismatic grains and laths of plagioclase (Pl<sub>2</sub>) and augite (Au<sup>1</sup>), and may contain sparse Ol<sub>2</sub>. These rocks are often highly altered (see Table 1); plagioclase grains which had original compositions of An<sub>35-60</sub> may now have compositions of An<sub>1</sub>, and secondary amphibole is common. The names of the rock units within this sequence are all new to this contribution, because the magnetite-gabbro unit has not been recognized in previous Russian studies and the "standard" Russian names for the rocks we call quartz diorite and prismatic gabbro are, respectively, quartz gabbrodiorite and gabbrodiorite; these Russian names have little meaning to Western geologists. In prismatic gabbro the cores of unaltered plagioclase grains are slightly more calcic than An<sub>50</sub> and in quartz diorite they are less calcic. We also note that some previous reference to the magnetite gabbro as "ferrogabbro" is inappropriate because the rocks do not contain Fe-rich pyroxene (cf., WAGER and BROWN, 1967; see Table 5 and Fig. 13). As noted in Table 1 and seen in Figures 8B, 8C, 8D, and 9A, relatively large, elongate grains of second-

generation plagioclase are common to the three rock types of the residual sequence. Especially notable are the abundance of quartz and micropegmatite in quartz diorite and of titanomagnetite in the magnetite gabbro.

Reference to Table 3, Appendix 2, and Figure 17 shows that, except for Cr and PGE contents, there are only subtle geochemical distinctions between prismatic gabbro and underlying olivine-bearing gabbrodolerite, despite a profound difference in texture (e.g., Figs. 9A and 9B). Tables 5 and 6 show that, also with the exception of Cr, the differences in clinopyroxene compositions in the two rock types are equally subtle, especially considering that the analyzed pyroxenes are from two different intrusions. Magnetite gabbro has highest  $\text{FeO}^{\text{T}}$  and  $\text{TiO}_2$  contents of any rock type in the intrusions; this obscures other chemical parameters, but rare-earth-element (REE) contents may be higher than those found in any rock type other than quartz diorite. Quartz diorite has relatively low contents of  $\text{Al}_2\text{O}_3$ ,  $\text{MgO}$ , and  $\text{CaO}$ , with elevated contents of  $\text{SiO}_2$ ,  $\text{Na}_2\text{O}$ ,  $\text{P}_2\text{O}_5$ , and S. Contents of Ta, Zr, and REE may reach three to five times those in magnetite or prismatic gabbro.

Magnetite gabbros from boreholes KZ-1799 and NP-29 are not only texturally (Figs. 8C and 8D) but chemically dissimilar. Those from borehole KZ-1799 contain significantly lower concentrations of  $\text{SiO}_2$ ,  $\text{Na}_2\text{O}$ , and incompatible trace elements and higher concentrations of  $\text{FeO}^{\text{T}}$ ,  $\text{K}_2\text{O}$ , S, Cu, and Cr (Table 3). The strong contrast in titanomagnetite habits shown in Figures 8C and 8D reflects a different crystallization history that is undoubtedly also responsible for the overall chemical contrasts between the two rock variants. In borehole NP-29, magnetite gabbro and olivine-bearing gabbrodolerite interfinger, such that the magnetite gabbro unit is split into three layers. A very unusual rock (sample NP-29-603), believed to represent an olivine-magnetite cumulate and containing abundant biotite, is found at the base of the lowermost magnetite-gabbro layer; it contains (wt%)  $\text{SiO}_2$ , 34.6, FeO, 36.6,  $\text{MgO}$ , 10.9,  $\text{TiO}_2$ , 4.1, S, 1.28, as well as 3000 ppm Cu and 200 ppb Pt; the Pd/Pt ratio is 0.55, quite different from Pd/Pt ratios in disseminated, sulfide ore and even lower than Pd/Pt ratios typical of basalts (Table 4; WOODEN et al., 1993; CZAMANSKE et al., 1994).

Overall similarity in the chemical compositions of prismatic gabbro and olivine-bearing gabbrodolerite suggests that the bulk of the residual sequence was produced largely during fractional crystallization and differentiation of the magmas that formed the olivine-bearing gabbrodolerite through olivine gabbrodolerite sequence. However, the residual sequence may have been at one time an essentially discrete, largely-liquid layer of melt, partly formed by processes of filter pressing or diapiric melt transfer (e.g., HELZ, 1987), coupled with concentration of volatiles. This possibility seems to best account for its irregular distribution and impoverishment in Cr, as well as for the common occurrence of (1) complex interfingering of prismatic gabbro with underlying olivine-bearing gabbrodolerite and (2) lenses of coarse-grained (1-1.5 cm) prismatic gabbro in olivine-bearing gabbrodolerite that range in thickness from a few centimeters to tens of centimeters. Prismatic crystals of plagioclase and

clinopyroxene grew large, perhaps in response to concentration of volatiles in late-crystallizing magma. Most compositional attributes of the residual sequence are compatible with fractional crystallization and interstitial-melt extraction; in addition, partial melting and assimilation of roof rocks probably was involved in the evolution of quartz diorite.

Olivine-bearing gabbrodolerite through olivine gabbrodolerite -- This important sequence of rocks ranges in thickness from 30 m to well over 100 m and forms the middle to upper part of all Noril'sk-type intrusions, from the base of the residual sequence to the relatively sharp discontinuity at the upper contact of picritic gabbrodolerite (e.g., Fig. 17). Olivine-bearing gabbrodolerite contains essentially the same modal proportion of plagioclase as rocks of the residual sequence, and may contain minor quartz and micropegmatite; in these aspects also, olivine-bearing gabbro and prismatic gabbro are similar. We have listed three rock types in Table 1 -- olivine-bearing gabbrodolerite, olivine-bearing to olivine gabbrodolerite, and olivine gabbrodolerite -- as these are firmly entrenched in local usage. However, compositional changes in this sequence are gradational (Fig. 17; Table 3; Appendixes 1 and 2) and we do not present data for olivine-bearing to olivine gabbrodolerite in Table 3.

These rocks are fine to medium grained (Figs. 9B, 9C, 9D, and 10A) and relatively plagioclase rich (highly zoned, An<sub>40-70</sub> in olivine-bearing gabbrodolerite and An<sub>45-85</sub> in olivine gabbrodolerite). They are distinguished by the virtual absence of fine-grained Ol<sub>1</sub>, and are characterized by downward-increasing concentrations of second-generation olivine, accompanied by gradual changes in olivine size and morphology from mainly large, anhedral oikocrysts (Ol<sub>2</sub><sup>3,4</sup>) to smaller, oikocrystic grains (Ol<sub>2</sub><sup>5,6</sup>). General increases in forsterite and Ni contents of olivine, from the top of the olivine-bearing gabbrodolerite unit to the base of the olivine gabbrodolerite unit, are complicated by minor reversals and ranges in olivine composition within individual samples (as discussed below). Roughly, the overall, downward change in average olivine composition is from Fo<sub>58</sub> and 0.05 wt% NiO to Fo<sub>76</sub> and 0.14 wt% NiO. Accompanying the downward transition from olivine-bearing to olivine gabbrodolerite is a modest decrease in augite content and a change in augite habit from subprismatic (Au<sup>2</sup>) to oikocrystic (Au<sup>3</sup>). Changes in the composition of this clinopyroxene are relatively insignificant through the 46 meters of this sequence present in borehole NP-29 (Table 6). Samples of olivine-bearing gabbrodolerite have an intergranular, sometimes trachytic texture; the latter is not well developed in the example shown as Figure 9B, and trachytic texture is not seen in olivine gabbrodolerite. Low in the sequence, in olivine gabbrodolerite, textures are poikilophitic and subophitic, reflecting the change in augite habit from subprismatic grains to oikocrysts (e.g., Fig. 9D). As olivine concentration increases downward in this sequence, there is a modest increase in whole-rock MgO content and a decrease in SiO<sub>2</sub> content. Contents of Al<sub>2</sub>O<sub>3</sub> and FeO<sup>T</sup> also slightly increase and decrease, respectively, except near the base of the sequence. Near its lower contact with picritic gabbrodolerite, olivine

gabbrodolerite is usually enriched in Cr-spinel and biotite; some recognize the biotite-rich rocks of this interval as olivine-biotite gabbrodolerite.

Picritic-like gabbrodolerite -- This transitional rock type is present in all four boreholes at the boundary between the olivine- and picritic-gabbrodolerite units; its thickness is typically measured in a few tens of centimeters, but reaches a few meters in borehole NP-29. In addition, picritic-like gabbrodolerite is interfingered with olivine gabbrodolerite throughout the entire olivine-gabbrodolerite unit in borehole KZ-1879, where that unit is unusually thick and rich in MgO (CZAMANSKE et al., 1994). Although MgO and olivine contents are similar,  $Ol_2$  is characteristic of picritic-like gabbrodolerite in borehole KZ-1879, whereas a significant component of  $Ol_1$  is present in the picritic-like gabbrodolerites found at the boundary of the picritic unit in boreholes KZ-1713, KZ-1799, and NP-29 (compare Figs. 10A and 10B). It appears that rocks which can be geochemically and modally classified as picritic-like gabbrodolerite may in some cases represent a thin, transitional layer between picritic and olivine gabbrodolerite and in others simply represent abnormal concentrations of olivine within the olivine-gabbrodolerite unit itself. Geochemical support for this argument is found in the higher  $Al_2O_3$  and CaO contents, but lower  $FeOT$ , Pd, Cu, and Cr contents of samples from borehole KZ-1879; in each case, measured concentrations are closer to those in olivine gabbrodolerite. The profound difference in the morphology of first- and second-generation olivine is revealed in comparison of Figures 9B, 9C, 9D, and 10A with Figures 10B, 10C, and 10D. Two small olivine grains included in the upper margin of the small plagioclase glomerocryst will assist the reader in recognizing the typical, fine-grained, first-generation olivine in the sample of picritic-like gabbrodolerite (Fig. 10B). Olivine in both varieties of picritic-like gabbrodolerite has compositions in the range  $Fo_{71-77}$  and contains 0.12 to 0.17 wt% NiO, as could be expected from the overall ranges in Table 7.

Picritic gabbrodolerite and olivine-rich picritic gabbrodolerite -- These rocks are of critical importance in understanding the evolution of the ore-bearing intrusions. Map outlines are drawn for the Noril'sk-type intrusions (e.g., Figs. 3 and 5A) where there is a coincidence of thinning of picritic gabbrodolerite and a sharp decrease in the thickness of the intrusion (to 30-50 m). The picritic-gabbrodolerite unit is commonly 10 to 30 m thick but may reach 120 m; it almost always carries disseminated sulfide (largely as globules 0.5-2 cm across), and discontinuities in concentrations of S, Cu, Ni, and PGE at the upper contact of the picritic-gabbrodolerite unit are remarkable (Fig. 17). Equally abrupt changes in major-element concentrations mark the transition from olivine gabbrodolerite, in which plagioclase is the most abundant phase, to picritic gabbrodolerite in which small, euhedral and resorbed grains of  $Ol_1$  may nearly reach close packing. Picritic gabbrodolerite is defined as containing 40 to 60 modal% olivine (Table 1), and olivine-rich, picritic gabbrodolerite as containing 60 to 80 modal% olivine. These rocks contain olivine with the highest average forsterite ( $Fo_{73-79}$ ) and NiO (0.16-0.28 wt%) contents. The average composition of

oikocrystic clinopyroxene differs little from that in overlying, olivine gabbrodolerite (Table 6). Picritic rocks may contain fine-grained fragments 2-6.5 cm across consisting of  $(Ol_2^8)_{30-80} (Pl_2^5)_{0-40} (Au^3)_{0-70}$  that may compose several modal% of the rocks. Glomerocrysts of  $Pl_1$  and  $Pl_2$  ( $An_{65-95}$ ) may reach 2 to 3 cm in size; they generally compose only a few percent of the unit, but their concentration may increase to more than 15 modal% near the base of the unit. Such glomerocrysts can be seen in Figure 12A. Rarely, large (2-3 cm), resorbed, plagioclase phenocrysts are present in the lower part of the picritic-gabbrodolerite unit (e.g., Fig. 12A).

Because of enrichment in olivine, picritic gabbrodolerite is relatively impoverished in all major elements except MgO (18.4 to 27 wt%) and  $FeO^T$ . Sulfur, Cu, Ni, and PGE contents are variable, but higher than those in any other unit except taxitic gabbrodolerite. In picritic gabbrodolerite, Cr-spinel is typically found in intercumulus plagioclase and clinopyroxene, rarely in  $Ol_1$ . Chromium contents may be the highest found in any rock type, but for our three boreholes in which the picritic unit is well expressed (KZ-1713, KZ-1799, and KZ-1879), Cr content is greatest in the upper part of this unit and decreases steadily downward (e.g., Fig. 17; Appendixes 1 and 2). Samples that are exceptionally rich in olivine are here called "olivine-rich, picritic gabbrodolerite" but have been called "olivinites" by several Russian petrologists. Additional enrichment in olivine simply results in further enrichment in MgO, to as much as 29 wt%, with further impoverishment in other major elements.

Taxitic gabbrodolerite.--The name of this important rock type reflects its exceptional variation in texture and chemical composition, as noted in Table 1 and reflected in the data of Table 3 and Appendixes 1 and 2. The unit ranges in thickness from 3 to 60 m (commonly 10-15 m); both its upper and lower contacts are usually gradational. Taxitic gabbrodolerite and picritic gabbrodolerite contain the economic, disseminated ores; Cu, Ni, and PGE contents are commonly higher in taxitic gabbrodolerite.

Plagioclase ( $An_{40-95}$ ) and clinopyroxene grains in taxitic gabbrodolerite may be several centimeters long, yet the unit contains a significant abundance of small fragments, rich in extremely small grains of olivine and pyroxene (e.g., Fig. 11A). Other small fragments contain zeolites. The significance of these fine-grained fragments, that may reach 2 x 3 cm in size, has yet to be determined, but some may represent xenoliths (KUNILOV, 1994). Forsterite and NiO contents of olivine are notably lower in taxitic gabbrodolerite than in overlying picritic gabbrodolerite. Data for borehole KZ-1799, in which olivine was analysed in a series of four samples, show that over an interval of only seven meters, average forsterite and NiO contents decrease downward from  $Fo_{75}$  and 0.16 wt% NiO to  $Fo_{64}$  and 0.10 wt% NiO.

As seen in Table 3, compositions of taxitic gabbrodolerite may encompass those of all rock types from olivine-bearing to picritic-like gabbrodolerite, but there is no straight-forward petrographic relation to any of those rock types.

Characteristic of taxitic gabbrodolerite, and requiring explanation in any adequate model for the origin of the intrusions, are Cr contents as low as those in contact and olivine-bearing gabbrodolerite and usually lower than those in olivine gabbrodolerite.

Contact gabbrodolerite -- While usually missing from the upper contacts of the ore-bearing intrusions, contact gabbrodolerite is almost continuously present along the base of these intrusions. In this contribution, the name contact gabbrodolerite is used in a much more restricted sense than has been done by many Russian geologists. We apply the term only to the fine-grained, quenched rocks 1-2 m thick that lie against the lower contact and not to the thicker, overlying zones (up to 10 m thick) that grade into taxitic rocks. Contact gabbrodolerite may contain a significant amount of devitrified glass (Table 1) and has the most uniform, fine grain size of any rock type in the intrusions (Fig. 11B), fitting the interpretation that these rocks represent rapid crystallization, against footwall sediments or basalt, of essentially phenocryst-free, mafic magma. First-generation, intratelluric olivine is never found. Small plagioclase phenocrysts have compositions of An<sub>75-85</sub>, whereas plagioclase needles in the groundmass are An<sub>50-70</sub>. Contact gabbrodolerite is similar to olivine-bearing gabbrodolerite in SiO<sub>2</sub> (48.9 to 51.0 wt%) and in MgO contents (6.9 to 8.0 wt%), as well as most other geochemical attributes. The common absence of upper contact gabbrodolerite must be addressed in credible models.

Disseminated sulfide -- It is beyond the scope of this paper to characterize the massive ores, and the veinlet-disseminated ores in metamorphosed country rocks that have been well described by others (e.g., GENKIN et al., 1981; DISTLER, 1994; STEKHIN, 1994; TORGASHIN, 1994). However, the disseminated ores within the intrusion are exceptional and their origin was integral to formation of the ore-bearing intrusions. All primary, disseminated ores, with the exception of minor sulfides in leucogabbro and in upper taxitic gabbrodolerite (DUZHIKOV et al., 1992; SLUZHENIKIN et al. 1994) are found in picritic and taxitic gabbrodolerite. Sulfide concentrations range from sparse disseminations to sideronitic, a texture rather seldom seen in which sulfide forms a matrix to the silicate minerals. Most typically, the disseminated ores consist of isolated sulfide globules or aggregates "suspended" among the silicate grains of the host rocks, among which fine-grained sulfide also is dispersed (e.g., Figs. 10D, 11A, and 12B); sulfide contents in both picritic and taxitic gabbrodolerite are commonly in the range 3 to 20 vol%, the bulk of the sulfide being contained in the relatively large, isometric masses. Ovoid globules from 0.5 to 2 cm across in picritic gabbrodolerite clearly represent solidified droplets of immiscible Fe-Cu-Ni-S-O melt (e.g., Fig. 12B). Xenomorphic sulfide aggregates as much as 3 to 4 cm across are typical of taxitic gabbrodolerite (e.g., Fig. 11A). Stretched bodies several centimeters across in either picritic or taxitic gabbrodolerite apparently were affected by local, late-stage compaction and slumping.

As remarkable as the suspension of the sulfide globules is the fact that within the picritic gabbrodolerite they are invariably layered, with coarse pyrrhotite and

pentlandite in the lower part of each globule and a copper-rich assemblage in the upper part. Such layering is not as evident in taxitic rocks, perhaps because most of the sulfide aggregates are xenomorphic. Monosulfide solid solution [mss; (Fe,Ni)S], crystallized at ~1000 °C from the Fe-Cu-Ni-S-O melt and sank to the bottom of each droplet, whereas subhedral magnetite grains that are quite large relative to those in the host rock crystallized along the margins of the droplets. Subsequently, the Cu-rich liquid in the upper part of each droplet crystallized as a Ni-bearing, intermediate solid solution [iss; (Cu,Fe)S]. The droplets probably were completely solid at ~800 °C. Ultimately, the accumulated mss recrystallized to form coarse-grained pyrrhotite and pentlandite and the iss broke down to form a complex intergrowth of Cu-Fe-Ni-sulfide phases (e.g., CZAMANSKE et al., 1992). Noteworthy discussions of the distribution and compositions of disseminated, veinlet, and massive sulfide ores within the intrusions have been presented recently by NALDRETT et al. (1994), ZIENTEK et al. (1994), and DISTLER and KUNILOV, eds. (1994).

### MINERAL CHEMISTRY

A detailed discussion of silicate- and oxide-mineral chemistry within the intrusions cannot be presented at this time, but we have obtained much new information about olivine compositions and some, new information about pyroxene, biotite, and Cr-spinel compositions. ZOLOTUKHIN et al. (1975, their Table 25) and RYABOV and ZOLOTUKHIN (1977, their Table 5) present data from chemical analysis of bulk plagioclase separates. Anorthite contents show little systematic variation and were reported as (mole%): olivine gabbrodolerite, 46-78; picritic gabbrodolerite, 69-76; and taxitic gabbrodolerite, 55-81. The wide-ranging plagioclase compositions typical of most rock types have been presented above, based on electron-microprobe analyses by ZEN'KO and LIKHACHEV and the report of LIKHACHEV (1994). The existence of two generations and numerous morphological types of plagioclase (Table 2), representing both intratelluric and *in situ* crystallization, coupled with extensive zoning for many morphological types and alteration in some rock types, presents a challenge for analysis and interpretation.

Numerous studies have shown that olivine compositions in mafic intrusions often reflect reequilibration, dependent on olivine modal abundance (e.g., BARNES, 1986; CHALOKWU and GRANT, 1987), and we strongly suspect that olivine reequilibration has taken place in the ore-bearing intrusions. In the four studied boreholes of the ore-bearing and Lower Talnakh-type intrusions, the most Mg-rich olivine is found in the picritic-gabbrodolerite unit, in which olivine and whole-rock, MgO contents are the highest (e.g., Figs. 16 and 17). The fact that the forsterite content of olivine decreases upward in the olivine through olivine-bearing gabbrodolerite sequence of all four boreholes is consistent with fractional crystallization; however, these rocks also contain progressively less olivine. In borehole KZ-1799, olivine also becomes increasingly iron rich downward in taxitic rocks as their MgO contents decrease (Fig. 16 and Appendix 2). In nine samples of olivine to picritic-like gabbrodolerite from borehole KZ-

1879 (samples KZ-1879-1718.4 through -1743.1; CZAMANSKE et al., 1994) in which MgO content varies irregularly between 10.3 and 17.3 wt%, average forsterite contents of Fo<sub>76</sub> to Fo<sub>69.5</sub> correlate well with MgO content. On the basis of these considerations, we hesitate to interpret the offset in olivine composition between the picritic- and olivine-gabbrodolerite units (Table 7; Fig. 16) as additional evidence for a discrete emplacement of picritic magma. In fully interpreting our olivine data, it will be essential to categorize analyses of individual olivine grains according to morphological type (Table 2) and textural relations, i.e., on grain boundaries or trapped in a pyroxene oikocrysts. Because we have analyzed an average of 10 grains per sample, this approach may ultimately allow evaluation of the extent of olivine reequilibration in these intrusions.

Because chalcophile elements partition strongly into sulfide liquid in preference to silicate melts and minerals, the NiO content of olivine has long been taken as a sensitive indicator of sulfide segregation (e.g. THOMPSON and NALDRETT, 1984, their Fig. 9). Nickel solubility in olivine is a strong function of forsterite content, and the data of Table 7 show that none of the olivine in the ore-bearing intrusions is Ni depleted, despite the range in NiO contents. These data argue strongly against the sulfide melts having been formed by an *in situ* segregation process, and indicate that olivine and Ni-bearing, sulfide liquid were essentially in equilibrium, either as a result of having been accumulated and emplaced together, or having been mixed together *in situ*.

For most analysed olivine grains there is <1 mole% zoning in Fo content from core-to-rim, but the forsterite contents of grains within individual thin sections may vary by 5 to 10 mole% (as also noted by RYABOV, 1991). Chromium contents are negligible (<0.02 wt% Cr<sub>2</sub>O<sub>3</sub>) in all of the analysed grains, whereas CaO contents range from 0.07 to 0.32 wt% and MnO contents from 0.22 to 0.70 wt%. CaO contents always decrease by 0.04 to 0.15 wt% from cores to rims of grains. MnO contents generally range from 0.26 to 0.40 wt% in picritic gabbrodolerite, but from 0.35 to 0.52 wt% in taxitic gabbrodolerite; above the picritic-gabbrodolerite unit, MnO contents also increase, reaching 0.47 to 0.62 wt% in olivine-bearing gabbrodolerite.

Orthopyroxene is a relatively minor constituent of the ore-bearing intrusions (Table 1); two average analyses from NP-29 samples are presented in Table 6. Analyses of clinopyroxene were obtained for 10 samples from the residual sequence of borehole KZ-1799 (KZ-1799-1214.8 through KZ-1779-1249.8) and ten samples from borehole NP-29 (NP-29-639.7 through NP-29-691.6) that range from olivine-bearing through taxitic gabbrodolerite. In general, 3 or 4 points were analysed from the cores and rims of 3 to 4 pyroxene grains per thin section, as summarized in Tables 5 and 6 and in Figure 13. (A subjective averaging procedure was used to prepare Tables 5, 6, 8, and 9; more than one average analysis is presented for a sample only when several elements show >20% covariation or when Cr is at dramatically different concentration levels.)



The data of Table 6 show that there is no systematic variation in the composition of clinopyroxene through 54 meters of the Noril'sk I intrusion, despite occurrence in four rock types (olivine-bearing through taxitic gabbrodolerite) and in both subprismatic ( $Au^2$ ) and oikocrystic ( $Au^3$ ) habits; clinopyroxene that was on the liquidus at the top of the olivine-bearing gabbrodolerite unit has virtually the same composition as clinopyroxene that crystallized after olivine in picritic gabbrodolerite. Chromium contents show that two generations of pyroxene are present in many samples. Late-crystallizing clinopyroxene has lower Cr content, as indicated by its occurrence on the edges of grains (e.g., sample NP-29-637.9) and consistent enrichment in Fe, Ti, and Mn. The existence of two generations of clinopyroxene is better documented by Russian workers (e.g., RYABOV and ZOLOTUKHIN, 1977; ZOLOTUKHIN, 1982) who refer to early, green (chromian) and late, brown (titaniferous) varieties, although Cr appears to show proportionately far greater change. As expected (e.g., HUEBNER, 1980), orthopyroxene contains less Cr, Al, and Na, but more Mn than coexisting clinopyroxene; corresponding to whole-rock compositions, orthopyroxene in picritic gabbrodolerite is somewhat richer in Mg and Cr than that in taxitic gabbrodolerite.

In the residual sequence of borehole KZ-1799, there is little systematic change in clinopyroxene composition through 30 meters of prismatic gabbro and 12 meters of magnetite gabbro, but clinopyroxene in the uppermost sample of magnetite gabbro (KZ-1799-1214.8) is notably enriched in Fe (Table 5; Fig. 13). As to be expected from whole-rock compositions, clinopyroxene in the residual sequence contains little Cr. Despite the fact that samples were analysed from both the Noril'sk I intrusion and the NE branch of the Talnakh intrusion, the Cr-poor clinopyroxene in the 15-m thickness of prismatic gabbro in borehole KZ-1799 differs only slightly in composition from that in the olivine-bearing through olivine-gabbrodolerite sequence of borehole NP-29 (e.g., Fig. 13). We have no explanation at this time for the fact that two clinopyroxene compositions are found in several samples of the residual sequence, but textures in thin section are suggestive that the clinopyroxene with relatively high Wo content crystallized later. In the three samples of magnetite gabbro, this clinopyroxene is relatively enriched in Si, and depleted in Fe, Al, Ti, and Na, in comparison with coexisting clinopyroxene; in the prismatic gabbro, these relations do not hold.

As seen in Figure 13, as well as for the Kharaelakh intrusion (ZEN'KO and CZAMANSKE, 1994a; their Fig. 21.6), the range of clinopyroxene compositions in the Noril'sk-type intrusions is much more restricted than those in such layered mafic intrusions as the Skaergaard Intrusion (WAGER and BROWN, 1967) or the Bushveld Complex (ATKINS, 1969). The bulk of the Noril'sk data define a trend that overlaps those of approximately the lower 4000 m of the Bushveld Complex (to the level of Main zone b) and the lower 600 m of the Skaergaard Intrusion (two-thirds through Lower Zone b). Although our data represent two intrusions, it is tempting to suggest that the somewhat more Wo-rich pyroxenes in the residual sequence of borehole NP-29 represent crystallization at slightly lower temperature (e.g., HUEBNER, 1980), perhaps caused by higher water content,

which might also be expected to enhance Wo content (GAETANI et al., 1993). A continuation of this effect could account for the compositions of the most Wo-rich clinopyroxenes from the magnetite gabbro in borehole KZ-1799, if they crystallized last.

A notable attribute of many of the mafic-ultramafic intrusions of Siberia is the presence of biotite. Traces of biotite may be found in most rock types, but it is most abundant in the lower part of the olivine-gabbrodolerite unit, and in picritic-like and picritic gabbrodolerite. In these rocks, biotite occurs in two ways (1) as anhedral, interstitial grains as large as 2 mm across (e.g., Figs 10B and 10C) and (2) in "books" of grains as large as 2-4 mm across associated with sulfide mineralization. The K<sub>2</sub>O contents of biotite-bearing rocks that we have analysed range from only 0.19 to 0.51 wt%, comparable to K<sub>2</sub>O contents in Mr<sub>2</sub>-Mk basalts (0.10 to 0.47 wt%; WOODEN et al., 1993) which geochemically most resemble the magmas that formed the intrusions. Crystallization of biotite rather than amphibole in the ore-bearing intrusions is related to the fact that (1) the concentrations of K<sub>2</sub>O in the interstitial melts of rocks enriched in cumulus phases were greater than those in the basaltic magma and (2) biotite may be stable at much higher temperatures than amphibole. Occurrence of coarse biotite in pockets next to sulfide aggregates strongly suggests the activity of a late, fluid phase.

The analyses of Table 8 indicate that, as a late-crystallizing phase, biotite composition was responsive to local variations in the compositions of late-stage melts/fluids. Thus, in sample KZ-1713-922.9 of the heterogeneous, taxitic unit, MgO contents in biotite range from 8.2 to 18.1 wt%, FeO contents from 14.4 to 28.9 wt%, TiO<sub>2</sub> contents from 0.31 to 5.5 wt%, and Cl contents from 0.45 to 4.32 wt%. Biotite in the taxitic- and olivine-bearing gabbrodolerite units, which bracket the main sequence in the intrusions, appears to be richer in Fe and Cl than that in the more olivine-rich, mid-section of the intrusions. Otherwise there are no perceptible trends with stratigraphic position. With one exception, contents of Cr are quite low, whereas TiO<sub>2</sub> contents over 5 wt% are not uncommon; Cl and F are regularly present. (Sparse apatite present near the upper contact of the picritic gabbrodolerite is rich in Cl.)

Analyses of biotite that occurs in leucogabbro and magnetite gabbro, as well as in 2-mm-thick booklets with sulfide in picritic gabbrodolerite of the Noril'sk I intrusion (sample 90MC22) are presented in Table 9. All contain significant amounts of Cl and F, and the biotite in sample 90MC22 contains a significant amount of Cr. Contents of Ti may be high, and the Fe contents of biotite in single samples of leucogabbro and magnetite gabbro are extremely high. Aside from containing less Ti, there is little difference between the chemistry of biotite in sample 90MC22 and that in the picritic gabbrodolerite of borehole KZ-1713 (Table 8). Biotite is a relatively abundant and coarse-grained constituent of sample NP-29-603, the magnetite-olivine cumulate, and its distinctly lower Fe content may reflect extensive withdrawal of Fe by magnetite crystallization.

In an effort to understand the Cr-concentration anomaly near the contact between olivine and picritic gabbrodolerite, we examined 16 polished thin sections of this critical interval in the four studied boreholes by cycling back and forth under low magnification on the electron microprobe, while observing back-scattered images. This process confirmed TATYANA ZEN'KO's microscopic determination that very few olivine grains contain oxide grains or sulfide inclusions. Instead, fine-grained, Cr-spinel is dispersed very irregularly in clinopyroxene, orthopyroxene, and especially, interstitial plagioclase in Cr-enriched samples of picritic gabbrodolerite. Whereas much plagioclase in each thin section may be free of Cr-spinel grains, other plagioclase grains are crowded with grains 20-40 microns across (e.g., Figs. 14A and 14B). Notable concentrations of Cr-spinel grains are present in samples NP-29-678.2, -681.2, and -683.6; KZ-1879-1752.5; and KZ-1713-879.5, -880, and -883.8. No such concentrations of grains were seen in any samples from borehole KZ-1799 or in the following three samples that contain >2000 ppm Cr -- NP-29-684.4, KZ-1713-879, and KZ-1713-883.6. Texturally most Cr-spinel grains trapped in olivine are rounded (e.g., Fig. 14A), whereas many grains included in pyroxene or plagioclase, or interstitial to those phases, are subhedral to euhedral.

We analyzed a representative number of Cr-spinel grains in each mineral host, as reported in Table 10 and shown in Figure 15. The compositional range observed in our analyses of these grains is remarkable and is the reason that we refer to these grains as Cr-spinel, rather than simply chromite. For 37 analyses, the overall ranges are (in wt%): Cr<sub>2</sub>O<sub>3</sub>, 4.58-38.4; MgO, 1.14-12.2; FeO<sup>T</sup>, 28.6-81.8; TiO<sub>2</sub>, 0.96-12.2; Al<sub>2</sub>O<sub>3</sub>, 3.25-21.4; V<sub>2</sub>O<sub>3</sub>, 0.31-1.93; MnO, 0.31-0.63; NiO, 0.00-0.17; SiO<sub>2</sub>, • 0.03. A stoichiometric spinel program was used to apportion FeO<sup>T</sup> and produce the estimates of FeO and Fe<sub>2</sub>O<sub>3</sub> reported in Table 10 and to allow calculation of Cr# and Mg# for plotting in Figure 15. In sample NP-29-678.2 (Fig. 14B), where there are two distinct Cr-spinel populations in close proximity to one another, the Cr-rich population is composed of the smaller, rounded, slightly darker grains on the left side of the photo. It appears to be typical that the larger, more euhedral grains which are commonly interstitial, contain lesser amounts of Cr (e.g., Table 10, Fig. 14A).

We are not prepared to discuss our preliminary analytical data at length because (1) the compositions of Cr-spinel grains range widely in individual samples (Table 10) and we have too few analyses to constrain this variation and (2) as with olivine, Cr-spinel reequilibrates in mafic rocks (e.g., SCOWEN et al., 1991). Other studies have indicated that Cr-spinels with TiO<sub>2</sub> contents near 1 wt%, Fe<sup>2+</sup>/Fe<sup>3+</sup> approaching 2, and Mg# >40 may approach magmatic compositions. As seen from Table 10, those grains trapped in plagioclase most nearly meet these criteria. Most likely, most of the analysed grains have reequilibrated in the subsolidus; those trapped in olivine have reacted with their host and the interstitial grains may have reacted both with interstitial melts and during late alteration. Extensive study will be required to fully appreciate what

can be learned about the formation of the intrusions from further analyses of the Cr-spinels.

## COMMENTS

Although core from boreholes NP-29 and KZ-1879 (CZAMANSKE et al., 1994) constituted a major part of the material made available to the U.S. Geological Survey in 1990, it was eventually recognized that, while of significant interest, these boreholes do not represent typical sections of the Noril'sk-type intrusions. The upper part of NP-29 contains a thick and complex residual sequence and an anomalously thin unit of picritic gabbrodolerite is present lower in the borehole. Conversely, olivine-bearing gabbrodolerite and the entire residual sequence is missing from borehole KZ-1879, in which the olivine-gabbrodolerite unit is anomalously thick and enriched in olivine, often with MgO contents falling in the range for picritic-like gabbrodolerite. Thus, initial sampling of boreholes KZ-1713 and KZ-1799 through the NE branch of the Talnakh intrusion was substantially augmented when it was realized that they would include a more complete and typical sequence of rock units. Data from these boreholes (Appendixes 1 and 2; Fig. 5 for location) has been used to construct Figures 16 and 17. While it is disturbing that all or parts of some units are missing from each of these two boreholes, vigorous efforts over three years to obtain a more complete rock sequence for these or other boreholes were unsuccessful. Note that the last digits of the sample numbers in Appendixes 1 and 2 represent the depth in the boreholes in meters, as also shown in Figure 17. The distance of each sample from the basal contact of each intrusion is given as the "Height" in Appendixes 1 and 2.

Because overall intrusion thicknesses and the thicknesses of individual rock units are quite variable, lithologic sequences and geochemical profiles for individual boreholes can best be compared on the basis of (1) their basal contacts upward (e.g., CZAMANSKE et al., 1994) or (2) the upper contact of the picritic-gabbrodolerite unit (e.g., Fig. 17). For the picritic gabbrodolerite and overlying rock units, samples from boreholes KZ-1713 and KZ-1799 have entirely comparable textural and geochemical characteristics; apparent differences in the lower parts of the intrusions (e.g., in  $\text{FeO}^T$ , S, Ca, Ni, and Pd) are largely due to the thinner, picritic-gabbrodolerite unit in borehole KZ-1799 and the lack of samples for taxitic gabbrodolerite in borehole KZ-1713. High modal proportions of olivine in picritic gabbrodolerite, Cr-spinel between picritic gabbrodolerite and olivine gabbrodolerite, and plagioclase in olivine gabbrodolerite are evident in the modal and geochemical data of Figures 16 and 17.

Our 25 samples of the olivine-bearing through olivine gabbrodolerite sequence of the three ore-bearing intrusions contain 50-174 ppm Cu, 2-17 ppb Pd and 1-33 ppb Pt, with an overall average Pd/Pt ratio of 0.88 (Table 4). These values are little different from those obtained for eight basalt samples from the Upper Morongovsky ( $\text{Mr}_2$ ) and Mokulaevsky suites of the Noril'sk region (Table 4; WOODEN et al., 1993). Thus, there is no evidence that the upper parts of the

intrusions contributed ore metals to the picritic and underlying units. Steep and rather smooth profiles of the PGE from Ir to Pd in the disseminated ores (Fig. 19; shown also by the relatively high Pd/Pt ratios in these ores) is evidence that PGE were scavenged from mafic silicate melt. High PGE concentrations (Table 4, low Cu/Pd ratios) show that large amounts of this melt were involved (the relative volume of basaltic melt processed during sulfide separation and accumulation is quantified as the R factor; e.g., NALDRETT, 1989; NALDRETT and WILSON, 1990).

Contact gabbrodolerite (e.g., samples KZ-1799-1340 and -1341.9) represents typical basaltic magma that contains 6.9 to 8.0 wt% MgO (Appendix 2). These two rocks have elevated PGE contents and their average Pd/Pt ratio of 2.63 is similar to that for sulfide ores, as can be noted by comparison with the Pd/Pt ratios in picritic gabbrodolerite (Table 4). It is not uncommon for small amounts of sulfide to have been introduced into the basal contact gabbrodolerite after its crystallization, just as such mineralization may be found in basaltic rocks of the exocontact of the Noril'sk I intrusion.

There are some regular changes in the chemical composition of magnetite gabbro in both the composite section for the Talnakh intrusion (Fig. 17) and in borehole NP-29 (CZAMANSKE et al., 1994, their Tables 23.1 and 23.4); SiO<sub>2</sub> content increases and MgO content decreases in the upper parts of each magnetite-gabbro sequence, and there is a significant upward increase in the concentrations of incompatible trace elements (e.g., Ta and La, Fig. 17).

Some general comments can be made about the behavior of incompatible trace elements in the differentiation process, using the Talnakh intrusion and Ta and La as examples. Figure 17 shows that contents of these elements regularly increase from the taxitic gabbrodolerite/picritic gabbrodolerite boundary to the upper part of the magnetite gabbro (with a small anomaly at the base of the magnetite gabbro). TiO<sub>2</sub> follows the incompatible trace elements, except in magnetite gabbro, where massive crystallization of titanomagnetite took place. Th/U, Ta/La, and La/Sm ratios are nearly constant up through the magnetite gabbro; however, these ratios show irregular and decoupled variation in the quartz diorite. This variation, elevated contents of Ta and La, and high Th/U ratios suggest that contamination by host rocks modified the composition of a late-stage, residual liquid, and that the quartz diorite is a hybrid rock type.

Evidence of significant lateral transport of silicate magmas is restricted to the upper parts of the intrusions in the boreholes we have studied; such evidence might be significantly more obscure in picritic gabbrodolerite (where the distribution of disseminated ore is clearly of irregular vertical distribution) or in the heterogeneous taxitic unit. We have noted that all upper units of the residual sequence are absent in KZ-1879 and that the magnetite gabbro is abnormally thick and repeated in section in boreholes NP-29 and KZ-1799 (Figs. 16 and 17). A very thin layer of olivine-bearing-gabbrodolerite layer is present in the upper part of the residual sequence in borehole KZ-1799 (Figs. 16 and 17), and interfingering of the texturally contrasting, prismatic gabbro and olivine-bearing gabbrodolerite units can often be recognized. Considering the various examples

mentioned, and broader views of the variation of lithologic sequence from place-to-place within the Noril'sk-type intrusions (e.g., LIKHACHEV, 1983, 1994, his Fig. 16.3) short-range migration and displacement of silicate magma must have taken place at all stages of intrusion history. Our discussion has indicated that, while generally comparable, the various lithologic units do not have constant proportions within the main bodies of the individual intrusions; Figure 18, based on averaging core logs from 23 boreholes from the intrusions of the Talnakh ore junction, is a tangible indication of this variation. The general presence of a substantial, leucocratic gabbro unit and the thin residual sequence that distinguish the Kharaelakh intrusion from the two branches of the Talnakh intrusion are notable. In terms of proportions of other units, variation in the thickness of the picritic-gabbrodolerite unit is most striking.

Migration of sulfide melt appears to have been common. Cross-cutting relations and emplacement of massive ore sheets beneath the floor of the intrusions is clear evidence that pools of sulfide melt were fluid and mobile, and it is not surprising that URVANTSEV (1971) came to believe that sulfide liquid was brought into the intrusion chambers as a separate, late event. Many mine geologists of the Noril'sk-Talnakh district still believe that these sulfide sheets were emplaced separately from the host intrusion, after consolidation of the silicate magmas (e.g., GENKIN et al., 1981; DUZHIKOV et al., 1992; STEKHIN, 1994).

The data of NALDRETT et al. (1994) and ZIENTEK et al. (1994) show that (1) disseminated ores represent relatively undifferentiated sulfide liquids; (2) massive ores represent strongly differentiated, sulfide accumulations; and (3) Cu-rich, disseminated ores in metamorphosed-host-rock and contact-gabbrodolerite halos around massive orebodies are enriched in Pt and Au with respect to Cu. A plot of relative Cu, Ni, and PGE concentrations shows that there are three distinct compositional groups among the studied, disseminated ores (Fig. 19). The first group includes ores of the Noril'sk ore junction (the Noril'sk I and Noril'sk II intrusions); it is characterized by the highest Ni and PGE contents in 100% sulfide,  $^{206}\text{Pb}/^{204}\text{Pb}$  ratios between 17.660 and 18.082, and  $\gamma\text{Os}$  values that average +5.8 (WALKER et al., 1994). The second group includes ores from the Talnakh intrusion and the northeastern part of the Kharaelakh intrusion (Gluboky mine segment, Fig. 3A); it has intermediate Ni and PGE contents in 100% sulfides,  $^{206}\text{Pb}/^{204}\text{Pb}$  ratios between 18.137 and 18.282, and  $\gamma\text{Os}$  values that average +7.7. The third group is related to the Main Kharaelakh orebody of the western part of the Kharaelakh intrusion (Fig. 3A); it has low Ni and PGE contents,  $^{206}\text{Pb}/^{204}\text{Pb}$  ratios between 18.122 and 18.172, and  $\gamma\text{Os}$  values that average +10.4. The Pb- and Os-isotopic compositions of these three groups require different source regions. Even the differences in Ni, Cu, and PGE concentrations cannot be explained by sulfide fractionation from a common, parental sulfide melt; because the PGE profiles are nearly parallel (Fig. 19), these differences must relate directly to differing R-factors. Evolution of the massive orebodies closely paralleled that of the disseminated ones, because Ni and PGE contents as well as Pb- and Os-isotopic compositions are comparable

for associated, massive and disseminated ores, and similarly distinct for the northeastern and western parts of the Kharaelakh intrusion. In terms of Cu/Ni covariations, the massive ores also correspond to the three groups discussed above (Fig. 20).

Disseminated and massive ores in the Gluboky-mine segment of the Kharaelakh intrusion (as sampled in borehole KZ-1879; Fig. 3A) resemble those of the Talnakh intrusion and are very different in metal concentrations and Pb- and Os-isotopic compositions from those in the western part of the Kharaelakh intrusion. Hundreds of boreholes show the Kharaelakh intrusion to be a single intrusive body, with a continuous lithologic sequence, yet one must conclude that at least the sulfide component of this body was emplaced from two discrete sources. On the basis of sulfide mineralogy, STEKHIN (1994) also recognized differences between the western and northeastern part of the Kharaelakh intrusion and proposed that the former was on the Oktyabr'sky "ore stream" and the latter on the Gluboky "ore stream."

## **MODELS AND DISCUSSION**

Many ideas about the formation of the Noril'sk-type, ore-bearing intrusions have been presented in the Russian literature over the past 60 years of investigation. They include differentiation of a single magma (e.g., KOROVYAKOV et al., 1963; GENKIN et al., 1981; ZEN'KO, 1983); emplacement of several, distinct magmas (LIKHACHEV, 1965; MITENKOV et al., 1977; FEDORENKO, 1994b); lava-conduit models (RAD'KO, 1991; NALDRETT et al., 1995); a recycling model (LIKHACHEV, 1994), and even proposals for a metasomatic origin for the ores (ZOLOTUKHIN et al., 1975) and the intrusions themselves (ZOTOV, 1979). No single idea predominates and even the two Russian co-authors of this paper have quite different ideas.

This report allows the reader the opportunity to consider factual information and to evaluate arguments for the single-magma-input model of TATYANA ZEN'KO and the multiple-magma-injection model of VALERI FEDORENKO. The lava-conduit model of NALDRETT et al. (1995) and the recycling model of LIKHACHEV (1994) are discussed in passing.

At the outset of this discussion, we acknowledge that several of the most puzzling attributes of these intrusions including their "insertion," thick metasomatic haloes, exceptional PGE enrichment in super-abundant sulfide melt, and evidences of lateral transport might be more readily understood if the main bodies of the Noril'sk-type intrusions served as magma conduits to the surface. However, whereas erosion has allowed the supposition that the Noril'sk I and Talnakh intrusions may have breached the surface, the close-spaced drilling that allows detailed contouring of the entire Kharaelakh intrusion (which lies in the deepest stratigraphic position) provides no indication of a major exit conduit. No sills or apophyses to the Noril'sk-type intrusions have ever been found to contain significant amounts of sulfide. Given present, factual knowledge, models for intrusion emplacement that are based on limited input of magma seem most appropriate.

**TATYANA ZEN'KO's model:** Crystallization differentiation of a single magma which contained intratelluric  $Ol_1$ ,  $Pl_1$ , and sulfide droplets can explain the following regularities of lithologic sequence in the main bodies of the intrusions (ZEN'KO, 1983).

(1) Much  $Pl_1$  was frozen to the roof of the intrusion chamber as leucocratic gabbro, because the rate of movement of the upper solidification front within the chamber was more rapid than the rate of settling of  $Pl_1$  phenocrysts.

(2) Enrichment of the lower part of the sequence in intratelluric  $Ol_1$ ,  $Pl_1$ , and sulfide droplets, and the distribution of these phases according to their density and size was controlled by Stokes Law settling. Massive sulfide orebodies at the bottom of the intrusion formed by accumulation of the largest sulfide droplets, after the lower contact gabbrodolerite had hardened. Taxitic gabbrodolerite is enriched in larger sulfide aggregates and large  $Pl_1$  glomerocrysts, and picritic gabbrodolerite in relatively small sulfide droplets and  $Ol_1$ . The distributions in plan of taxitic gabbrodolerite, picritic gabbrodolerite, disseminated ore, and massive orebodies are practically coincident everywhere.

(3) Rocks of the middle part of the sequence (olivine through olivine-bearing gabbrodolerite) contain predominately second-generation minerals. The vertical distribution of these minerals (decreasing olivine and increasing augite contents upward) and the accompanying change in augite morphology from oikocrystic ( $Au^3$ ) to subprismatic ( $Au^2$ ) agrees with the expected order for *in situ* crystallization of magma ( $Pl + Ol$  followed by  $Pl + Ol + Au$ ).

(4) Enrichment of the residual sequence in quartz, micropegmatite, titanomagnetite, and apatite, and the relatively coarse-grain size of the main rock-forming minerals in this sequence reflects crystallization from buoyant, residual magma, enriched in volatiles,  $SiO_2$ , K, Na, Ti, P, and ITE.

(5) Sulfide droplets and  $Ol_1$  are absent from the lower contact gabbrodolerite because suspended phases may be in low abundance along the margins of conduits through which magma has flowed. Thus, the composition of the contact gabbrodolerite approximates that of the liquid fraction of the parental magma, and is characterized by low Mg content.

The Kruglogorsky-type sills (bordering apophyses; ZEN'KO, 1986, 1989) surrounding the main bodies of the intrusions formed from magma enriched in  $Pl_1$  phenocrysts, which had minimum density. A greater proportion of leucogabbro was frozen to the roof of the bordering apophyses because the rate of movement of the upper solidification front in the thinner apophyses (usually 10-50 m thick) was faster than that in the main bodies of the intrusions. Lower parts of these apophyses underwent slight differentiation according to the scheme outlined for the main bodies. Apophyses sometimes contain taxitic and picritic-like gabbrodolerite near the main bodies of the intrusions, but picritic gabbrodolerite and massive sulfide orebodies are not found. The geometry of the zones of transition between the main bodies of the intrusions and the



surrounding apophyses is comparable everywhere and the geochemical and petrographic characteristics of the rocks in the apophyses are similar to those of the comparable lithologic units in the main bodies of the ore-bearing intrusions. The volumes of magma represented by the bordering apophyses are estimated to be twice those found in the main bodies of the Kharaelakh and Talnakh intrusions (ZEN'KO, 1994; ZEN'KO and CZAMANSKE, 1994b). These larger volumes allow better understanding of the exceptionally high contents of sulfide ore and extensive hornfels aureoles associated with the ore-bearing intrusions.

Horizontal displacement of magma during the differentiation process led to the following distinctions in individual sections through the ore-bearing intrusions: absence of some rock units, variation in their thicknesses, and interfingering of rock units. Splitting of the intrusions in section is largely restricted to the ends (or frontal parts) of the intrusions, where they simultaneously rise to higher stratigraphic positions. The relatively high fluidity and lower solidification temperatures of the sulfide-melt fraction in the lower part of the sequence allowed continued movement after much of the intrusion had hardened. Thus, there is almost everywhere a sharp discontinuity at the upper contact of the picritic gabbrodolerite and, along the length of the Talnakh intrusion, a more uniform thickness for picritic, taxitic, and contact gabbrodolerite than for the middle and upper parts of the lithologic sequence (LIKHACHEV, 1994). Enrichment of Cr-spinel and biotite near the mobile zone at the upper contact of the picritic gabbrodolerite may be partly due to concentration of volatiles.

Magmas parental to individual, ore-bearing intrusions contained different amounts of intratelluric  $Ol_1$ ,  $Pl_1$ , and sulfide melt; in addition, the concentrations of these suspended phases changed *in situ*, as bordering apophyses developed. As a result, individual ore-bearing intrusions contain different proportions of massive sulfide ore and of the individual rock units of the lithologic sequence. The major geological regularities of placement and construction of the ore-bearing intrusions are considered to have been influenced by the relative densities of these parental magmas. Because parental magmas of the ore-bearing intrusions were enriched in sulfides in comparison to Lower Talnakh-type and weakly-mineralized intrusions: (1) all ore-bearing intrusions are situated mainly in the central parts of Talnakh and Noril'sk ore junctions; (2) the main bodies of these intrusions, which contain almost all ore, are situated lowest in stratigraphic section; and (3) decreasing total sulfide content in the intrusion succession -- Kharaelakh - Talnakh - Noril'sk I -- caused the intrusions to be emplaced at increasingly higher stratigraphic positions (an overall interval of ~1,100 m).

The parental magmas of the ore-bearing intrusions adapted to decreasing lamination in their host rocks because, in the same succession -- Kharaelakh - Talnakh - Noril'sk I, there are changes in: (1) the shapes of the intrusions in plan (respectively, roughly triangular, elongate, and arcuate), in section (from layer-like to trough-like), and in maximum thickness (respectively 220, 260, and 350 m); (2) the abruptness of change in thickness at the margins of the main bodies of the intrusions (from gradual to very abrupt); (3) the orientation of bordering

apophyses with respect to bedding in the host strata (from conformable to steeply dipping); and (4) the maximum extent of the apophyses (from extensive to limited).

**VALERI FEDORENKO's model:** FEDORENKO (1994a and 1994b) considers the formation of the ore-bearing intrusions as inseparably involved in the evolution of the flood-basalt sequence and relates them to the conclusion of Middle-assemblage volcanism. Activity which immediately preceded, and was related to, formation of the Noril'sk-type, ore-bearing intrusions included eruption of the Tuklonsky to Lower Morongovsky lavas and emplacement of the Lower Talnakh-type intrusions. Magma evolution is suggested to have taken place in an extensive, subhorizontal, crustal chamber that underlay the entire Noril'sk region. Mixing of two different, mantle-derived, magma types, crustal contamination, fractionation, and sulfide precipitation all took place in this chamber. Sulfide saturation and precipitation occurred during generation of the Nd<sub>1</sub> and, probably, Nd<sub>2</sub> lavas, as these basalts are notably depleted in chalcophile elements and PGE (NALDRETT et al., 1992, BRÜGMANN et al., 1993; FEDORENKO, 1994a). Immiscible sulfide droplets sank through the chamber and interacted extensively with Lower Talnakh-type magma located in the lower part of the chamber, causing strong depletion in PGE without sulfur depletion in this magma. This interaction also allowed Pb-isotopic equilibration between the Lower-Talnakh magma type and the Noril'sk-type, sulfide ores (WOODEN et al., 1992; CZAMANSKE et al., 1994). When the Lower Talnakh-type intrusions were emplaced, remnants of the Lower-Talnakh magma type, containing sulfide disseminations, remained in the chamber, along with pools of sulfide liquid that lay on the chamber floor. The isotopic and geochemical compositions of these pools differed slightly, owing to the complexity of their formation within the extensive chamber. The chamber then received a new influx of mantle-derived magma, and its mixing with residual Lower Talnakh-type magma gave rise to the magmas which formed the ore-bearing intrusions. After differentiation of this mixture, basaltic liquid lay above picrite-like magma that contained phenocrysts of olivine and plagioclase, as well as sparse disseminations of sulfide droplets. Further differentiation in the lower part of the chamber led to formation of leucogabbroic (enriched in plagioclase) and picritic (enriched in olivine) magmas.

The first event recorded in the near-surface was withdrawal of basaltic magma from the upper part of the intermediate magmatic chamber to form dolerite sills (the Makusovsky subtype of the Noril'sk-type intrusions). In some intrusive systems of the Noril'sk area, no further activity took place, e.g., in the Mikchanda River area to the SE of the Kharaelakh depression. However, in the majority of the known intrusive systems a second event took place shortly after the first -- leucogabbroic magma entered the still-liquid, dolerite sills. Thus, the Kruglogorsky-subtype, leucogabbro sills were formed.

The leucogabbro sills solidified before formation of the main bodies of the ore-bearing intrusions, and for a time, there were no near-surface expressions of the intrusive system. Meanwhile, the intermediate magmatic chamber, was

being replenished with a new portion of fresh, mantle-derived magma similar to the Mr<sub>2</sub> geochemical type of the lava sequence. A new layer of basaltic liquid developed at the top of the chamber. Picrite-like magma, accumulating in the lower part of the chamber, contained olivine, plagioclase, and small sulfide droplets, while sulfide liquid pooled lowermost in the chamber.

The third event in formation of the ore-bearing intrusions was a second episode of basaltic-magma emplacement, which caused inflation of the elongate areas that became the main bodies of the intrusions and produced numerous lenses and short sills of dolerite around the main bodies. The composition of the magma (7-8 wt% MgO) is thought to be represented by the basal, contact gabbrodolerite of the intrusions; if this is true, the magma was comparable to magmas represented by the Mr<sub>2</sub> and Mk basalts, except in K<sub>2</sub>O content. This magma was commonly emplaced just below the leucogabbro sills, as seen in the Kharaelakh and Noril'sk I intrusions. Hardened leucogabbro fragments occasionally fell into this underlying magma and are now found in the olivine-bearing- and olivine-gabbrodolerite units of the intrusions. Rarely, part of the main body developed above a leucogabbro sill, as seen by the fact that the Gabbrovy intrusion (Kruglogorsky subtype; a bordering apophysis according to ZEN'KO, 1989 and ZEN'KO and CZAMANSKE, 1994b) extends to the east (and slightly to the west) from the keel of the northern part of the Talnakh intrusion. The third and following events did not occur in all intrusive systems, e.g., only leucogabbroic sills are found in the Arylakh-Mastakhsala system to the NE of the Kharaelakh depression. Formation of intrusions of the Dvugorbinsky subtype concluded with this second episode of basaltic-magma emplacement.

The fourth event was emplacement, into the main bodies of the intrusions, of picrite-like magma carrying small, disseminated sulfide droplets; this occurred when the basaltic magma within the intrusion chambers was still liquid and only 1-2 m of contact gabbrodolerite had crystallized against the basal contact. The picrite-like magma fountained into the basaltic magma and sometimes reached and intruded the leucogabbroic roof of the chamber (IVANOV et al., 1971). Because picrite-like magma mixed with basaltic magma in turbulent fountains, this mixture was able to differentiate and form the regular sequence in the main bodies of the intrusions, from picrite gabbrodolerite, through gabbrodolerites containing decreasing amounts of olivine, to the upper residual sequence. Contact gabbrodolerite that had solidified against the floor was not affected by this influx. Taxitic gabbrodolerite developed as dense phases of the picritic magma settled into solidifying, basaltic magma that lay above the lower contact gabbrodolerite. This fourth event terminated development of the majority of the Noril'sk-type intrusions that are weakly mineralized and are designated as the Chernogorsky subtype; Noril'sk II, Chernogorka, Tangaralakh, Imangda, and several other intrusions belong to this subtype.

Development of the intrusions carrying economic mineralization continued with the fifth and sixth events, each of which essentially involved inputs of sulfide melt. Event five took place when the upper part of the intrusions (from olivine gabbrodolerite through the residual sequence) was still liquid, and picritic and

taxitic gabbrodolerite were partially solidified. Turbulent fountains of sulfide liquid were injected into the silicate magma and dispersed to form relatively large globules (up to 3 cm) and small droplets. Being of great density, they fell quickly to the upper boundary of the dense picritic magma and then slowly descended into the picritic and taxitic units, giving rise to economic, disseminated mineralization. This explains both (1) the basaltic Pd/Pt ratios and lack of PGE depletion that are typical for olivine-bearing and olivine gabbrodolerite (Table 4) and (2) the presence of small, trapped droplets of immiscible sulfide that cause some samples to have elevated Pd and Pt concentrations (Fig. 17) and Pd/Pt ratios (DISTLER and KUNILOV, eds., 1994; their Fig. 13). It is also an explanation for the coincidence between the mutual upper boundaries of economic ore and picritic gabbrodolerite -- there was a dramatic decrease in the rate of settling of the sulfide droplets as they encountered dense, picritic magma. Probably, several sequences of sulfide-liquid fountaining took place, as suggested by the irregular distribution of ore grades in vertical profiles through the picritic- and taxitic-gabbrodolerite units.

The final, sixth event took place after solidification of the silicate intrusions with their disseminated ores. Massive orebodies formed when sulfide magma pools were emplaced into the lowermost units of the ore-bearing intrusions and underlying metasedimentary rocks.

The successive injections of different silicate and sulfide magmas are considered to have used the same feeder dikes, which were located just beneath the main bodies of the intrusions along virtually their entire lengths. Several dikes may have fed some complex intrusions, e.g., the Kharaelakh intrusion. In this intrusion, there is no detectable difference in the composition of the silicate magmas, but sulfide compositions in the west and northeast branches of the Kharaelakh intrusion are distinct, and may represent separate accumulation pools in the intermediate chamber.

Formation of the main bodies of intrusions was dependent on the third through sixth events. The necessity of each of these events can be judged on the basis of the typical lithologic section, as represented by Figs. 6 and 17. Olivine (and Mg) were concentrated in picritic gabbrodolerite, Cr-spinel (and Cr) at the picritic-olivine-gabbrodolerite boundary, plagioclase (and Al) in olivine gabbrodolerite, clinopyroxene (and Ca) in the lower part of the olivine-bearing gabbrodolerite unit, and Ti and incompatible trace elements in the residual sequence. The lower part of the picritic layer commonly contains plagioclase glomerocrysts (several to 15 modal%) and may contain large (2-3 cm) resorbed crystals of intratelluric plagioclase (Fig. 12A). This regularity is consistent with Stoke's Law differentiation of a magma that contained intratelluric plagioclase, olivine, and Cr-spinel -- large plagioclase phenocrysts settled to near the bottom of the intrusion chamber, smaller olivine grains accumulated higher in the chamber, and tiny grains of Cr-spinel did not settle far. Crystal differentiation then took place, accompanied by crystallization of second-generation olivine and plagioclase, and then clinopyroxene, leading to evolution of residual liquid. This conspicuous regularity led GODLEVSKY (1959), KOROVYAKOV et al. (1963), and

ZEN'KO (1983) to conclude that differentiation of a single magma took place in the intrusion chambers. However, they supposed a single input of magma. Such a model can not explain: (1) the composition of contact gabbrodolerite and the absence of  $Ol_1$  and  $Pl_1$  in this quenched unit; (2) the relatively low MgO contents of contact gabbrodolerite and the lower part of the taxitic layer; and (3) the relatively low Cr content of the lower part of the picritic layer.

Two magma types -- basaltic and picritic -- seem essential to intrusion construction. One could assume that the picritic magma did not mix with the basaltic magma, but simply spread and differentiated itself, giving rise to the picritic layer and participating in development of the lower taxitic gabbrodolerite. Such an assumption explains the concentration of large plagioclase crystals in taxitic gabbrodolerite and the lower part of the picritic layer. However, it cannot explain the relatively low Cr concentrations (~500 ppm) often found in the middle-to-lower parts of the picritic layer, which compare with Cr concentrations in many samples of olivine and olivine-bearing gabbrodolerite and are higher than those (100-200 ppm) in basaltic magma (Fig. 17; Appendixes 1 and 2). Only separate intrusions of basaltic and picritic magmas into an intrusion chamber, followed by mixing and differentiation of this mixture, seems capable of explaining the regularities of the intrusion section and the observed exceptions to these regularities.

A significant question concerns whether the picritic magma carried a substantial amount of sulfide, or was relatively sulfide-free. Of course, it contained some disseminated sulfide, because every analyzed sample of picritic gabbrodolerite has elevated PGE concentrations and "ore-type" Pd/Pt ratios, even if the sulfide component is not visible. However, it seems unlikely that the total sulfide component of economic, disseminated ores, was brought into the chambers in picritic magma. As seen from Figure 17, there has been almost perfect differentiation of the basaltic/picritic mixture for the silicate-rock sequence. The picritic layer itself is differentiated, with large plagioclase grains concentrated in the lower part and Cr-spinel in the upper part. Similar concentration of the sulfide component did not take place. The upper boundary of economic, disseminated ores usually coincides with the upper boundary of picritic gabbrodolerite and large sulfide droplets are often present near this boundary. Sulfide fountaining into silicate magma provides one mechanism to explain the observed relations. This explanation may not be readily accepted and will be willingly abandoned in favor of a more satisfactory explanation for: (1) the fact that basaltic PGE concentrations and Pd/Pt ratios are characteristic of most olivine-bearing- and olivine-gabbrodolerite samples, but "ore-type" Pd/Pt ratios are found in some samples with elevated PGE concentrations (Table 4); (2) the coincidence of the upper boundaries of picritic gabbrodolerite and economic, disseminated ores (Fig. 17); and (3) the globule texture of much of the sulfide in the picritic, disseminated ores.

**CZAMANSKE's perspective:** The senior author finds FEDORENKO's arguments for sequential input of leucogabbroic, basaltic, and picritic magmas to most adequately address the formation of the intrusions as a whole, and of the

leucocratic gabbro and contact gabbrodolerite in particular. However, the idea of first fountaining picritic magma and then sulfide liquid into the intrusion chambers is not attractive. On the one hand, it may be questioned whether Stokes Law settling can account for the general absence of small, rounded grains of  $Ol_1$  and interstitial sulfide from rocks immediately overlying picritic gabbrodolerite. And, on the other hand, it is not easy to envision how the momentum could be acquired to cause fountaining of these two dense magmas into basaltic liquid. If the intrusions developed from a single input of silicate magma, or by thorough mixing *in situ* of basaltic, picritic, and sulfide magmas, one might have expected to find a more gradational transition in rock texture and composition, modal mineralogy, olivine morphology, and ore-metal content than is typical (e.g., Fig. 17; compare Figs. 9B, 9C, 9D, and 10A with Figs. 10B, 10C and 10D). ZEN'KO's argument that late movement is in some way responsible for the observed, sharp transition at the upper contact of the picritic gabbrodolerite seems inadequate, because this transition is comparable everywhere; i.e., the picritic gabbrodolerite magma is required to have moved everywhere, making it essentially a separate intrusive event. With the ore-metal contents of basalt and comparable overall composition, the olivine through olivine-bearing gabbrodolerite sequence seems to represent a semi-independent layer of differentiated magma (e.g., Table 3; Fig. 17). Upward percolation of interstitial melt from the consolidating picritic layer, fractionation within the olivine through olivine-bearing gabbrodolerite unit as a whole, and possible settling of olivine might all have contributed to the somewhat higher MgO contents of olivine gabbrodolerite, compared to olivine-bearing gabbrodolerite.

The distribution of Cr in the lower part of the ore-bearing intrusions is not that to be expected from fractional crystallization of a single magma input or with Cr-spinel having been carried in with picritic magma; rather, it is consistent with the fact that Cr-spinel grains are rarely present in  $Ol_1$ . As seen in Figure 17 and Appendixes 1 and 2, Cr concentration increases downward to the base of the olivine gabbrodolerite unit, and may reach 2750 ppm in rocks containing <16 wt% MgO. It may or may not increase further (to > 4500 ppm) in the uppermost, analyzed picritic rocks several meters below, which contain >25 wt% MgO. Within 5 m below this contact, Cr contents begin to fall quickly; in the lower parts of the picritic-gabbrodolerite unit and in the taxitic unit, Cr contents may be less than they are in the middle of the olivine-gabbrodolerite unit. This Cr-distribution pattern may represent settling of Cr-spinel from a largely liquid layer that slightly differentiated *in situ* and solidified as the olivine gabbrodolerite through olivine-bearing gabbrodolerite sequence. Cr-spinel appears to have been trapped (conceivably redissolved and redistributed?) in the upper few meters of the hot, picritic-gabbrodolerite unit, rich in intratelluric olivine. The observed Cr-distribution pattern also does not appear compatible with the intrusions having been built as conduits for eruption of lavas (e.g., NALDRETT et al., 1995).

Lifting of essentially pure sulfide melt has been argued as being credible (e.g., CZAMANSKE et al., 1992; NALDRETT et al., 1992) and is still considered a possibility, if extrusive pressures were generated by movement of irregular fault

surfaces in an appropriate stress system or, perhaps, by collapse of an intermediate staging chamber. As cited by CZAMANSKE et al. (1992), magnetite flows of comparable density have been erupted. However, it seems possible that both the massive and disseminated ores were lifted as an immiscible sulfide component with the crystal-rich, picritic magmas. FEDORENKO's model can be simplified if virtually all of the sulfide associated with the ore-bearing intrusions had been turbulently mixed with, and entrained in, the picritic magmas during their evacuation from the intermediate chamber and transport to the subvolcanic, ore-bearing chambers. As magma flow changed from subvertical to subhorizontal, the largest masses and droplets of immiscible-sulfide melt could be expected to quickly settle out, to form accumulations near the feeders to the main bodies of the intrusions. The picritic magmas would have contained a greater proportion of silicate melt than they did when they came to rest within the intrusions, and during flowage along the length of the intrusion many of the next larger droplets might be expected to reach the base of the picritic layer. Centimeter-size droplets remained suspended during flow of this dense, olivine-laden magma. Ore grades in picritic gabbrodolerite are highly variable, and the general absence of systematic, downward increase in the concentration of disseminated ore in this unit seems difficult to reconcile with a model of gravitational settling through the whole body of the intrusion, but quite compatible with subhorizontal flowage of sulfide-bearing magma.

Sulfide textures in typical magmatic-sulfide ore deposits involve sulfide-mineral aggregates that were trapped interstitially to silicate minerals, consistent with the lower solidus temperature of sulfide liquid. In such deposits, there is an increase in the proportion of sulfide towards the lower contact of the intrusion, often culminating in massive ore; such relations are consistent with gravitational setting (Stoke's Law) of dense sulfide liquid. Globular textures that represent solidified droplets of Fe,Cu,Ni-sulfide liquid are uncommon in magmatic-sulfide ores, and reminiscent of the small immiscible sulfide globules in quenched ocean-ridge basalt (e.g., CZAMANSKE and MOORE, 1977). The consistent, vertical segregation of *iss* over *mss* in the globules, which is characteristic of picritic gabbrodolerite in the ore-bearing intrusions, shows that they were liquid when they came to rest, yet the molten sulfide was unable to percolate downward. Remarkable conditions were required to prevent settling of dense sulfide-melt droplets as large as 2 cm, while generally preserving their globular shapes and only modestly wetting silicate grains at their margins.

Taxitic gabbrodolerite is a very complex rock type, containing fine-grained xenoliths and areas of micro-pegmatoid, with some signatures of a magmatic breccia. It is envisioned to have formed as sulfide-bearing, picritic magma ripped up and mixed with partly solidified, basaltic magma that lay above solidified, contact gabbrodolerite. The proposal that the taxitic unit may represent an inner-contact zone or magmatic breccia is not new (e.g., MITENKOV et al., 1977). The substantial amount of sulfide now found in taxitic rocks could have been derived both from sulfide liquid that was dropped near the feeder zones and carried along at the base of flowing, picritic magma, and from the

continued settling of sulfide melt from this magma. Further evidence against simple differentiation and settling from well-mixed magmas is the fact that gradations of increasingly-rich, disseminated (globule or xenomorphic) ore into massive ore are not found.

Two additional observations seem most compatible with the sulfide liquid having been introduced with picritic magma that generally underwent little mixing, except to form taxitic gabbrodolerite: (1) NALDRETT et al. (1994) and ZIENTEK et al. (1994) showed that the compositions of disseminated ores are closest to those assumed for primitive sulfide liquid. Compositions of both massive ores and disseminated, exocontact ores show variable and progressive evidence of fractionation. (2) Consideration of the elongate NE branch of the Talnakh intrusion (Fig. 5) as a series of 100-m segments shows that along its length, the mass of sulfide-free differentiates (olivine gabbrodolerite through quartz diorite) fluctuates more than the mass of picritic, taxitic, and contact gabbrodolerite (LIKHACHEV, 1994; LIKHACHEV and JAMNOVA, in prep.). LIKHACHEV and JAMNOVA have calculated that the ubiquitous, disseminated ores in these units contain roughly 10% more sulfide than is contained in the massive ores at the base of the intrusion (in the Kharaelakh intrusion, massive ore contains a much greater proportion of the sulfide).

## DISCUSSION

Although it is commonly said that massive sulfide concentrations are greatest near the frontal parts of the intrusions, this is debatable and, if true, the question remains as to how this might have occurred. Many have thought that the sulfide was pushed to the ends (frontal parts) of the intrusions by advancing magma. LIKHACHEV (1994) and LIKHACHEV and JAMNOVA (in prep.) proposed that magmas flowed the entire length of the intrusion chambers, dropping their load of suspended sulfide-melt droplets where the cross-sectional areas of the main bodies changed and in the frontal areas, before cycling back to, and down, the feeder zones.

There is no reason not to consider the possibility that much sulfide liquid accumulated down slope from feeder zones, but there is no good evidence available to us as to which directions those might have been. The Valyok saddle, which separates the Noril'sk and Talnakh ore junctions (Fig. 1), is a later structure. However, the extensive drilling provides clear evidence of pre-Tunguskaya folding within the ore junctions, and small folds and anticlines in the Talnakh ore junction appear to have influenced intrusion morphology. One tight anticline has long been known to extend for many kilometers, sub-parallel to the Noril'sk-Kharaelakh fault zone as currently mapped (e.g., ZEN'KO and CZAMANSKE, 1994b).

Many had thought that the Kharaelakh intrusion was emplaced from a northern feeder zone, but GENKIN et al. (1981; see ZEN'KO and CZAMANSKE, 1994a) proposed that it had a centrally-located feeder zone. Sulfide geochemistry and Pb- and Os-isotopic data appear to require that it had at least two feeders. The possibility that the NE and SW branches of the Talnakh



intrusion were predominantly fed from multiple, feeders located near the Noril'sk-Kharaelakh fault has been widely proposed (e.g., STEKHIN, 1994). NALDRETT et al. (1995) challenged conventional concepts of flow direction for the ore-bearing intrusions of both districts on the basis of a northward decrease in the concentrations of Pt, Pd, Rh, and Au in the sulfides of the NE branch of the Talnakh intrusion, and because it suited them to propose (and conveniently destroy) an extremely high-level, processing chamber between the two ore junctions.

That sulfide melts continued to be extremely mobile and commonly migrated downward is evident from their general occurrence near the base of the thickest parts of the concave-downward intrusions, often in footwall hornfels, several meters below the intrusions. The present authors have no information which rules out the possibility that the Main Kharaelakh ore body (Fig. 3A; STEKHIN, 1994; TORGASHIN, 1994) is so enormous because it was downslope from the feeder system. Accumulations of sulfide melt could have been pushed ahead of advancing picritic magma and we certainly do not disallow this possibility; however, gravity also may have been a significant cause of motion and Stekhin's "ore streams" may have been real paths of downward flow. Occasional occurrences of picritic rocks and Cu-rich, exocontact mineralization near the upper contacts of the ore-bearing intrusions seem best explained by relatively rare complications during construction of the intrusions. Picritic magma may have encountered and penetrated into solidified leucogabbro or upper contact gabbrodolerite along the roof, in areas that had not yet been fully inflated (IVANOV et al., 1971).

Relatively "complete" sulfide pools, such as the Main Kharaelakh ore body, mimic on a vast scale the immiscible sulfide droplets that were trapped in picritic gabbrodolerite, i.e., they contain a very Cu-rich upper zone (e.g., CZAMANSKE et al., 1992; TORGASHIN, 1994). Knowledge of other massive ore bodies of the Talnakh and Kharaelakh intrusions suggests that occasionally a still liquid, Cu-rich pool was displaced from a mss-rich, cumulate pile to form an unusually Cu-rich orebody and leave behind a Cu-poor orebody (e.g., STEKHIN, 1994). Massive ore in borehole KZ-1713 (ZIENTEK et al., 1994) and most other massive ores in the NE branch of the Talnakh intrusion show enrichment in mss, but Cu-rich ores are not known (e.g., Fig. 19). Clear evidence that sulfide melt was mobilized along faults is seen in the cross-cutting veins that are relatively common in the intrusions. Copper-rich breccia ores near the upper contact of an intrusion probably resulted from tapping the upper part of a differentiated, sulfide melt pool near the base of the intrusion.

Two facts not well explained by any proposal are the inordinate masses of hornfels associated with the ore-bearing intrusions and the isotopically-heavy sulfur contained in the ores ( $\delta^{34}\text{S}$  of +9 to +12‰). TUROVTSEV (1973, 1986, personal communication, 1995) has reported that the combined thickness (above and beneath the intrusion) of these alteration halos varies from 150-250 m and that the mass of hornfels above the intrusions is 2 to 4 times that found

beneath them. The haloes consist of 20-60% hornfels and 40-80% metasomatites; rocks of the pyroxene-hornfels, hornblende-hornfels, and muscovite-hornfels facies are represented, with average proportions of 5:4:1. Temperatures of pyroxene-hornfels formation are estimated at 700-1050°C; rocks in the spurrite-merwinite subfacies (900-1050°C) of the pyroxene-hornfels facies extend from a few, to 10-15 m from intrusion contacts. Metasomatites formed mainly after hornfels and replaced them near the intrusions.

Curiously, thick halos not only accompany thick, ore-bearing intrusions, but sometimes thin, weakly-mineralized, Noril'sk-type intrusions. The best example is the Tomulakh intrusion, located NE of the W end of the Kharaelakh intrusion; its thickness is 6-35 m. The intrusion is composed predominately of olivine to olivine-bearing gabbrodolerite, with rare picritic-like rocks and very minor disseminated sulfide. According to TUROVTSEV (1986, personal communication, 1995), the contact halo of this intrusion may reach 400 to 450 m in thickness. About 80% are metasomatites, but 40 to 65-m-thick packets of pyroxene-hornfels-facies, brucite marble are present in the halo, indicating that temperatures reached 700°C about 200 m above the intrusion. Extremely high enrichment of Noril'sk-type magma with fluids is emphasized by many investigators (e.g., ZOLOTUKHIN et al., 1975), and TUROVTSEV (1986, personal communication, 1995) has concluded that formation of such thick, contact halos is impossible in terms of a conductive model of heat transfer, but required fluids as the main carriers of heat.

TUROVTSEV has compiled comparative data concerning the haloes of associated metasomatized and metamorphosed sedimentary rocks for several intrusion types. For the four intrusion types (Fig. 2) -- Noril'sk (N), Lower Talnakh (LT), Kruglogorsky (K), and Daldykansky (D; post-volcanic, undifferentiated trap sills) -- the ratios of halo thickness to intrusion thickness are: N, 1.5-2.5; LT, 0.5-1.5; K, 0.4-0.6; and D, 0.2-0.5. Ratios of halo thickness above/below the intrusions are: N, 2-4; LT, 1.2-2; K, 1.1-1.3; and D, 1.2-1.5. Ratios for the thickness of pyroxene-, amphibole-, and muscovite-facies hornfels average: N, 5:4:1; LT, 1:6:3; K, 1:5:4; and D, 1:5:4. These data show little distinction between the contact haloes associated with the Kruglogorsky and Daldykansky sill types. Clearly a combination of factors caused the Noril'sk-type, ore-bearing intrusions to alter a proportionately far greater volume of material at higher average temperatures.

Because it is difficult to understand how volumes of hornfels could be created that have twice the mass of the intrusions themselves, it is appealing to propose that the main bodies of the intrusions, as limited by the distribution of picritic gabbrodolerite and abrupt thinning of the intrusions, did not account for the entire hornfels halo. ZEN'KO (1994) and ZEN'KO and CZAMANSKE (1994b) calculated that the total volume of magma represented by the main bodies and bordering apophyses of the Kharaelakh and Talnakh intrusions is about three times the volume found in the main bodies. However, it is indeterminate as to how much of the material contained in these apophyses can be considered to have passed through the main bodies of the intrusions, as LIKHACHEV (1965)

and FEDORENKO argue that they represent sills that formed before the main bodies took shape. As noted earlier, the enigma of the extensive hornfels halos is mitigated by the proposal of LIKHACHEV (1994) and LIKHACHEV and JAMNOVA (in prep.) that over a long period, magmas dropped immiscible sulfide as they flowed the length of the intrusion and then circulated back to and down the feeder channel.

It would be convenient if some intrusions could be shown to have served as conduits for large amounts of mafic magma. As well as ample quantities of mafic magma from which to extract PGE, the proposals of RAD'KO (1991) and NALDRETT et al. (1995), that the main bodies of the intrusions served as conduits to feed surface lava flows, also provide for a long-lasting heat source. However, the intrusion types that are certainly comagmatic with some lava units (e.g., the Ergalasky intrusions and Ivakinsky lavas, Fig. 2) have very weak contact haloes, and the combined geochemical and isotopic signatures for the important intrusion types that are associated with thick metasomatic haloes -- the Noril'sk and Lower Talnakh types -- do not correlate well with the signatures for any of the lava suites (e.g., WOODEN et al., 1993).

It is conceivable that the unprecedented volumes of associated hornfels may be partly the result of a unique combination of factors: (1) a generally elevated thermal regime as a consequence of emplacement during major, flood-basalt volcanism, including emplacement of numerous sub-volcanic sills and the Lower Talnakh-type intrusions only slightly earlier, and commonly only a few tens of meters below positions soon to be occupied by the ore-bearing intrusions (ZEN'KO, 1989; ZEN'KO and CZAMANSKE 1994a, 1994b); (2) a long history of formation of the main bodies of the intrusions, perhaps including as many as six inputs of new silicate and sulfide magma; (3) emplacement of mafic magmas rich in fluids, as evidenced by the common occurrence of biotite in relative abundance in picritic and olivine gabbrodolerite, extensive alteration to amphibole in the residual sequence, and high proportions of vesicular and tuffaceous basalt in the associated flood-basalt sequence; (4) emplacement of the intrusions into relatively hydrous, and/or reactive sedimentary strata; (5) possible passage through the intrusion chambers of several times the volume of magma represented in the main bodies of the intrusions (now represented by the sill-like apophyses to the main bodies); and (6) the presence of unprecedented proportions of sulfide liquid in the intrusions, estimated as 0.2 to 7 wt% of their total mass.

NALDRETT et al. (1994, 1995) took the extensive hornfels aureoles as support for their lava-conduit model, yet LIKHACHEV and JAMNOVA (in prep.) note that none of the apophyses to the ore-bearing intrusions are bordered by the expected, thick hornfels selvages; i.e., there is no indication that truly vast amounts of magma exited the intrusion chambers. The model of NALDRETT et al. (1995) is little different from that proposed by RAD'KO (1991), except that their model is more quantitative and calls upon a separate, high-level chamber in which a sulfide-melt phase formed and accumulated prior to formation of the ore-bearing intrusions. Their model is predicated on initially extracting metals from

the magmas that were erupted to form the Early and Middle Nadezhdinsky (Nd<sub>1</sub> and Nd<sub>2</sub>) basalts, as first proposed by NALDRETT et al. (1992) in a model that proposed processing of the basaltic magmas in a deeper, crustal chamber. The initial processing chamber proposed by NALDRETT et al. (1995) was at a very high crustal level, near the stratigraphic level of the ore-bearing intrusions themselves. They interpreted the main bodies of the ore-bearing intrusions as representing the principal exit conduits from this chamber, with the implication that sulfide melt was initially carried to the main bodies of the intrusions and then enriched by scavenging Cu, Ni, and PGE from large volumes of basaltic melt that were enroute to the surface.

It is most difficult to imagine that the depletion in chalcophile elements and PGE that so uniformly characterize the Nadezhdinsky basalts can be directly ascribed to processing in a single chamber at the stratigraphic level of the ore-bearing intrusions. These basalts are widespread and show remarkably little variation in composition; they commonly have a combined thickness of 150 to 500 m over much of the Noril'sk region (~45,000 km<sup>2</sup>) and a calculated volume of ~14,000 km<sup>3</sup> (FEDORENKO, 1981). In contrast, within the same area, the estimated total volume represented by the differentiated and weakly-differentiated intrusions of the Noril'sk, Lower Talnakh, and Ruiny types is only about 100 km<sup>3</sup>. A much larger and deeper chamber, with an extensive feeder system seems essential for delivery of the amount of magma represented by the metal-depleted, Nadezhdinsky basalts. The model of NALDRETT et al. (1995) does not address the details and complexities of intrusion stratigraphy that form the basis of this report. In particular, it is difficult to envision how the globular textures in picritic ore would have formed or been preserved during the proposed *in situ* enrichment process, or why maximum Cr concentrations should be found at the upper contact of the picritic-gabbrodolerite unit.

The isotopically-heavy sulfur in the ores is perplexing, yet seems to be characteristic of most ore-bearing and weakly-mineralized intrusions throughout the entire region (e.g., L. N. GRINENKO, unpublished data; R. R. SEAL, II, unpublished data). Explanations range from incorporation of sulfur from host rocks in a high-level chamber (e.g., NALDRETT et al., 1995) or interaction with sour gas (GRINENKO, 1984), to a variety of deeper settings in which a magma-processing chamber accessed marine evaporites. If one believes that the source of the ore metals was the processing of Nadezhdinsky magma, it can be argued that the isotopically-heavy sulfur that characterizes the ores was caused by contamination in a crustal reservoir, as suggested by other isotopic characteristics of the Nadezhdinsky lavas (e.g., WOODEN et al., 1993). An alternative is that the mantle beneath Noril'sk was the source of highly unusual, but not unique, isotopically-heavy sulfur (e.g., see discussion in WOODEN et al., 1992).

At this point in time, it seems important to retain an open-minded attitude and to continue to seek critical information. In our opinion, no current proposal satisfactorily addresses all enigmas of these remarkable intrusions. With the

exception of the Kharaelakh intrusion, which is uneroded, defined by hundreds of boreholes, and ultimately splits in vertical section and rises to higher stratigraphic levels along its flank and frontal parts, there seems to be little certainty about how many ends of intrusions actually represent frontal parts, or in which direction magmas flowed. Similarly, there is no definitive evidence regarding the placement or number of feeders for each intrusion. Although geochemical and isotopic compositions of sulfide ores require distinct feeders for the west and northeast branches of the Kharaelakh intrusion, a central, vertical feeder was proposed for this intrusion by GENKIN (1981) and again by ZEN'KO (1987) on the basis of the distribution of mss- and iss-rich massive sulfides and normative compositions of olivine and plagioclase in the picritic gabbrodolerite. FEDORENKO's proposal for dike-like, vertical feeders beneath the ore-bearing intrusions, with relatively little lateral movement of magma, is somewhat different and must be evaluated against the more prevalent view that most of the magma was emplaced from the flexure zone that preceded breakage along the Noril'sk-Kharaelakh fault (e.g., STEKHIN, 1994, his Fig. 18.9).

### **FACTUAL CONSTRAINTS**

The primary intent of this paper has been to present a factual basis for broader understanding and contemplation of the physical attributes, petrography, and geochemistry of the Noril'sk-type, ore-bearing intrusions. In addition, a variety of genetic models for the development of these intrusions have been presented. In a future report, we will attempt to develop a comprehensive petrologic model for evolution of the intrusions and ores on the basis of our extensive accumulation of geochemical and Sr-, Pb-, Nd-, and Os-isotopic data. Until such time, it seems appropriate to let the reader draw his own conclusions as to how the ore-bearing intrusions formed and to review here only the the most significant factual constraints for such deliberations.

Any worthy new model for the formation of the ore-bearing intrusions must account for (1) their relation to the Siberian flood-basalt sequence and associated, weakly-mineralized and unmineralized intrusions; (2) the specific sequence of events involved in their construction; and (3) their numerous, currently enigmatic aspects. On the basis of this and earlier investigations, the factual constraints for such a model must include the following:

(1). On the whole, Noril'sk-type intrusions are geochemically quite similar to the Upper Morongovsky and Mokulaevsky basalts, but they contain somewhat more Mg, Cr, and K, and slightly more radiogenic Sr (WOODEN et al., 1993; CZAMANSKE et al., 1994; LIGHTFOOT et al., 1994).

(2). The magmatic system was extensive and complex, and clearly capable of delivering diverse magmas to a single locality. The two, coeval intrusion types that characterize the two ore junctions -- the Noril'sk, ore-bearing type and the Lower Talnakh type-- differ markedly in chemical and isotopic compositions.

(3). The main body of each intrusion is situated in the lowest stratigraphic position occupied by that intrusion, and contains the disseminated and massive

ore and the picritic rocks. At the margins of the main bodies, the intrusions consistently rise to higher stratigraphic position, decrease sharply in thickness, and usually split in section or in plan at the ends. The main bodies of the intrusions may be flanked by one or two, weakly-mineralized, weakly-differentiated sills (the Kruglogorsky type). Exploration drilling has shown that short sills and lenses of dolerite also may be well developed around the ore-bearing intrusions.

(4). The main bodies of the differentiated, Noril'sk- and Lower Talnakh-type intrusions appear to largely occupy space formerly occupied by host strata. This relation is quite dissimilar to that seen for trap sills, which appear to have spread apart the host-rock sequence. Isotopic and trace-element data give no evidence of significant *in situ* contamination of these intrusions, except for the quartz diorite unit and some parts of the leucogabbro and taxitic units from near the upper and lower contacts of the ore-bearing intrusions. The Lower Talnakh-type intrusions were formed by magmas that were contaminated at depth.

(5). The Noril'sk-type, ore-bearing intrusions and some thin, weakly-mineralized intrusions have abnormally thick halos of high-temperature, contact metamorphic and metasomatic rocks, including pyroxene hornfels.

(6). The three ore-bearing intrusions are composed of rocks of entirely comparable petrographic and geochemical characteristics, and a generalized sequence of rock units and geochemical regularities can be established. The distributions in plan of picritic gabbrodolerite, taxitic gabbrodolerite, and disseminated ore are practically coincident everywhere; if massive orebodies are present, they underlie parts of the intrusions in which picritic or taxitic gabbrodolerite is present.

(7). Variation among the lithological sections within individual intrusions may have been caused by lateral movement of stratified magma. However, there is significant variation between intrusions in the thickness of important units, suggesting that the intrusions may have somewhat different average compositions, whether from input of single magmas of more or less evolved composition or from inputs of differing proportions of distinct magma compositions.

(8). Trace-element compositions, isotopic compositions, distributions of mineral phases, and mineral chemistry through the lithologic sequence show that if the intrusions were formed by multiple injection of magma, these magmas were very closely related.

(9). The upper contact of the ore-bearing, picritic gabbrodolerite unit is the most definitive contact in the lithologic sequence. Above this relatively sharp contact (i) MgO content commonly drops by more than 15 wt%; (ii) Ni, Cu, and PGE contents commonly drop to those typical of the flood basalts; and (iii) virtually no fine-grained, intratelluric olivine is present.

(10). There are many other relations within the intrusions that suggest a complex evolutionary history -- low-MgO content in the lower, contact

gabbrodolerite; extensive development of taxitic gabbrodolerite; leucogabbro fragments in olivine gabbrodolerite; maximum Cr contents near the upper contact of picritic gabbrodolerite; plagioclase glomerocrysts in picritic gabbrodolerite; etc.

(11). There is evidence of lateral displacement and interfingering among the upper units of the intrusions, particularly of magnetite gabbro and prismatic gabbro with olivine-bearing gabbrodolerite. Small lenses of prismatic gabbro are common in olivine-bearing gabbrodolerite.

(12). Chromium distribution may be one of the keys to understanding the processes involved in formation of the intrusions. Maximum Cr concentrations are found near the upper contact of the picritic gabbrodolerite unit, and decrease quickly down through that unit and toward the base of the intrusion. Most Cr-spinel grains are hosted in plagioclase or pyroxene, rather than olivine. The upper, residual sequence is extremely depleted in Cr.

(13). Sulfide-free rocks of the ore-bearing intrusions are not depleted in Cu, Ni, and PGE in comparison with geochemically-related, Upper Morongovsky and Mokulaevsky basalts.

(14). Olivine in the ore-bearing intrusions is not Ni depleted, yet high PGE concentrations and Pd/Pt ratios in the disseminated and massive ores reflect PGE scavenging from large amounts of mafic magma.

(15). Although the silicate portions of all Noril'sk-type intrusions are geochemically comparable, three geochemical types of ores have been identified which are not related to one another through fractionation; they apparently represent discrete sources at depth. The Kharaelakh intrusion, a single body in terms of lithology and silicate geochemistry, contains geochemically and isotopically dissimilar sulfide ores in its west and northeast branches.

(16). The upper boundary of economic, disseminated ore coincides closely with the upper boundary of picritic gabbrodolerite, and picritic and taxitic gabbrodolerite almost universally contain disseminated ore. The textures of the disseminated ores are highly unusual, 0.5-2 cm globules are prominent in picritic gabbrodolerite and 3-4 cm xenomorphic aggregates (that may represent large sulfide-melt droplets) in taxitic gabbrodolerite. Commonly, concentrations of disseminated sulfide are greatest in the middle of the taxitic unit and decrease irregularly toward the lower, contact gabbrodolerite, which contains sulfide only when it has been introduced at a late stage.

(17). The massive sulfide orebodies that occur in close proximity to disseminated ores in the intrusions always have similar geochemical and isotopic characteristics. However, there is no evidence of massive ore accumulation from disseminated ores, and massive ores are always fractionated in comparison with unfractionated, disseminated ores. Geologic relations show that sulfide melt was commonly mobile, and often emplaced as a late, intrusive phase into the lower exocontact, the lower units of the ore-bearing intrusions, and, occasionally, as veins reaching the roof of the intrusion.

## ACKNOWLEDGEMENTS

The support of Igor Migachev, Director of TsNIGRI, Vladimir Kunilov, Chief Geologist of the Noril'sk State Nickel Concern, Victor Lul'ko of the Noril'sk Expedition, and Ivan Sidorov and Oleg Simonov of the Taymyrian Geological Committee is deeply appreciated. Michael Zientek provided extensive critical and incisive commentary that substantially improved our presentation. Shunso Ishihara invited the senior author to participate in the Symposium in Sapporo and to contribute to this volume. Susan Garcia is responsible for the clear presentation of all tables and construction of several figures by computer graphics. Lowell Kohnitz gave splendid assistance with the photomicrographs.

## REFERENCES

- ATKINS, F. B. (1969): Pyroxenes of the Bushveld Intrusion, South Africa. *Jour. Petrol.*, **10**, 2, 222-249.
- BARNES, S. J. (1986): The effect of trapped liquid crystallization on cumulus mineral compositions in layered intrusions. *Contrib. Mineral. Petrol.*, **93**, 524-531.
- BRÜGMANN, G. E., NALDRETT, A. J., ASHE, M., LIGHTFOOT, P. C., GORBACHEV, N. S. and FEDORENKO, V. A. (1993): Siderophile and chalcophile metals as tracers of the evolution of the Siberian Trap in the Noril'sk region, Russia. *Geochim. Cosmochim. Acta.*, **57**, 2001-2018.
- CAMPBELL, I. H., CZAMANSKE, G. K., FEDORENKO, V. A., HILL, R. I. and STEPANOV, V. (1992): Synchronism of the Siberian Traps and the Permian-Triassic boundary. *Science*, **258**, 1760-1763.
- CHALOKWU, C. I. and GRANT, N. K. (1987): Reequilibration of olivine with trapped liquid in the Duluth complex, Minnesota. *Geology*, **15**, 71-74.
- CZAMANSKE, G. K. and MOORE, J. G. (1977): Composition and phase chemistry of sulfide globules in basalt from the Mid-Atlantic Ridge rift valley near 37°N lat. *Geol. Soc. Am. Bull.*, **88**, 587-599.
- CZAMANSKE, G. K., KUNILOV, V. E., ZIENTEK, M. L., CABRI, L. C., LIKHACHEV, A. P., CALK, L. C. and OSCARSON, R. L. (1992): A proton-microprobe study of magmatic sulfide ores from the Noril'sk-Talnakh district, Siberia. *Can. Mineral.*, **30**, 249-287.
- CZAMANSKE, G. K., WOODEN, J. L., ZIENTEK, M. L., FEDORENKO, V. A., ZEN'KO, T. E., KING, Bi-S. W., KNIGHT, R. J. and SIEMS, D. F. (1994): Geochemical, Pb, and Sr-isotopic constraints on the petrogenesis of the Noril'sk-Talnakh ore-forming system. *In Proceedings of the Sudbury-Noril'sk Symposium* (P. C. LIGHTFOOT and A. J. NALDRETT, eds.). Ontario Geol. Surv. Spec. Vol. 5, 313-342.



- DALRYMPLE, B. G., CZAMANSKE, G. K., FEDORENKO, V. A., SIMONOV, O. N., LANPHERE, M. A. and LIKHACHEV, A. P. (1995): A reconnaissance  $^{40}\text{Ar}/^{39}\text{Ar}$  geochronological study of ore-bearing and related rocks, Siberian Russia. *Geochim. Cosmochim. Acta.*, **59**, 2071-2083.
- DISTLER, V. V. (1994): Platinum mineralization of the Noril'sk deposits. *In* Proceedings of the Sudbury-Noril'sk Symposium (P. C. LIGHTFOOT and A. J. NALDRETT, eds.). Ontario Geol. Surv. Spec. Vol. 5, 171-183.
- DISTLER, V. V. and KUNILOV, V. E., eds. (1994): Geology and Ore Deposits of the Noril'sk Region. VII International Platinum Symposium Guidebook, Moscow, 67 p.
- DUZHIKOV, O. A., DISTLER, V. V., STRUNIN, B. M., MKRTYCHYAN, A. K., SHERMAN, M. L., SLUZHENIKIN, S. S. and LURYE, A. M. (1992): Geology and Metallogeny of Sulfide Deposits, Noril'sk Region, U.S.S.R. *Soc. of Econ. Geol. Spec. Publ.* 1, 242 p.
- EVANS, B. W. and FROST, B. R. (1975): Chrome-spinel in progressive metamorphism--a preliminary analysis. *Geochim. Cosmochim. Acta.*, **39**, 959-972.
- FEDORENKO, V. A. (1981): Petrochemical series of extrusive rocks of the Noril'sk region. *Soviet Geol. Geophys.*, **22**(6), 66-74.
- FEDORENKO, V. A. (1991): Tectonic control of magmatism and regularities of Ni-bearing localities on the northwestern Siberian platform. *Soviet Geol. Geophys.* **32**(1), 41-47.
- FEDORENKO, V. A. (1994a): Evolution of magmatism as reflected in the volcanic sequence of the Noril'sk region. *In* Proceedings of the Sudbury-Noril'sk Symposium (P. C. LIGHTFOOT and A. J. NALDRETT, eds.). Ontario Geol. Surv. Spec. Vol. 5, 171-183.
- FEDORENKO, V. A. (1994b): Model of genetic relationships between flood basalts, ore-bearing intrusions, and Cu-Ni-Pt ores in the Noril'sk region, NW Siberian platform, Russia. VII International Platinum Symposium, Moscow, Abstr., p. 26.
- FEDORENKO, V. A., STIFEEVA, G. T., MAKEEVA, L. V., SUKHAREVA, M. S. and KUZNETSOVA, N. P. (1984): Mafic and alkali-mafic intrusions of the Noril'sk region; their co-magmatic relation to the volcanic formations. *Soviet Geol. Geophys.*, **25**(6), 54-61.
- GAETANI, G. A., GROVE, T. L. and BRYAN, W. B. (1993): The influence of water on the petrogenesis of subduction-related igneous rocks. *Nature*, **365**, 332-334.
- GENKIN, A. D., DISTLER, V. V., GLADYSHEV, G. D., FILIMONOVA, A. A., EVSTIGNEEVA, T. L., KOVALENKOR, V. A., LAPUTINA, I. P., SMIRNOV, A. V. and GROKHOVSKAYA, T. L. (1981): Sulfide Copper-Nickel Ores of the Noril'sk Deposits. Nauka, Moscow, 234 p. (in Russian).

- GENKIN, A. D., DISTLER, V. V., LAPUTINA, J. P. (1979): Chromitic mineralization of differentiations intrusions and conditions of its formation. *In* Conditions of formation of magmatic occurrences, Nayka, Moscow, 105-126 p.
- GODLEVSKY, M. N. (1959): Traps and Ore-bearing Intrusions of the Noril'sk Region. Gosgeoltekhizdat, Moscow, 68 p. (in Russian).
- GRINENKO, L. N. (1984) Hydrogen sulfide-containing gas deposits as a source of sulfur for sulfurization of magma in ore-bearing intrusions of the Noril'sk area. *Internat. Geol. Rev.* **27**, 290-292).
- HAWKESWORTH, C. J., LIGHTFOOT, P. C., FEDORENKO, V. A., BLAKE, S., NALDRETT, A. J., DOHERTY, W. and GORBACHEV, N. S. (1995): Magma differentiation and mineralization in the Siberian continental flood basalts. *Lithos*, **34**, 61-88.
- HELZ, R. T. (1987): Differentiation behavior of Kilauea Iki lava lake, Kilauea Volcano, Hawaii: An overview of past and current work. *In* Magmatic Processes: Physicochemical Principles (B. O. MYSEN, ed.) *Geochem. Soc. Spec. Pub.* **1**, 241-258.
- HORAN, M. F., WALKER, R. J., CZAMANSKE, G. K., and FEDORENKO, V. A. (in press): Os and Nd isotopic constraints on the temporal and spatial evolution of flood basalt sources, Siberia. *Geochim. Cosmochim. Acta*.
- HUEBNER, J. S. (1980): Pyroxene phase equilibria at low pressure. *In* Reviews in Mineralogy (C. T. Prewitt, ed.). *Mineral. Soc. Am. Reviews in Mineral.*, Vol.7, Chap. 5, 213-288.
- IRVINE, T. N. and FINDLAY, T. C. (1972): Alpine-type peridotite with particular reference to the Bay of Islands Igneous Complex. *Publ. Earth Physics Branch, Dept. Energy, Mines and Resources, Ottawa, Canada*, **42**(3), 97-128.
- IVANKIN, P. F., LUL'KO, V. A. and REMPEL, G. G. (1971): Morphogenetic peculiarities of the Noril'sk region ore junctions. *Doklady AN SSSR* **199**(3), 674-676 (in Russian).
- IVANOV, M. K., IVANOVA, T. K., TARASOV, A. V. and SHATKOV, V. A. (1971): Petrology and ore mineralization peculiarities of differentiated intrusions of the Noril'sk ore junction (Noril'sk I, Noril'sk II and Chernaya Mountain deposits). *In* Petrology and Ore Mineralization of the Talnakh and Noril'sk Differentiated Intrusions. *Trudy NIIGA, Nedra, Leningrad*, **167**, 197-305 (in Russian).
- KAMO, S. L., CZAMANSKE, G. K. and KROGH, T. E. (in prep.) The minimum U-Pb age for Siberian flood-basalt volcanism (and the Permian-Triassic boundary?) is 251 Ma.

- KOROVYAKOV, I. A., NELYUBIN, A. E., RAYKOVA, Z. A. and KHORTOVA, L. K. (1963): Origin of the Sulfide Copper-Nickel Ore-Bearing Noril'sk Trap Intrusions. *Trudy VSEGEI, novaya seriya, vypusk 9*. Gosgeoltekhizdat, Leningrad, 102 p. (in Russian).
- KUNILOV, V. Ye. (1994): Geology of the Noril'sk region: The history of the discovery, exploration, and mining of the Noril'sk deposits. *In Proceedings of the Sudbury-Noril'sk Symposium* (P. C. LIGHTFOOT and A. J. NALDRETT, eds.). Ontario Geol. Surv. Spec. Vol. 5, 203-216.
- LIGHTFOOT, P. C., NALDRETT, A. J., GORBACHEV, N. S., DOHERTY, W. and FEDORENKO, V. A. (1990): Geochemistry of the Siberian trap of the Noril'sk area, USSR, with implications for the relative contributions of crust and mantle to flood basalt magmatism. *Contrib. Mineral. Petrol.*, **104**, 631-644.
- LIGHTFOOT, P. C., HAWKESWORTH, C. J., HERGT, J., NALDRETT, A. J., GORBACHEV, N. S., FEDORENKO, V. A. and DOHERTY, W. (1993): Remobilization of the continental lithosphere by a mantle plume: Major-, trace-element, and Sr-, Nd- and Pb-isotopic evidence from picritic and tholeiitic lavas of the Noril'sk District, Siberia. *Contrib. Mineral. Petrol.*, **114**, 171-188.
- LIGHTFOOT, P. C., HAWKESWORTH, C. J., HERGT, J., NALDRETT, A. J., GORBACHEV, N. S., FEDORENKO, V. A. and DOHERTY, W. (1994): Chemostratigraphy of Siberian trap lavas, Noril'sk District, Russia: Implications for the evolution of flood basalt magmas. *In Proceedings of the Sudbury-Noril'sk Symposium* (P. C. LIGHTFOOT and A. J. NALDRETT, eds.). Ontario Geol. Surv. Spec. Vol. 5, 283-312.
- LIKHACHEV, A. P. (1965): The role of leucocratic gabbro in the formation of Noril'sk differentiated intrusions. *Izv. Akad. Nauk SSSR Geol. Series 10*, 75-88 (in Russian).
- LIKHACHEV, A. P. (1983): Geology and classification of copper-nickel deposits. *West. All-Union Mineral. Soc. Issue 1*, 14-27 (in Russian).
- LIKHACHEV, A. P. (1994): Ore-bearing intrusions of the Noril'sk region. *In Proceedings of the Sudbury-Noril'sk Symposium* (P. C. LIGHTFOOT and A. J. NALDRETT, eds.). Ontario Geol. Surv. Spec. Vol. 5, 185-201.
- LIKHACHEV, A. P. and JAMNOVA, V. V. (in prep.): The peculiarities and causes of distribution of PGE and other ore components in the Talnakh ore-bearing intrusion. Prepared for the proceedings of the 7th International Platinum Symposium, Moscow, 1994.
- LIND, E. N. and ANDREEVA, L. P. (1983): Methodical recommendations for using complex physical characteristics for division of trap magmatic rocks: SNIIGGiMS Press, Novosibirsk, 48 p. (in Russian).

- LIND, E. N., KROPOTOV, S. V., CZAMANSKE, G. K., GROMMÉ, S. C. and FEDORENKO, V. A. (in press): Paleomagnetism of the continental flood basalts of the Noril'sk region: A constraint on eruption duration. *Internat. Geol. Rev.*
- MACKENZIE, W. S., DONALDSON, C. H. and GUILFORD, C. (1982): *Atlas of Igneous Rocks and Their Textures*. John Wiley, New York, 148 p.
- MASLOV, G. D. (1963) Igarka-Noril'sk region tectonic and ore-bearing structures. *In Siberian Tectonics, Vol. 2*. Nauka, Novosibirsk, 336-350. (In Russian)
- MITENKOV, G. A., KHINEYKO, A. L. and SHISHKIN, N. N. (1977): Structure of the taxitic layer of the Talnakh ore-bearing intrusion and its genetic significance. *Doklady Earth Sciences Section* **237**, 170-173.
- NALDRETT, A. J. (1989): *Magmatic Sulfide Deposits*. Oxford University Press, New York, 186 p.
- NALDRETT, A. J. and WILSON, A. H. (1990): Horizontal and vertical variation in the noble metal distribution in the Great Dyke of Zimbabwe: A model for the origin of the PGE mineralization by fractional segregation of sulfide. *Chem. Geol.*, **88**, 279-300.
- NALDRETT, A. J., LIGHTFOOT, P. C., FEDORENKO, V., DOHERTY, W. and GORBACHEV, N. S. (1992): Geology and geochemistry of intrusions and flood basalts of the Noril'sk region, USSR, with implications for the origin of the Ni-Cu ores. *Econ. Geol.*, **87**, 975-1004.
- NALDRETT, A. J., ASIF, M., GORBACHEV, N. S., KUNILOV, V. E., STEKHIN, A. I., FEDORENKO, V. A. and LIGHTFOOT, P. C. (1994): The composition of the Ni-Cu ores of the Oktyabr'sky deposit, Noril'sk region. *In Proceedings of the Sudbury-Noril'sk Symposium* (P. C. LIGHTFOOT and A. J. NALDRETT, eds.). Ontario Geol. Surv. Spec. Vol. 5, 357-371.
- NALDRETT, A. J., FEDORENKO, V. A., LIGHTFOOT, P. C., KUNILOV, V. E., GORBACHEV, N. S., DOHERTY, W. and JOHAN, Z. (1995): Ni-Cu-PGE deposits of the Noril'sk region, Siberia: Their formation in conduits for flood basalt volcanism. *Trans. Inst. Mining and Metall.*, London, **104**, B18-B36.
- RAD'KO, V. A. (1991): Model of dynamic differentiation of intrusive traps in the northwestern Siberian platform. *Soviet Geol. and Geophys.*, **32**(11), 15-20.
- RYABOV, V. V. (1991): Problem of nickel source of sulfide deposits on the Siberian platform. *Soviet Geol. and Geophys.*, **32**(7), 70-77.
- RYABOV, V.V. (1992): Olivines of the Siberian Traps as Indices of Petrogenesis and Ore Formation. Nauka, Novosibirsk, 117 p. (in Russian).
- RYABOV, V. V. and ZOLOTUKHIN, V. V. (1977): *Minerals of Differentiated Traps*. Nauka, Novosibirsk, 392 p. (in Russian).

- SCOWEN, P. A. H., ROEDER, P. L. and HELZ, R. T. (1991): Reequilibration of chromite within Kilauea Iki lava lake, Hawaii. *Contrib. Mineral. Petrol.*, **107**, 8-20.
- SLUZHENIKIN, S. F., DISTLER, V. V., DUZHIKOV, O. A., KRAVTSOV, V. F., KUNILOV, V. E., LAPUTINA, I. P. and TUROVTSEV, D. M. (1994): Sulfide-poor platinum mineralization in the Noril'sk differentiated intrusions. *Geologiya rudnykh mestorozhdeniy* **36**(3), 195-217 (in Russian).
- STEKHIN, A. I. (1994): Mineralogical and geochemical characteristics of the Cu-Ni ores of the Oktyabr'sky and Talnakh deposits. *In Proceedings of the Sudbury-Noril'sk Symposium* (P. C. LIGHTFOOT and A. J. NALDRETT, eds.). Ontario Geol. Surv. Spec. Vol. 5, 217-230.
- STRECKEISEN, A. L. (1973): Plutonic rocks: Classification and nomenclature recommended by the IUGS Subcommittee on the Systematics of Igneous Rocks. *Geotimes*, October, 26-30.
- THOMPSON, J. F. H. and NALDRETT, A. J. (1982): Sulphide-silicate reactions as a guide to Ni-Cu-Co mineralization in central Maine, U.S.A. *In Sulphide Deposits in Mafic and Ultramafic Rocks* (D. L. BUCHANAN and M. J. JONES, eds.). Inst. Mining and Metall. (London), 103-113.
- TORGASHIN, A. S. (1994): Mineralogical and geochemical characteristics of the Cu-Ni ores of the Oktyabr'sky and Talnakh deposits. *In Proceedings of the Sudbury-Noril'sk Symposium* (P. C. LIGHTFOOT and A. J. NALDRETT, eds.). Ontario Geol. Surv. Spec. Vol. 5, 132-241.
- TUROVTSEV, D. M. (1973): Morphology of contact halos of the differentiated trap intrusions of the Talnakh ore junction. *Transactions of TsNIGRI*, Issue 108, 35-37 (in Russian).
- TUROVTSEV, D. M. (1986): Types of contact metamorphic halos of the sulfide-free and ore-bearing intrusions of the Noril'sk region, with implications for criteria of nickel-bearing magmatic complexes. *Transactions of TsNIGRI*, Issue 209, 28-33 (in Russian).
- URVANTSEV, N. N. (1971): Genetic characteristics of copper-nickel deposits of the Noril'sk region as criteria for predicting massive ores of this type within the Yeniseisky nickel-bearing province. *In Geology and Deposits of the Noril'sk Region Materials II*, Noril'sk Geological Conference, Noril'sk, 234-238 (in Russian).
- WAGER, L. R. and BROWN, G. M. (1967): *Layered Igneous Rocks*. W. H. Freeman, San Francisco, 588 p.
- WALKER, R. J., MORGAN, J. W., HORAN, M. F., CZAMANSKE, G. K., KROGSTAD, E. J., FEDORENKO, V. A. and KUNILOV, V. E. (1994): Re-Os-isotopic evidence for an enriched-mantle source for the Noril'sk-type, ore-bearing intrusions, Siberia. *Geochim. Cosmochim. Acta.*, **58**, 4179-4197.

- WOODEN, J. L., CZAMANSKE, G. K., BOUSE, R. M., KNIGHT, R. J. and BUDAHN, J. R. (1992): Pb isotopic data indicate a complex, mantle origin for the Noril'sk-Talnakh ores, Siberia. *Econ. Geol.*, **87**, 1153-1165.
- WOODEN, J. L., CZAMANSKE, G. K., FEDORENKO, V. A., ARNDT, N. T., CHAUVEL, C., BOUSE, R. M., KING, Bi-S. W., KNIGHT, R. J. and SIEMS, D. F. (1993): Isotopic and trace-element characterization of the Siberian continental flood basalts of the Noril'sk area. *Geochim. Cosmochim. Acta.*, **57**, 3677-3704.
- ZEN'KO, T. E. (1983): Mechanism of formation of the Noril'sk ore-bearing intrusions. *Izv. Akad. Nauk SSSR Geol. Series 11*, 21-39 (in Russian).
- ZEN'KO, T. E. (1986): Regularities of localization and construction of intrusions of the western part of the Talnakh region. *Transactions of TsNIGRI, Issue 209*, 21-28 (in Russian).
- ZEN'KO, T. E. (1987): About the supposed zone of injection of the Talnakh ore-bearing intrusions. *Izv. Acad. Nauk SSSR Geol. Series 7*, 130-134 (in Russian).
- ZEN'KO, T. E. (1989): Zonation and peculiarities of construction of intrusions of the Talnakh region. *Transactions of TsNIGRI, Issue 230*, 15-32 (in Russian).
- ZEN'KO, T. E. (1992): Regularities in localization and structure of intrusions of the Noril'sk commercial copper-nickel ore fields. *Russian Geol. Geophys.*, **33**(12), 44-52.
- ZEN'KO, T. E. (1994): Quantitative genetic-geological models of Noril'sk-type ore fields and deposits. *Rudy i metally, No. 3-5*, 57-72 (in Russian).
- ZEN'KO, T. E. and CZAMANSKE, G. K. (1994a): Spatial and petrologic aspects of the intrusions of the Noril'sk-Talnakh ore junctions, Siberia. *In Proceedings of the Sudbury-Noril'sk Symposium (P. C. LIGHTFOOT and A. J. NALDRETT, eds.)*. Ontario Geol. Surv. Spec. Vol. 5, 263-282.
- ZEN'KO, T. E. and CZAMANSKE, G. K. (1994b): Tectonic controls on ore-bearing intrusions of the Talnakh ore junction: Position, morphology, and ore distribution. *Internat. Geol. Rev.*, v. 36, p. 1033-1057.
- ZIENTEK, M. L., LIKHACHEV, A. P., KUNILOV, V. E., BARNES, S.-J., MEIER, A. L., CARLSON, R. R., BRIGGS, P. H., FRIES, T. L. and ADRIAN, B. M. (1994): Cumulus processes and the composition of magmatic ore deposits: Examples from the Talnakh district, Russia. *In Proceedings of the Sudbury-Noril'sk Symposium (P. C. LIGHTFOOT and A. J. NALDRETT, eds.)*. Ontario Geol. Surv. Spec. Vol. 5, 373-392.
- ZOLOTUKHIN, V. V. (1982): On the process of magma differentiation in certain intrusives of the Noril'sk type. *Soviet Geol. Geophys.*, **23**(6), 54-63.
- ZOLOTUKHIN, V. V., RYABOV, V. V., VASIL'EV, Yu. R. and SHATKOV, V. A. (1975): Petrology of the Talnakh Ore-bearing Differentiated Trap Intrusions. *Nauka, Novosibirsk*, 432 p. (in Russian).

ZOTOV, I. A. (1979): Genesis of Trap Intrusions and Metamorphic Formations of Talnakh. Nauka, Moscow, 155 p.

## FIGURES



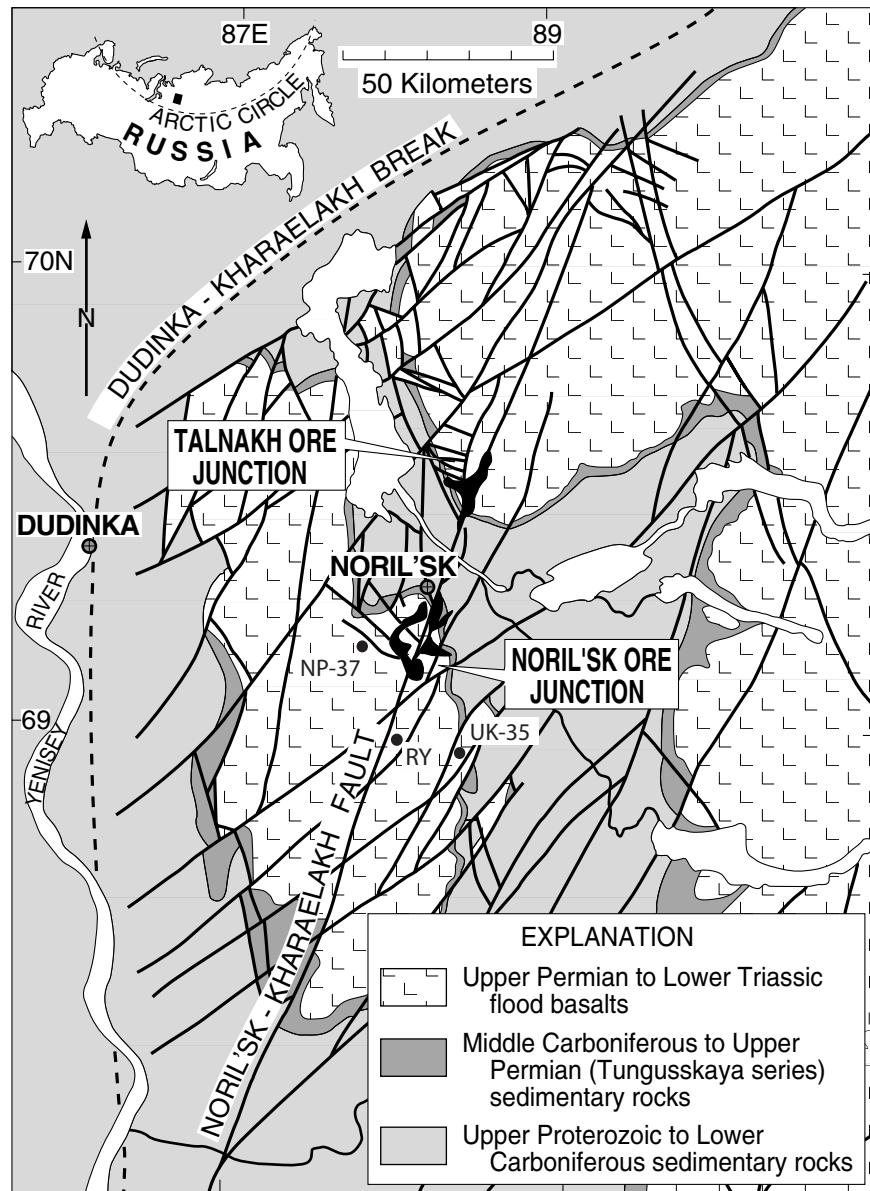


Fig. 1. Simplified geologic map of the Noril'sk-Talnakh district, showing major structural features and subsurface outlines of the Noril'sk-type, ore-bearing intrusions (black, true scale). The Kharaelakh and Noril'sk depressions are the ovoid areas, astride the Noril'sk-Kharaelakh fault and defined by the outcrop areas of basalt, which extend, respectively, north from the Talnakh ore junction and south from the Noril'sk ore junction.

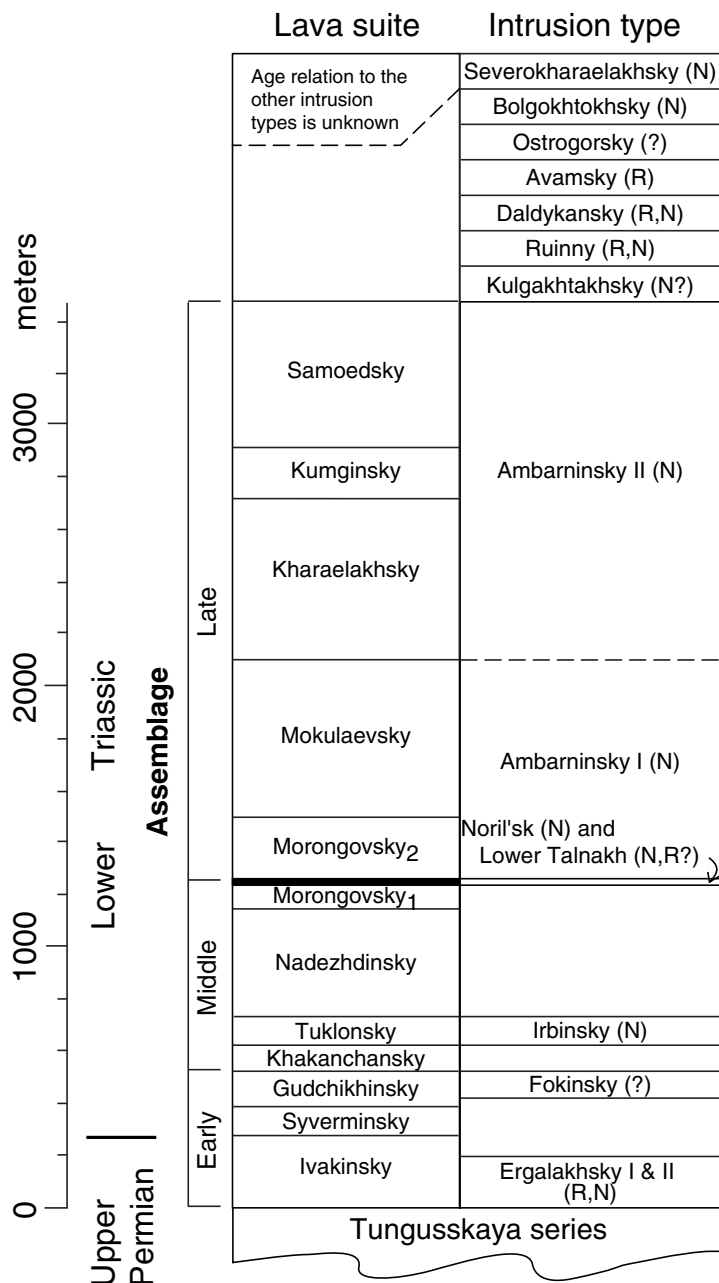


Fig. 2. Correlation chart relating the flood-basalt stratigraphy of the Noril'sk region (with division into the Early, Middle, and Late assemblages) to the intrusion types; thickness proportions approximately correct for the volcanic rocks. Emplacement of the Noril'sk-type, ore-bearing and the Lower Talnakh-type, weakly-mineralized intrusions may be correlative with the thick tuff unit (black band) in the Morongovsky suite. Age relations between basalt suites and intrusion types of the Noril'sk region are based on cross-cutting geologic relations, geochemical data, and preliminary paleomagnetic and magnetic signatures of the intrusion types. With the exception of the Ivakinsky suite (and possibly the uppermost flows of the Samoedsky suite) all suites of the flood-basalt sequence near Noril'sk have normal polarity (LIND et al., in press). Magnetic-polarities presented for the intrusions are based on laboratory measurements (LIND and ANDREEVA, 1983) and aeromagnetic maps.

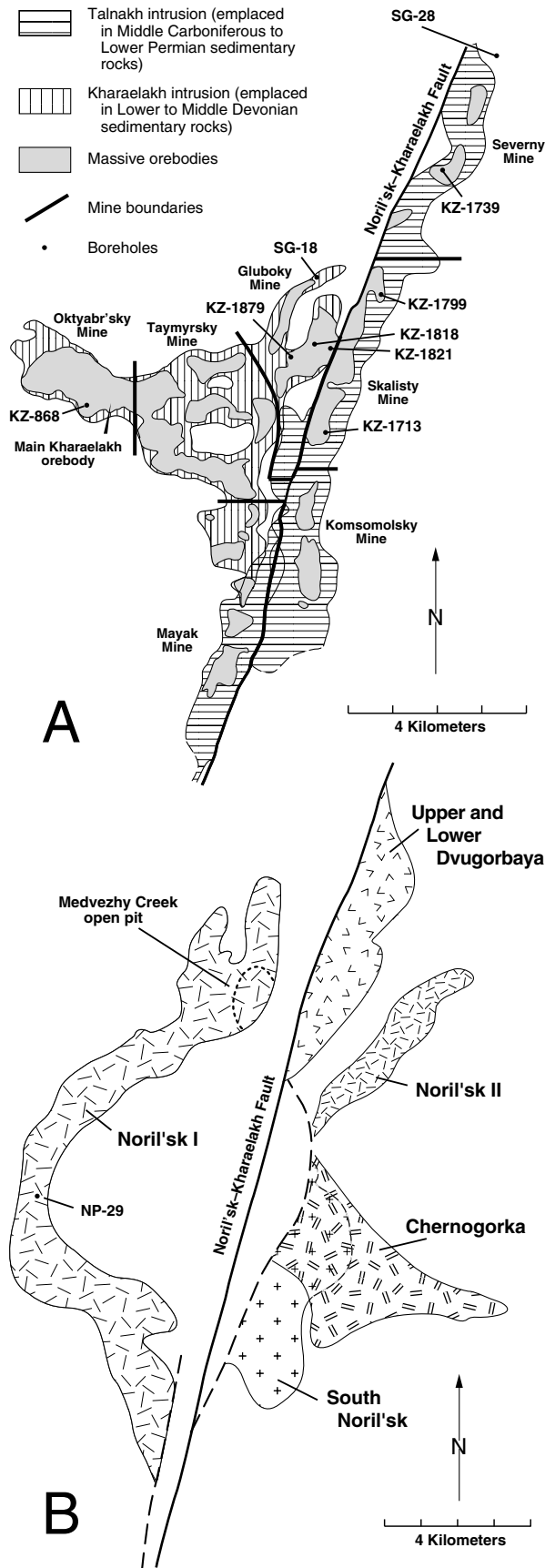


Fig. 3. Sketch maps showing subsurface outlines of the main bodies of the Noril'sk-type, ore-bearing and weakly-mineralized intrusions of the Talnakh (A) and Noril'sk (B) ore junctions. Outlines of massive orebodies, located at or just beneath the lower contacts of the intrusions, are shown for the intrusions of the Talnakh ore junction (flat-lying veins of massive sulfide that lay in the north end of the Noril'sk I intrusion have been mined out). The ore junctions are separated by ~20 km along the Noril'sk-Kharaelakh fault (Fig. 1). Boreholes referenced in the text are marked, as is the Main Kharaelakh orebody. Intrusions distinguished by pattern and name. Note that the outer margins of the main bodies of the intrusions of the Talnakh ore junction have been drawn where there is coincidence of thinning of the picritic gabbrodolerite and a sharp decrease in the thickness of the intrusion, usually to 30-50 m. Because picritic gabbrodolerite is well represented only in the Noril'sk I intrusion of the Noril'sk ore junction, intrusion boundaries for that ore junction have been drawn at the 50-m contour. Also note that the outlines of massive orebodies shown in Figure 3A are draw at zero thickness and are different in detail from other accurate outlines which show these bodies to be less extensive, based on a cutoff at 1-m thickness and mining criteria for Ni content (e.g., ZEN'KO and CZAMANSKE, 1994, their Fig. 21.2). The Upper and Lower Dvugorbaya intrusions essentially overlie one another and were emplaced, respectively, in the flood-basalt sequence and Lower Devonian sedimentary rocks.

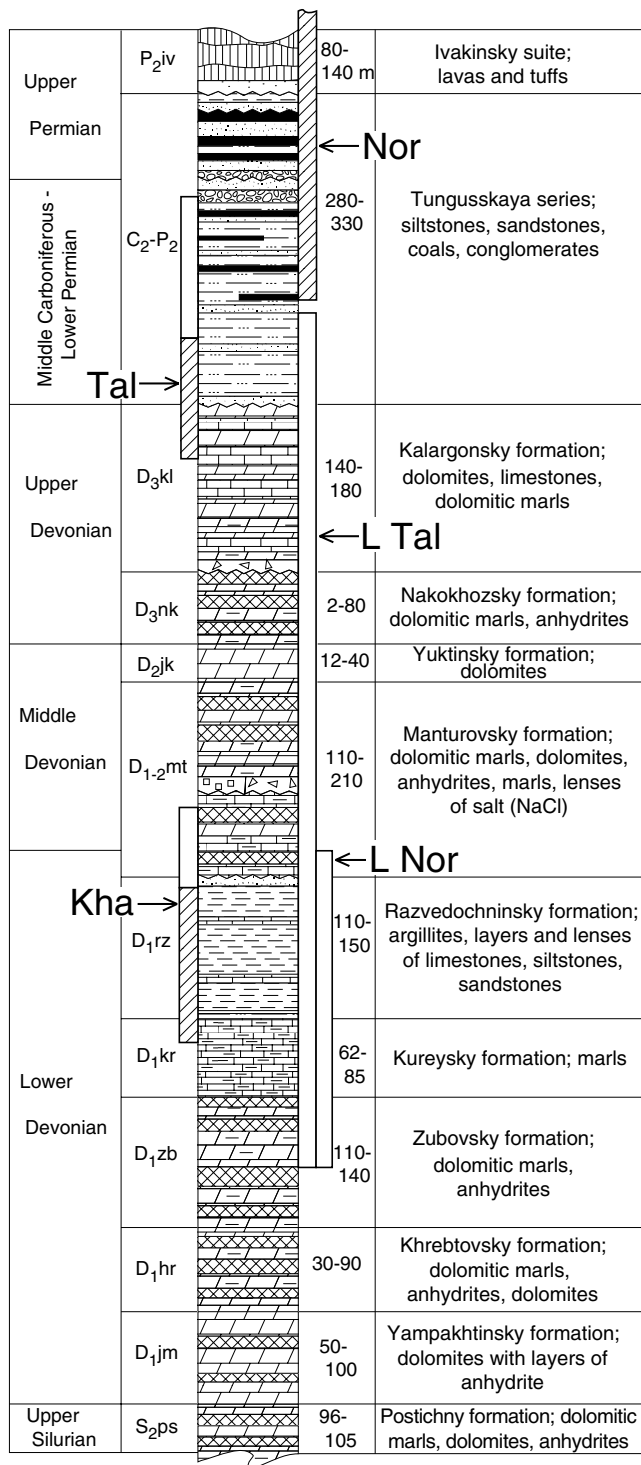
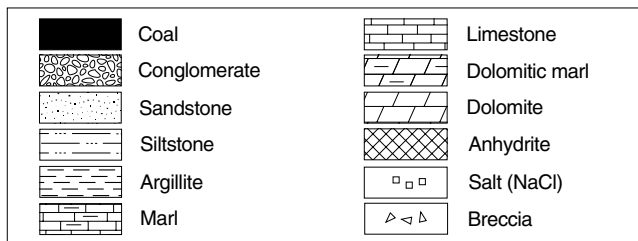


Fig. 4. Generalized stratigraphic column for Silurian to Permian formations based on typical stratigraphic thicknesses for the Talnakh ore junction. Vertical bars show the approximate ranges in stratigraphic position of the base of each intrusion: Nor, Noril'sk I; L Nor, Lower Noril'sk; Tal, Talnakh; Kar, Kharaelakh; and L Tal, Lower Talnakh. For each ore-bearing intrusion, the lower part of the bar (patterned) represents the main body and the upper part (unpatterned) the frontal parts of the intrusion. Stratigraphic positions are not shown for the flanks and bordering apophyses of these intrusions. In places, the Noril'sk I intrusion cuts as many as six of the lowermost basalt suites. Note that the northern tip of the NE branch of the Talnakh intrusion lies in the Zubovsky, Kureysky, and Razvedochninsky formations due to a washout along the axis of a pre-Tungusskaya anticline, such that the Tungusskaya series lies directly on the Razvedochninsky, Kureysky, and Zubovsky formations (Fig. 5B).



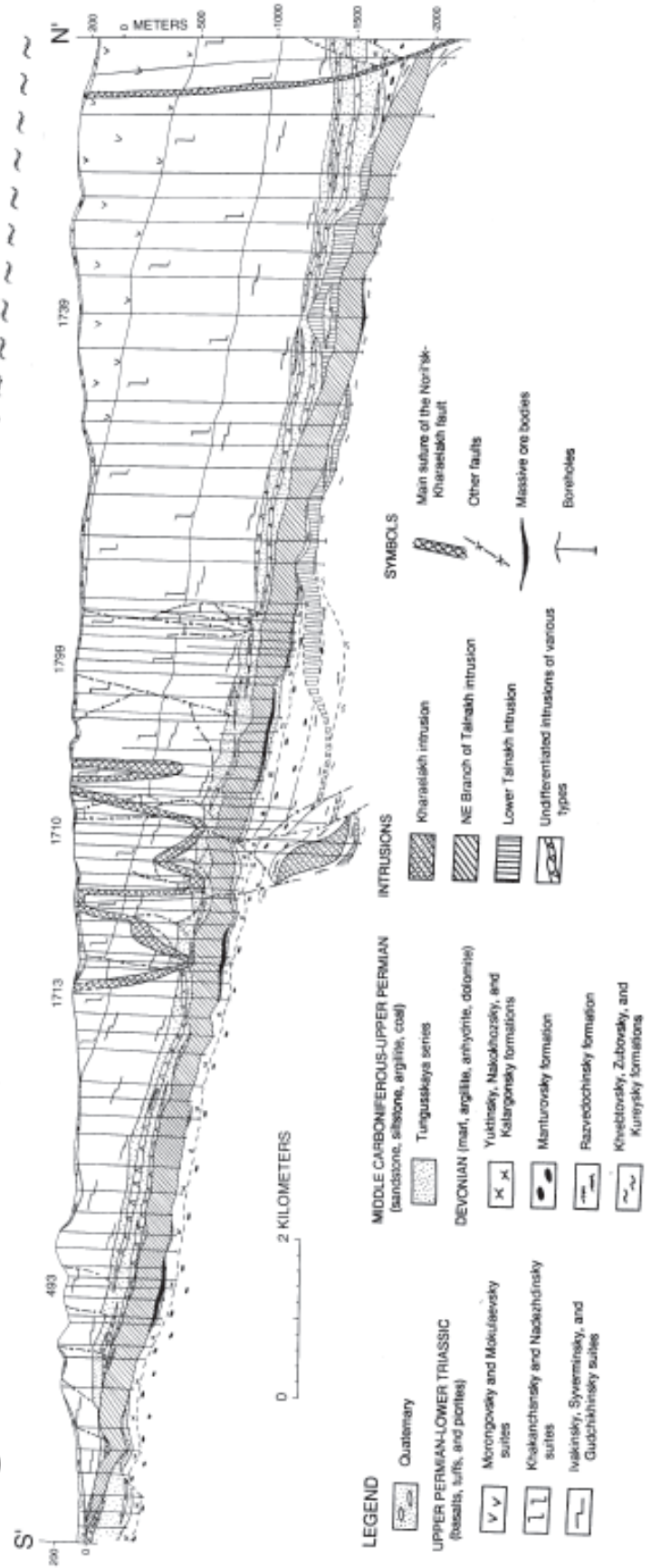
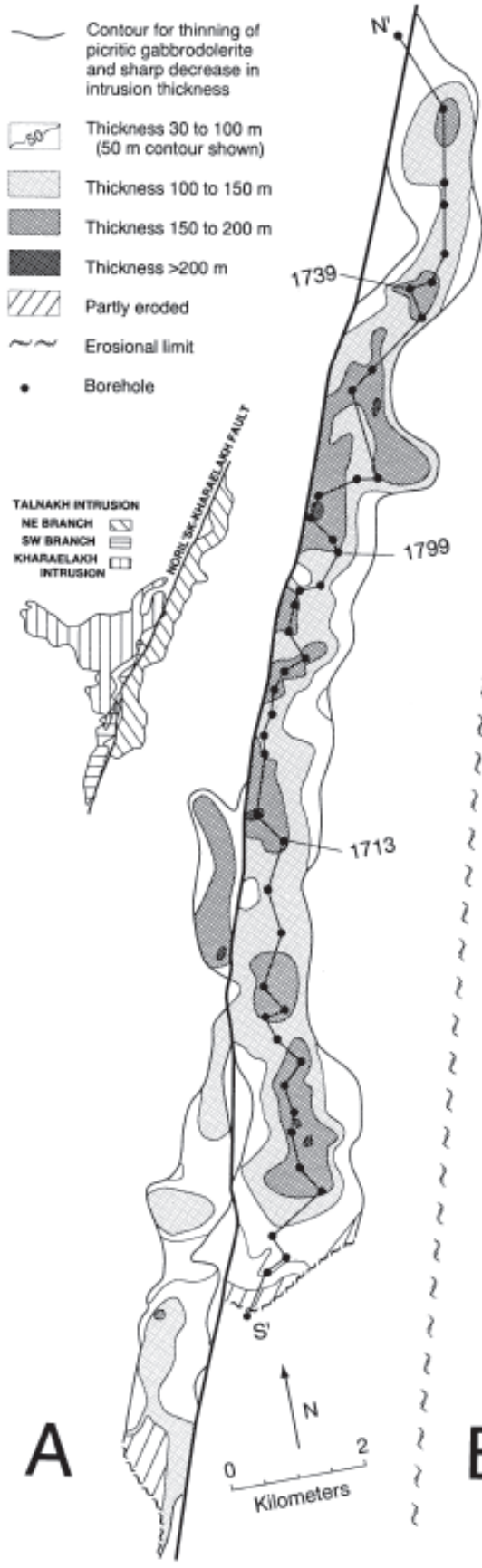
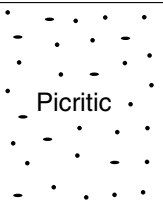




Fig. 5 (A) Projection to the surface of the outlines of the main bodies of the NE and SW branches of the Talnakh intrusion, with contours for intrusion thickness. Note that the outer margins of the main bodies have been drawn where the picritic gabbrodolerite thins and there is a sharp decrease in the thickness of the intrusion, usually to 30-50 m. The trace N'-S' relates to the cross-section (B), which follows the thickest part of the NE branch of the intrusion. Many of the boreholes that control this cross-section have been omitted to simplify the figure.

Fig. 6. Generalized lithologic section for the "fully differentiated," main bodies of the ore-bearing intrusions. Dotted patterns, disseminated ore (predominately globular in picritic gabbrodolerite and xenomorphic in taxitic gabbrodolerite); solid black ellipses, massive ore. Relative thicknesses of rock units are typical for an intrusion thickness of ~140 m. An upper taxitic unit may be present with, or in place of, leucocratic gabbro. Contact gabbrodolerite is seldom found along the upper contacts of the intrusions.

Rock unit	Modal % olivine	MgO wt %	Notable phases	
Leucocratic gabbro	0-3	4-8	Pl <sub>1</sub>	
Quartz diorite (Russian: quartz gabbrodiorite)	0	1.2-1.7	Pl <sub>2</sub> + Aug + Qtz	
Magnetite gabbro	0-4	4.4-7	Pl <sub>2</sub> + Aug + Mt	
Prismatic gabbro (Russian: gabbrodiorite)	0-5	6-7	Pl <sub>2</sub> + Aug	
GABBRODOLERITE	Olivine-bearing	3-7	6-8	Pl <sub>2</sub> + Aug + Ol <sub>2</sub>
	Olivine	10-27	9-12	Pl <sub>2</sub> + Aug + Ol <sub>2</sub> + sparse Pl <sub>1</sub>
	 Picritic	40-80	18-29	Ol <sub>1</sub> + Pl <sub>2</sub> + Aug + Sulfide + Pl <sub>1</sub> glom + sparse Pl <sub>1</sub>
	 Taxitic	7-18	9-16	Pl <sub>2</sub> + Ol <sub>2</sub> + Aug + Sulfide + Pl <sub>1</sub> glom
	Contact 	10-15	7-8	Pl <sub>2</sub> + Aug + Ol <sub>2</sub>

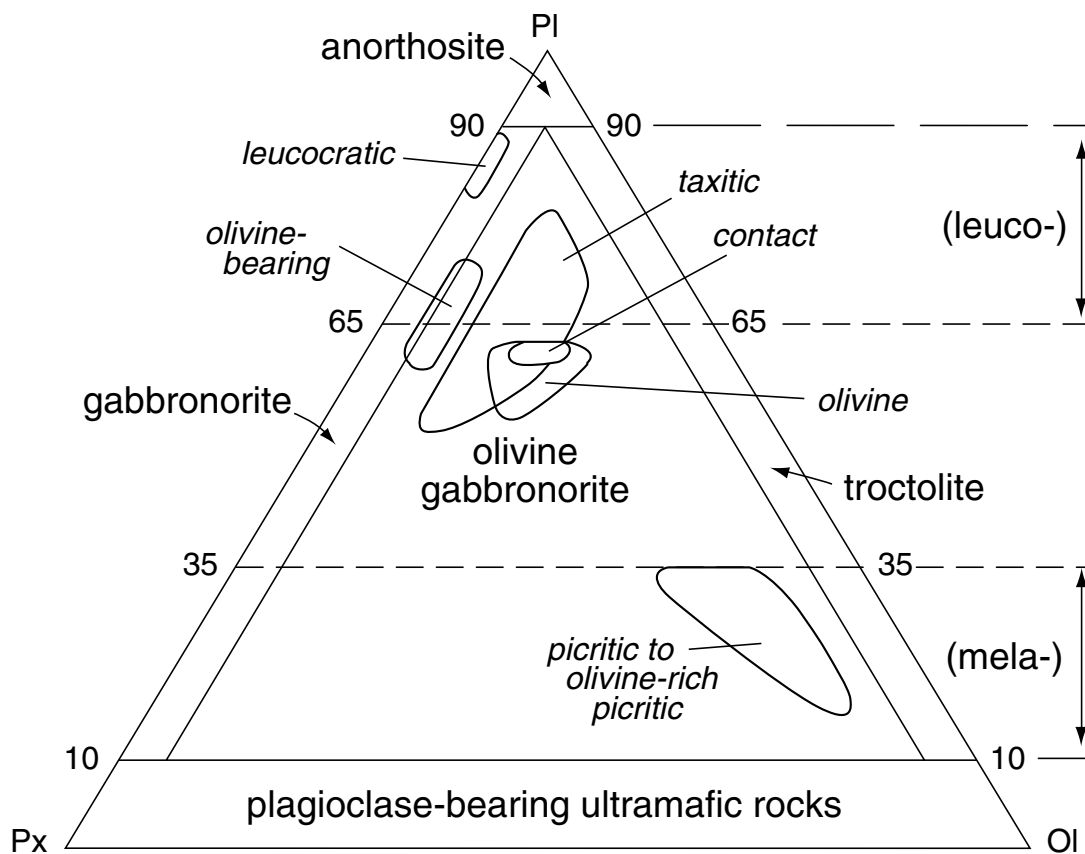


Fig. 7. Fields for the rock types that compose the Noril'sk-type, ore-bearing intrusions presented on the triangular diagram of IUGS nomenclature for gabbroic rocks (STRECKEISEN, 1973). Rock names used in this report are shown in italics, with omission of the term "gabbro" following leucocratic and "gabbrodolerite" following the other rock names. Field boundaries are approximate, after ignoring magmatic sulfide and other mineral constituents.

Fig. 8. Photomicrographs of representative rock types from the Noril'sk-type, ore-bearing intrusions. (A) Leucocratic gabbro, KZ-1818-1757.1 (crossed nicols). Note the coarse grain size of tabular, zoned plagioclase of the first generation and intergranular clinopyroxene. About 35 grains of olivine are present, ranging in size from ~2 mm across (cracked grain just below middle of right edge) to 0.5 mm (four grains aligned just below in clinopyroxene oikocryst). (B) Quartz diorite, KZ-1799-1194. Abundant quartz is late and fine-grained in this relatively coarse-grained unit. The elongate, altered grains were plagioclase of the second generation and clinopyroxene (now replaced by amphibole). Titanomagnetite is predominantly interstitial, but sometimes subhedral. (C) Magnetite gabbro (Type A), NP-29-599.8 (crossed nicols). Note the euhedral to skeletal shapes of oxide networks after early-formed titanomagnetite, the coarse-grained, and prismatic to subprismatic clinopyroxene (Au<sup>1,2</sup>). The texture contrasts with that of sample KZ-1799-1229 (Fig. 8D); however, sample NP-29-603 has titanomagnetite textures identical to those of KZ-1799-1229. (D) Magnetite gabbro (Type B), KZ-1799-1229 (crossed nicols). Note the distinctive early-crystallized titanomagnetite, which appears to have been partly resorbed. Altered laths of and subprismatic Au<sup>2</sup> predominate. Fields of all photos ~16 x 22 mm. Where not otherwise indicated, the photomicrographs have been taken with plane light.



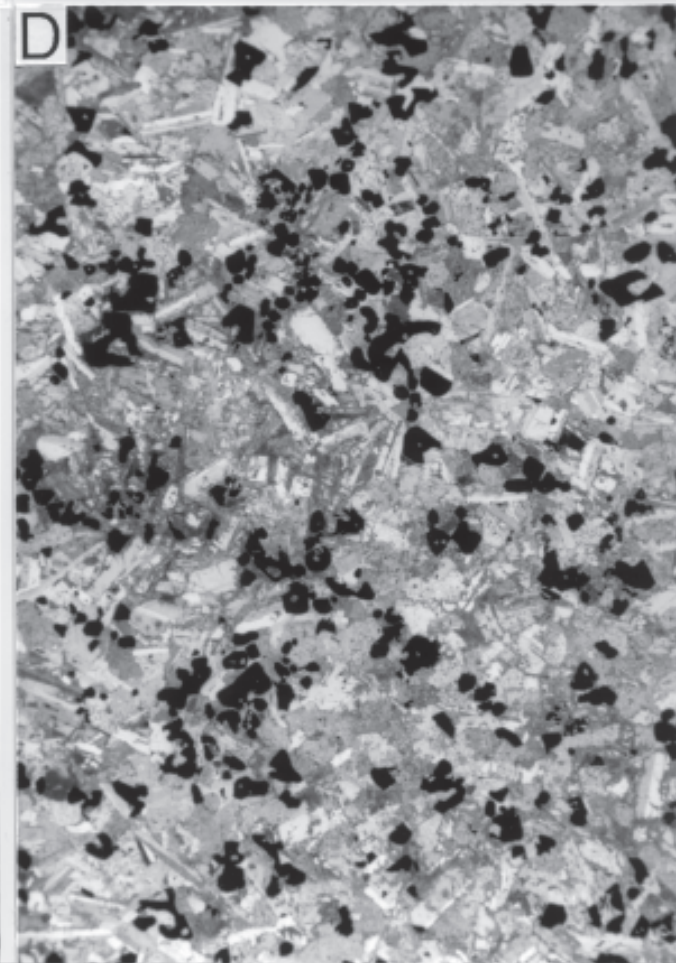
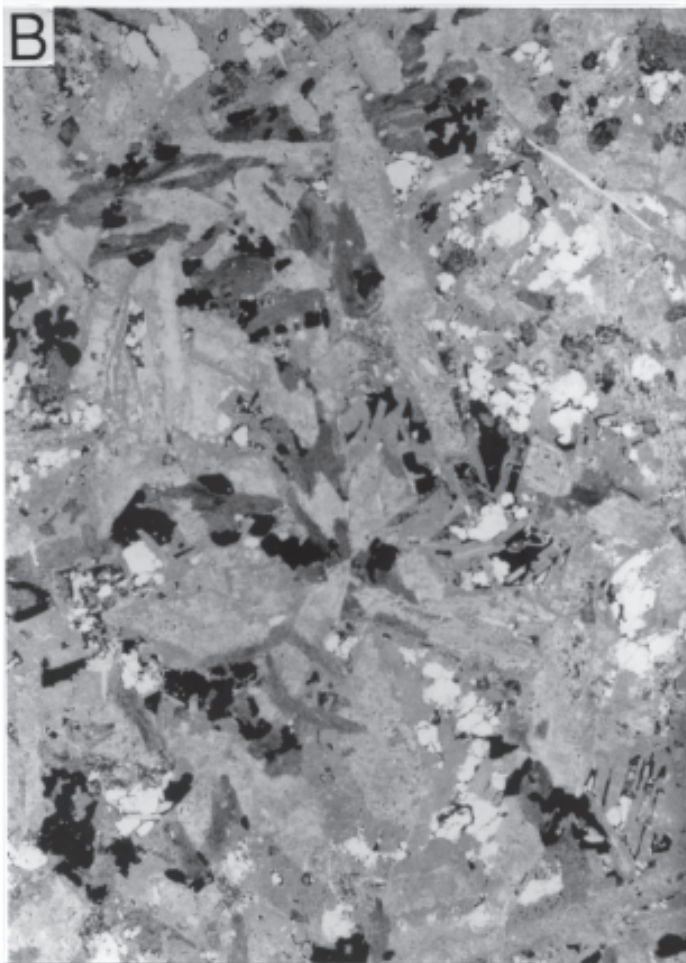
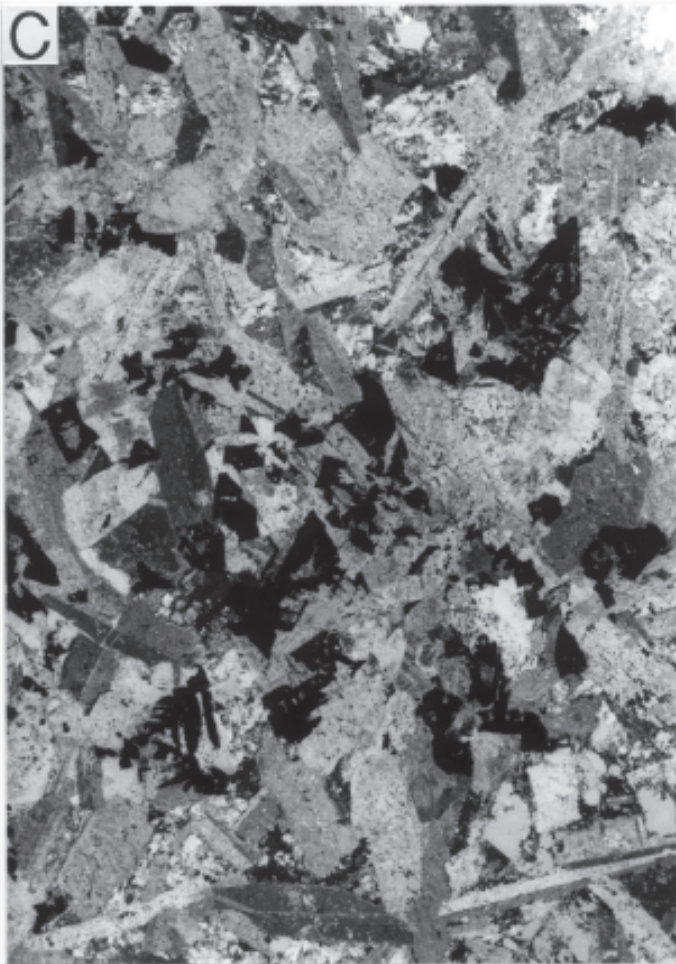


Fig. 9. Photomicrographs of representative rock types from the Noril'sk-type, ore-bearing intrusions. (A) Prismatic gabbro, KZ-1799-1249.8 (crossed nicols). Note the relatively coarse grain size of, subprismatic clinopyroxene ( $Au^2$ ), and interstitial titanomagnetite. A small amount of quartz is white. (B) Olivine-bearing gabbrodolerite, KZ-1713-840.5. Several olivine grains are completely altered and some altered along margins, but partial growth of olivine around earlier plagioclase laths is evident. Clinopyroxene is subprismatic ( $Au^2$ ) and titanomagnetite is interstitial. (C) Olivine-bearing to olivine gabbrodolerite, NP-29-655.7 (crossed nicols). More or less altered remnants of ~20 grains of  $Ol_2$  are present in this section, in which clinopyroxene appears transitional from subprismatic to oikocrystic. Because the nicols are crossed, the high-relief olivine grains range from nearly colorless (vertically elongate group of four grains just in from left-center edge of photo) to medium grey (two relatively large grains directly across, toward right side of photo). (D) Olivine gabbrodolerite, KZ-1713-860. Note the universally oikocrystic clinopyroxene ( $Au^3$ ) and the irregular shapes of the high-relief olivine grains, which often partly enclose plagioclase and are typically smaller than those present in olivine-bearing gabbrodolerite (e.g., samples KZ-1713-840.5 and NP-29-655.7). Titanomagnetite is the primary opaque mineral, as the Cr and S contents of the rock are only 335 ppm and 0.05 wt%, respectively. Fields of all photos ~16 x 22 mm.

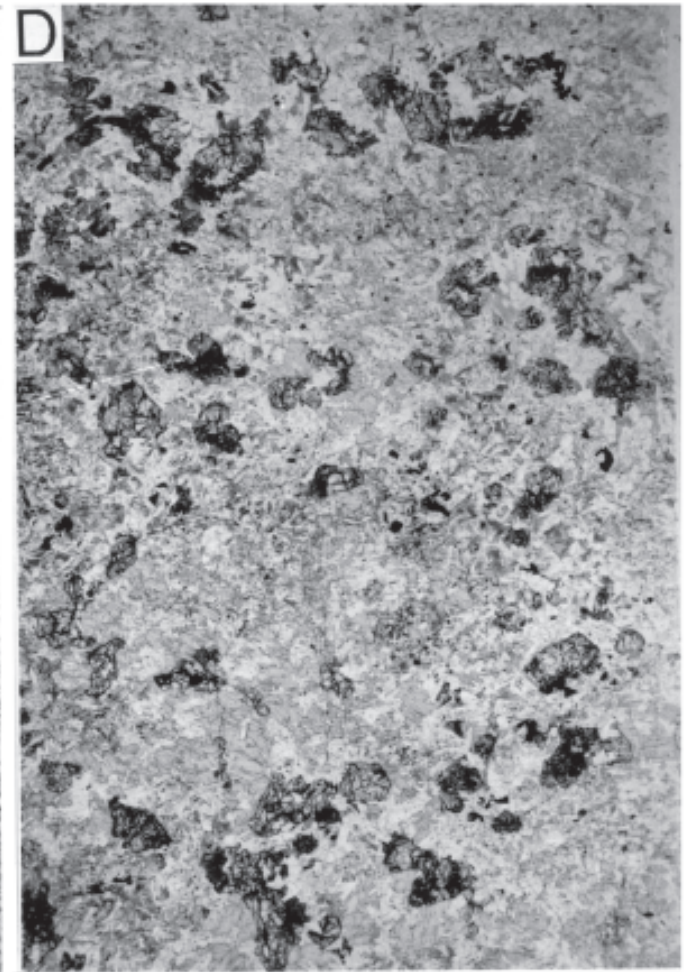
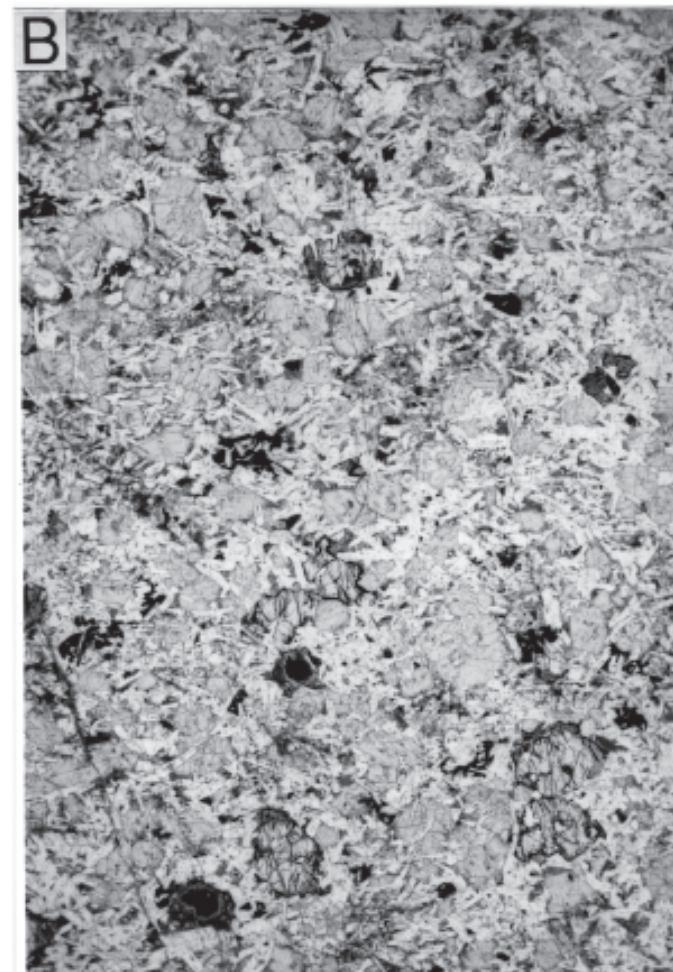
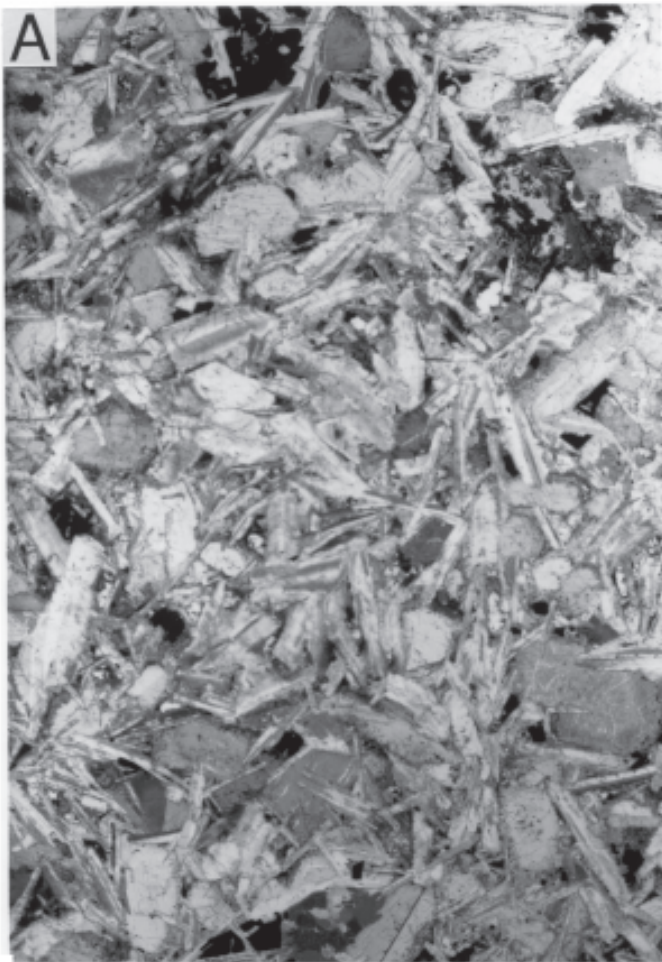
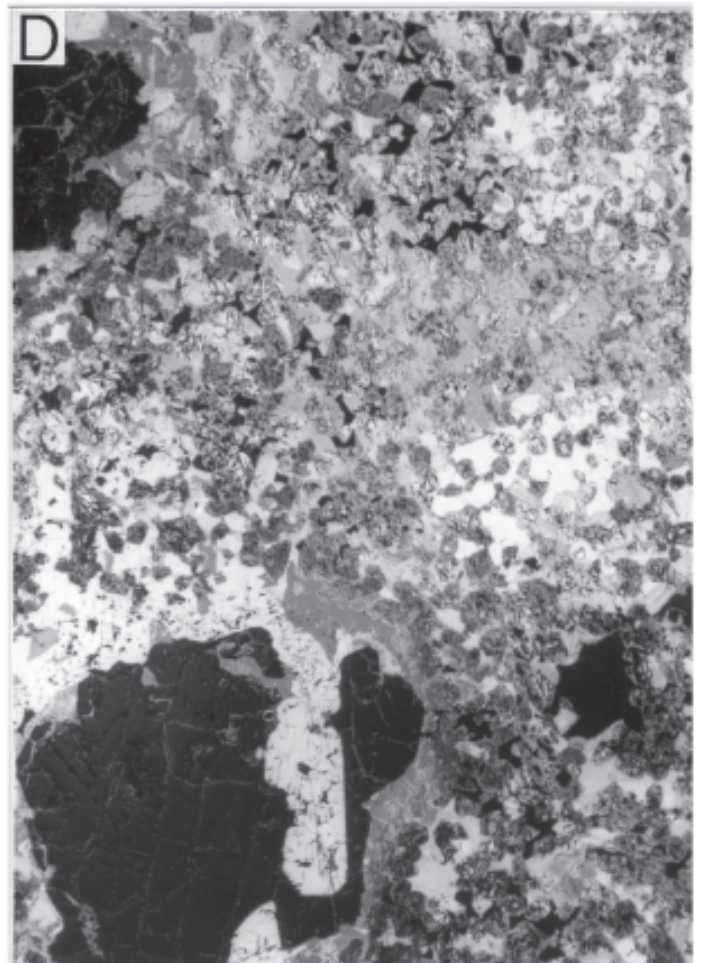
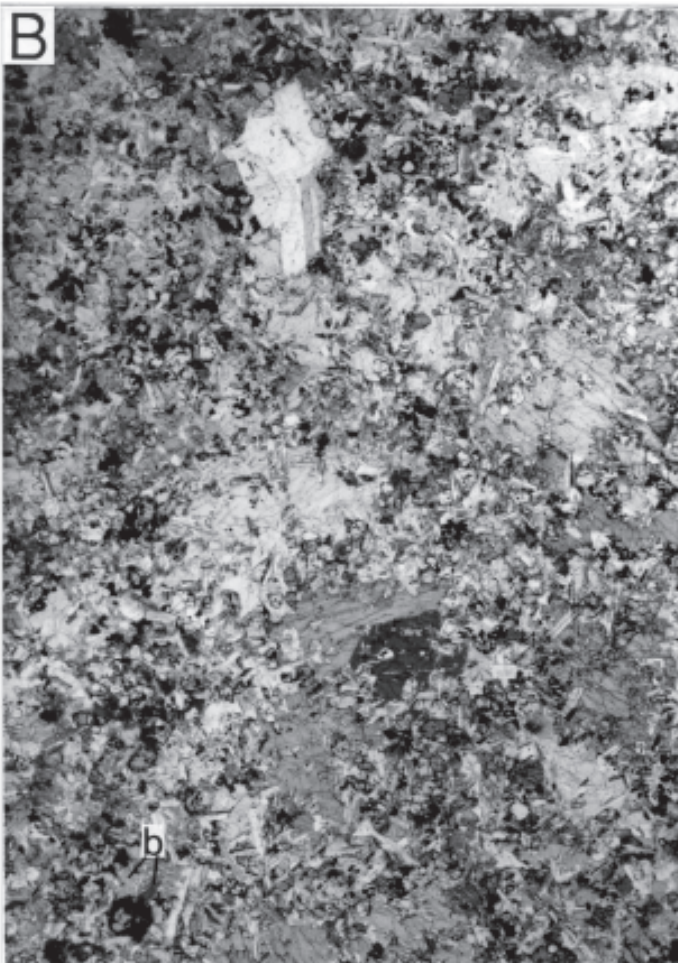
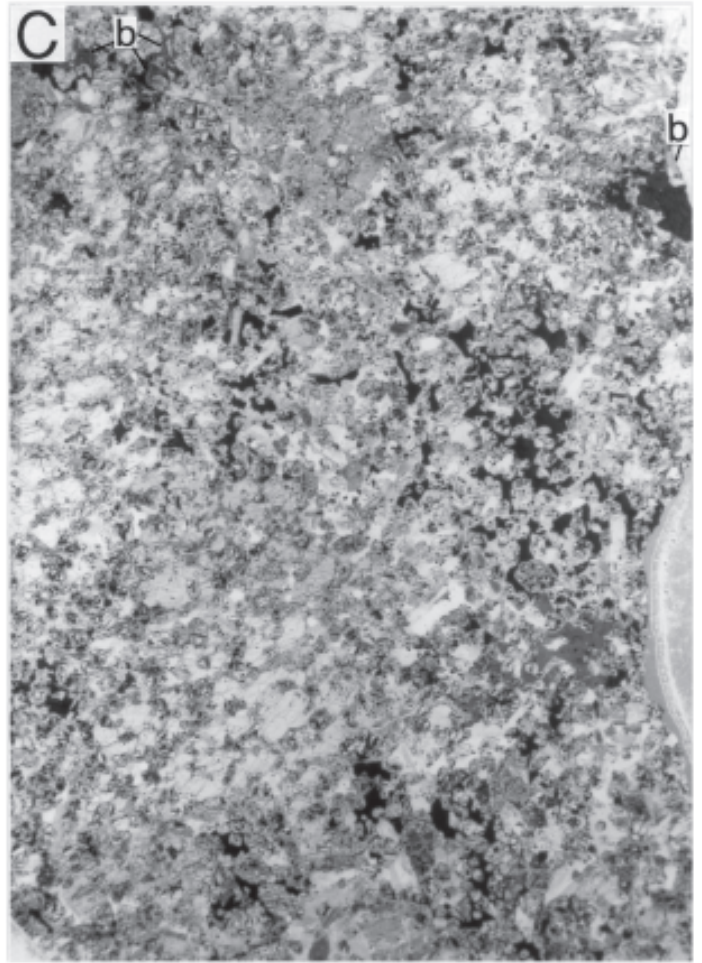
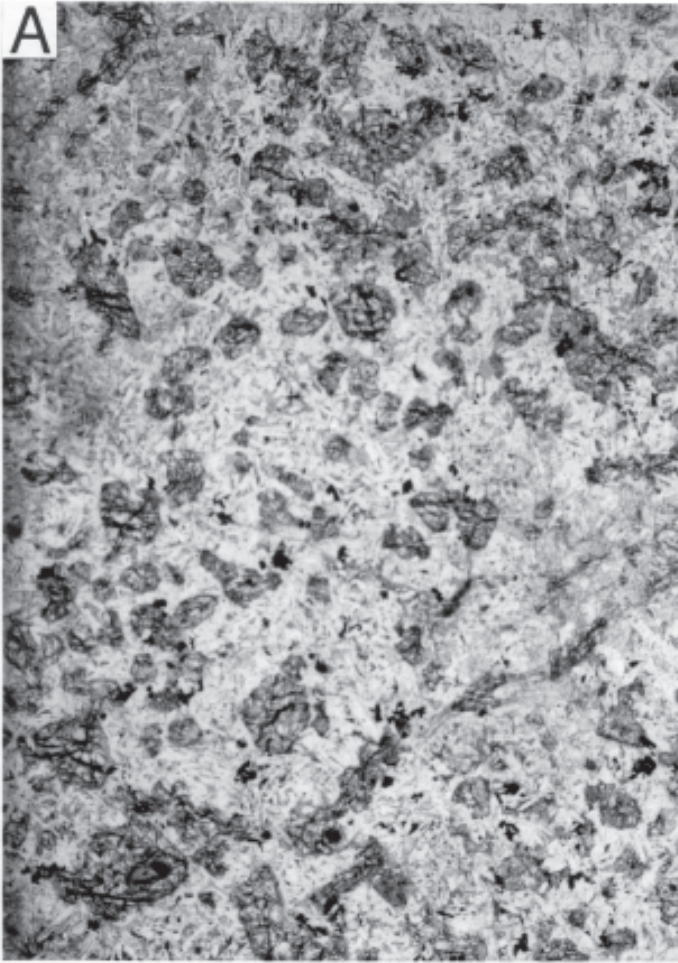


Fig. 10. Photomicrographs of representative rock types from the Noril'sk-type, ore-bearing intrusions. (A) Picritic-like gabbrodolerite, KZ-1879-1731.8. Compare the morphology of second-generation olivine in this rock with that of first-generation olivine in picritic-like gabbrodolerite sample NP-29-678.2 (Fig. 10B). Titanomagnetite is the primary opaque mineral, as the Cr and S contents of the rock are 405 ppm and 0.04 wt%, respectively. (B) Picritic-like gabbrodolerite, NP-29-678.2 (crossed nicols). Fine-grained, first-generation olivine is most readily seen in clinopyroxene oikocrysts ( $\text{Au}^3$ ) and at the margin of the small glomerocryst of . Compare this olivine morphology to that in sample KZ-1879-1731.8. The sample contains small, euhedral Cr-spinel grains; Cr and S contents are 2700 ppm and 0.04 wt%, respectively. The two relatively large grains of biotite (b) are marked. (C) Olivine-rich, picritic gabbrodolerite, KZ-1713-888.3. Fine-grained, first-generation olivine, oikocrystic clinopyroxene ( $\text{Au}^3$ ), and interstitial sulfide are typical for this rock type. This sample contains 3700 ppm Cr and 1.88 wt% S. The four relatively large grains of biotite (b) are marked. (D) Olivine-rich, picritic gabbrodolerite, KZ-1713-896.9. Dark areas are globular and interstitial sulfide. Although small plagioclase grains are present, the large crystals intergrown with the sulfide globule in the lower left are clinopyroxene, as are the light-colored upper margin to the globule and the light oikocrysts which host olivine. (Altered areas associated with the sulfide globules are a flat, medium gray.) This sample contains 930 ppm Cr and 4.65 wt% S. Fields of all photos ~16 x 22 mm.



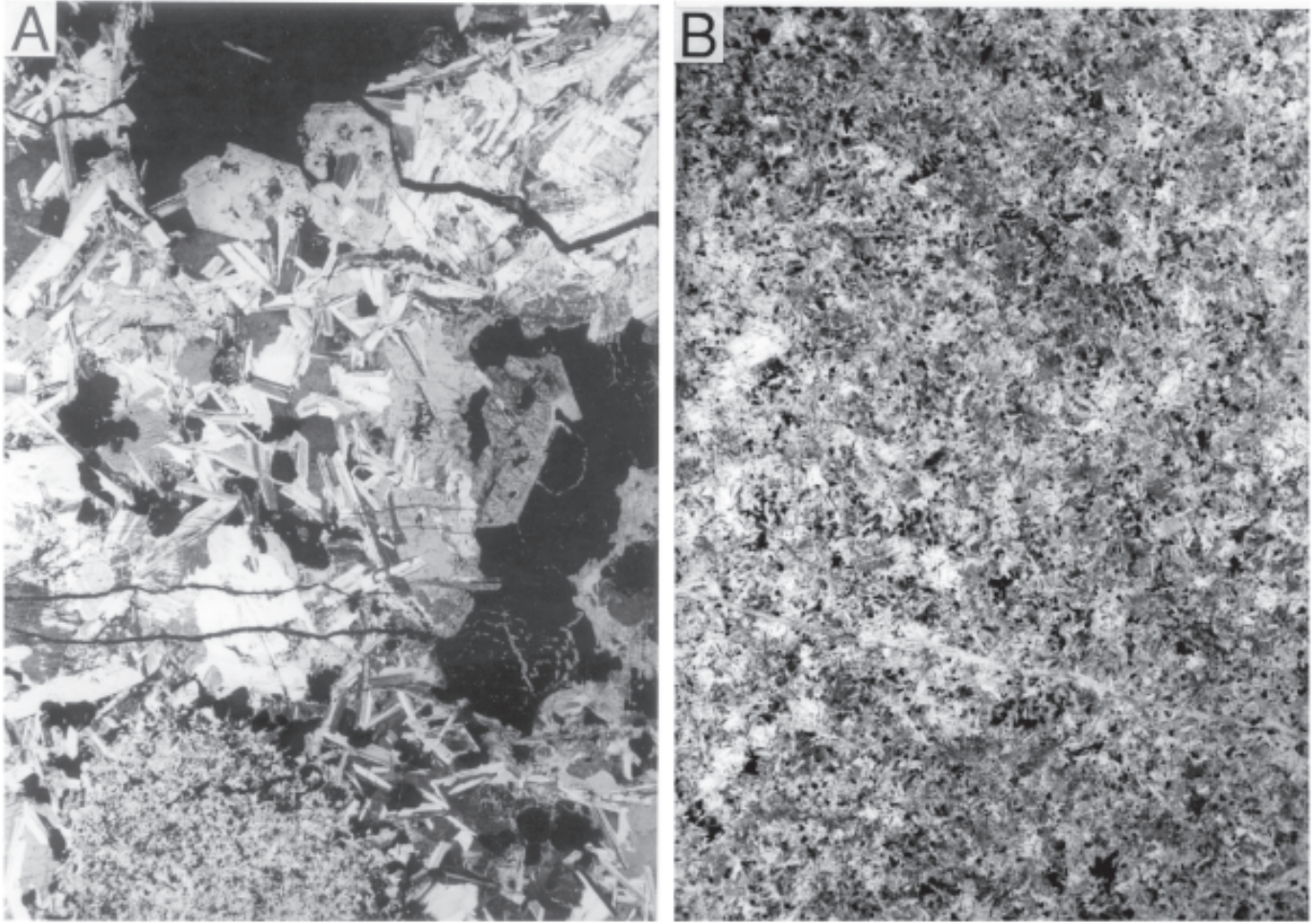


Fig. 11. Photomicrographs of representative rock types from the Noril'sk-type, ore-bearing intrusions. (A) Taxitic gabbrodolerite, KZ-1713-922.9 (crossed nicols). Large, xenocrystic sulfide aggregates; a typical, fine-grained patch (lower right); and large, subhedral clinopyroxene (e.g., imbedded in sulfide, upper center), and plagioclase grains are evident in this section. The upper, right corner of the photo shows part of a plagioclase glomerocryst 2 cm across. As is common, the area surrounding the sulfide aggregate on the lower right is altered. This sample contains 170 ppm Cr and 4.66 wt% S. (The upper dark crack resulted from breakage during preparation, the lower veinlets are filled with an alteration phase.) (B) Contact gabbrodolerite, KZ-1879-1798.1. Note the extremely fine grain size of this contact unit. In addition to small laths of , the rock contains small oikocrysts of  $Au^3$  and small, rounded grains of . Small dark grains are virtually all titanomagnetite, as the rock contains only 0.04 wt% S and 130 ppm Cr. Fields of all photos  $\sim 16 \times 22$  mm.

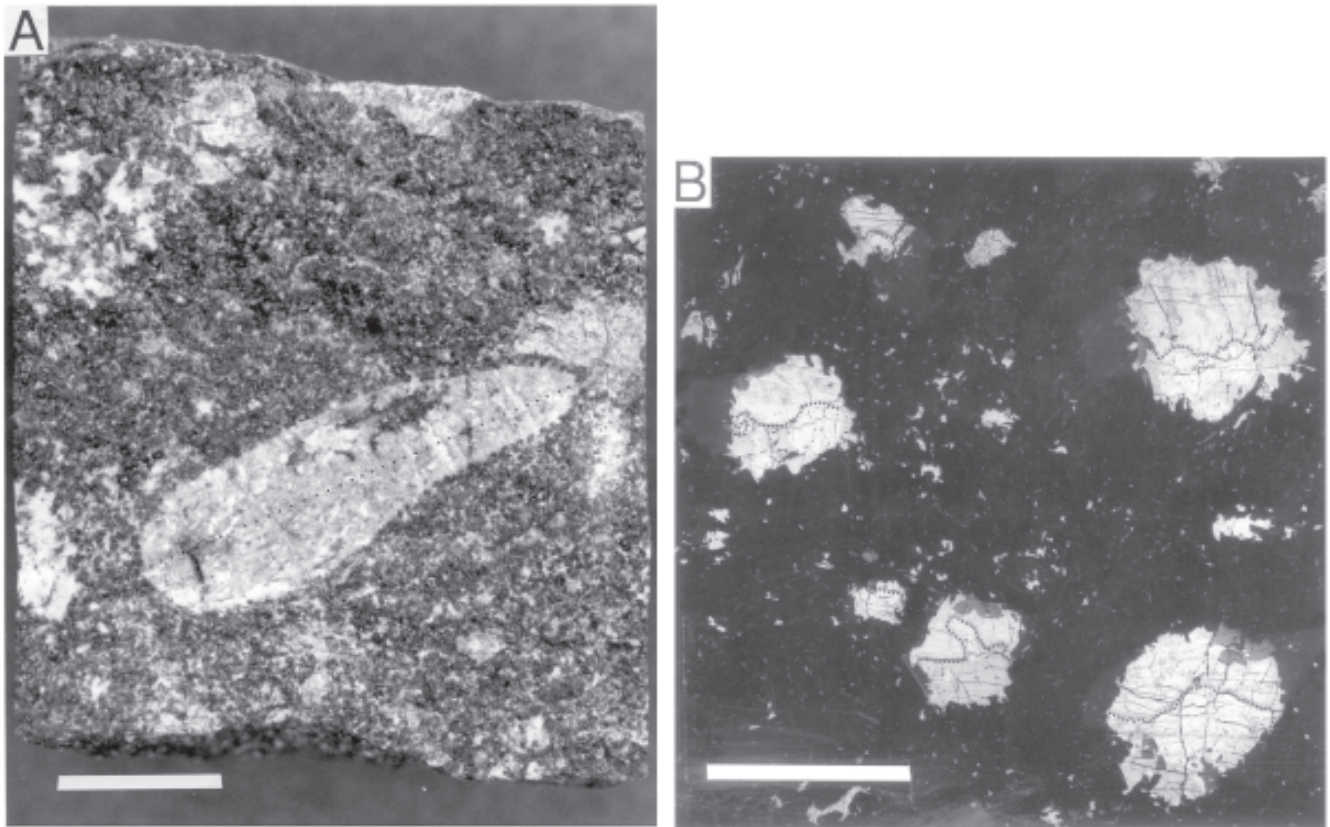


Fig. 12. (A) Photograph of split drillcore from the lower part of the picritic-gabbrodolerite unit showing a resorbed plagioclase phenocryst 3 cm long (NE branch of the Talnakh intrusion). Dots highlight a twin plane that runs the length of the grain. The broken gray area just above the right tip of the plagioclase phenocryst is sulfide, as are the two areas of similar size at, and near, the top of the specimen. Eight to ten other small patches of sulfide <2 mm across are present. Plagioclase glomerocrysts are seen at the left edge of the photo — to the left of the phenocryst and near the upper edge, to the lower left of the 6 mm sulfide aggregate. Bar = 1 cm. (B) Reflected-light photograph of globular ore in picritic gabbrodolerite sample 90MC10 from the Medvezhy Creek open pit mine, Noril'sk I intrusion. For six globules, the contact representing the base of the main mass of the former Cu-rich liquid is enhanced by dots. The lower part of each globule consists of coarse-grained pyrrhotite and pentlandite, recrystallized after early-formed crystals of monosulfide solid solution (mss) had accumulated at the bottom of the sulfide-melt droplets. Note the subhedral grains of magnetite (dark gray) at the margin of each globule. Bar = 1 cm.

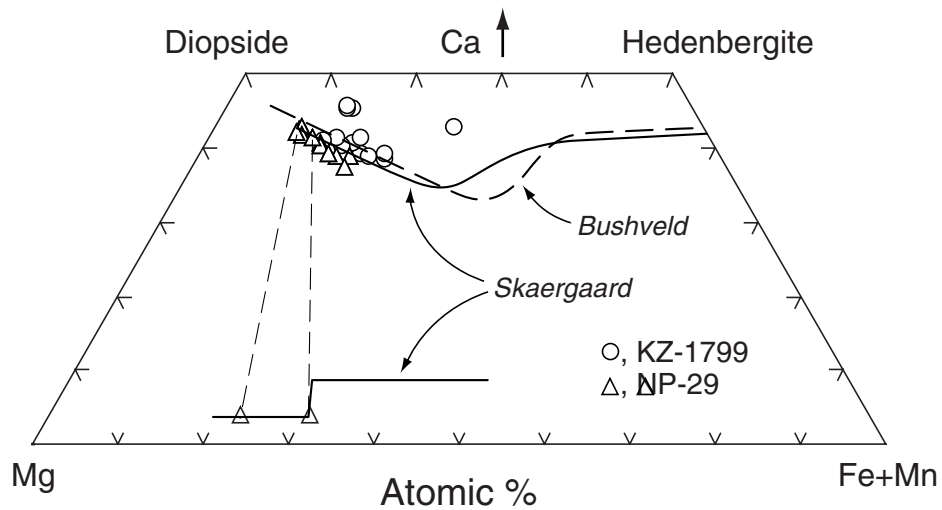


Fig. 13. Plot of the pyroxene compositional data of Tables 5 and 6 in terms of the wollastonite-enstatite-ferrosilite endmembers. Data for pyroxenes from borehole NP-29 are represented by triangles and those from borehole KZ-1799 by circles. Reference lines are for pyroxenes from the Skaergaard Intrusion (WAGER and DEER, 1967, their Fig. 19) and Bushveld Complex (ATKINS, 1969, his Fig. 3). Tie-lines connect coexisting clinopyroxene and orthopyroxene (Table 6).



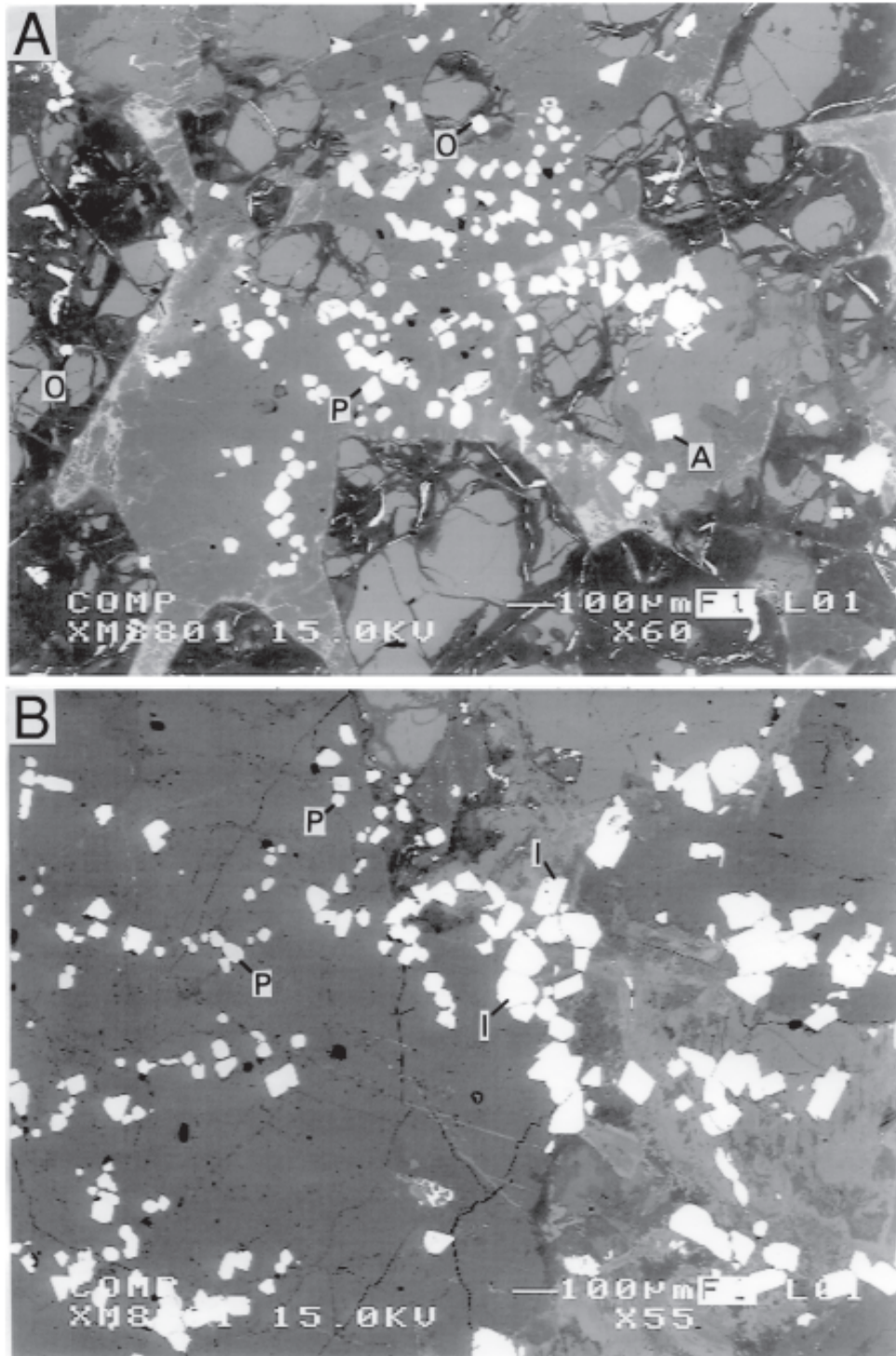


Fig. 14. Back-scattered-electron images. (A) Cr-spinel grains trapped in olivine (O), plagioclase (P), and orthopyroxene (A); picritic gabbrodolerite sample KZ-1713-880 (4100 ppm Cr). Note remnants of 15-16 grains of Ol<sub>1</sub> and 100-micron scale. Analyses presented in Table 10. (B) Cr-spinel grains in trapped in plagioclase (P) and largely interstitial to plagioclase grains, amid patches of alteration (I); picritic gabbrodolerite sample NP-29-678.2 (2700 ppm Cr). Analyses of the marked grains are presented in Table 10.

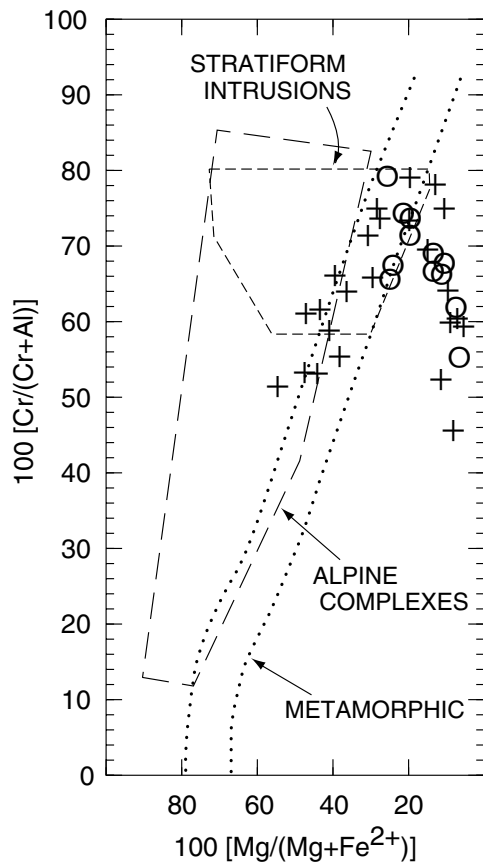


Fig. 15. Plot of recalculated electron-microprobe analyses for Cr-spinel grains on the conventional diagram  $100 [\text{Mg}/(\text{Mg}+\text{Fe}^{2+})]$  against  $100 [\text{Cr}/(\text{Cr}+\text{Al})]$ . Cr-spinel grains trapped in olivine shown by circles, interstitial grains and grains trapped in plagioclase or pyroxene shown by crosses. Fields are shown for metamorphic, secondary spinels in serpentinite and allied rocks (EVANS and FROST, 1975), as well as stratiform intrusions and alpine complexes (IRVINE and FINDLAY, 1972).

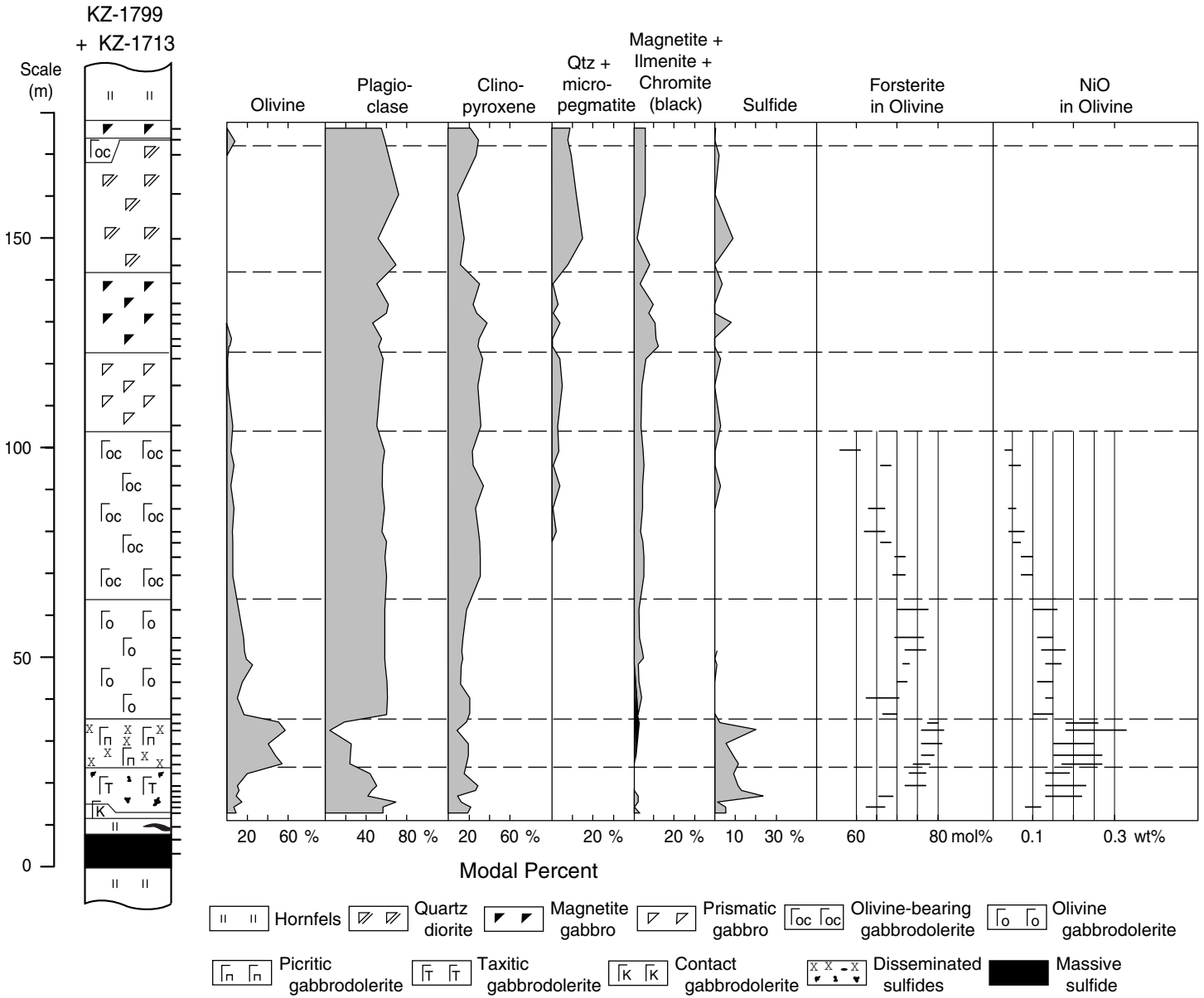


Fig. 16. Composite lithologic section, based on boreholes KZ-1713 and KZ-1799 (Appendixes 1 and 2; Fig. 17), with estimated modal proportions of significant mineral phases and ranges of forsterite and NiO contents in olivine, as determined by electron-microprobe analysis.

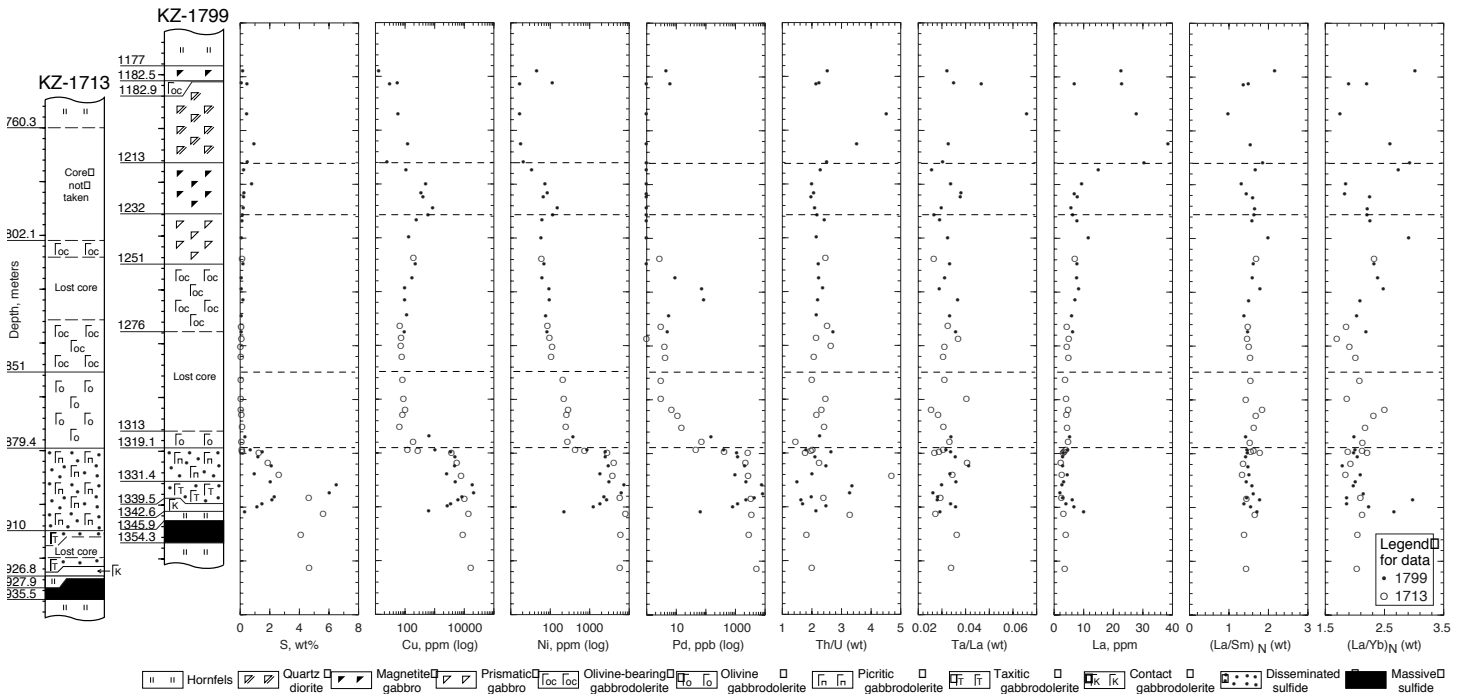
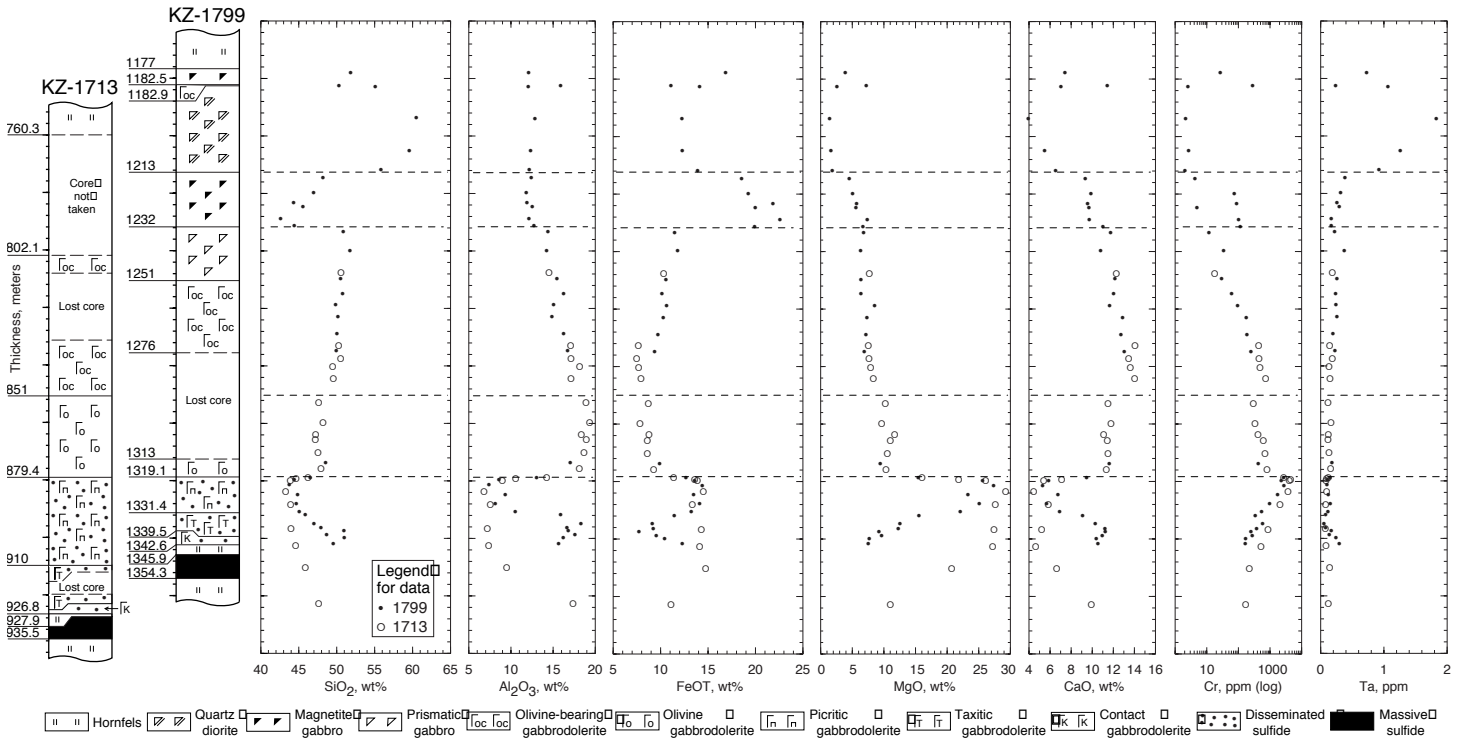


Fig. 17. Major- and trace-element variations with respect to stratigraphic position and rock type for a composite section for the NE branch of the Talnakh intrusion, based on complementary boreholes KZ-1713 and KZ-1799 (Fig. 5; Appendixes 1 and 2). Alignment of the two lithologic sections is at the upper contact of the picritic-gabbrodolerite unit.

# TALNAKH

## KHARAE LAKH (6 sections)

## SW branch (5 sections)

## NE branch (12 sections)

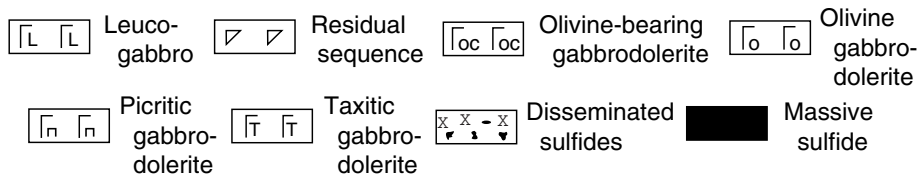
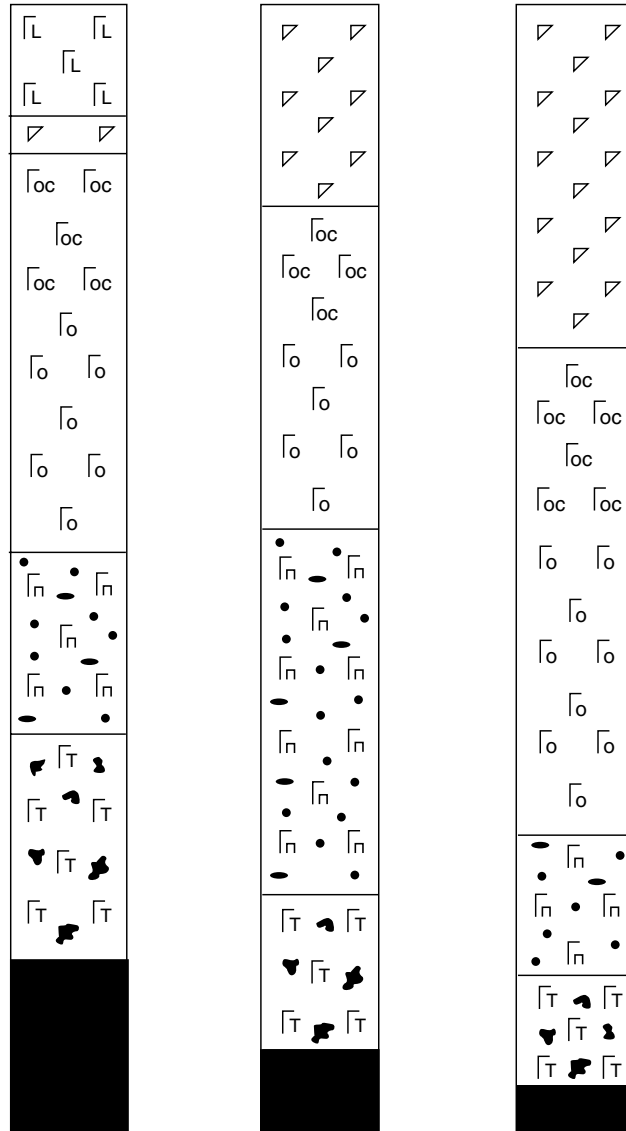


Fig. 18. Lithologic columns showing variation in average thickness of the main lithologic units in the three, ore-bearing bodies of the Talnakh ore junction. Columns have been normalized for comparative purposes. Actual thicknesses for the Kharaelakh intrusion and the SW and NE branches of the Talnakh intrusion range from 47 to 167 m, 77 to 120 m, and 87 to 185 m, respectively. Black bodies represent occurrence of globular, disseminated ore in picritic gabbrodolerite and xenomorphic, disseminated ore in taxitic gabbrodolerite.

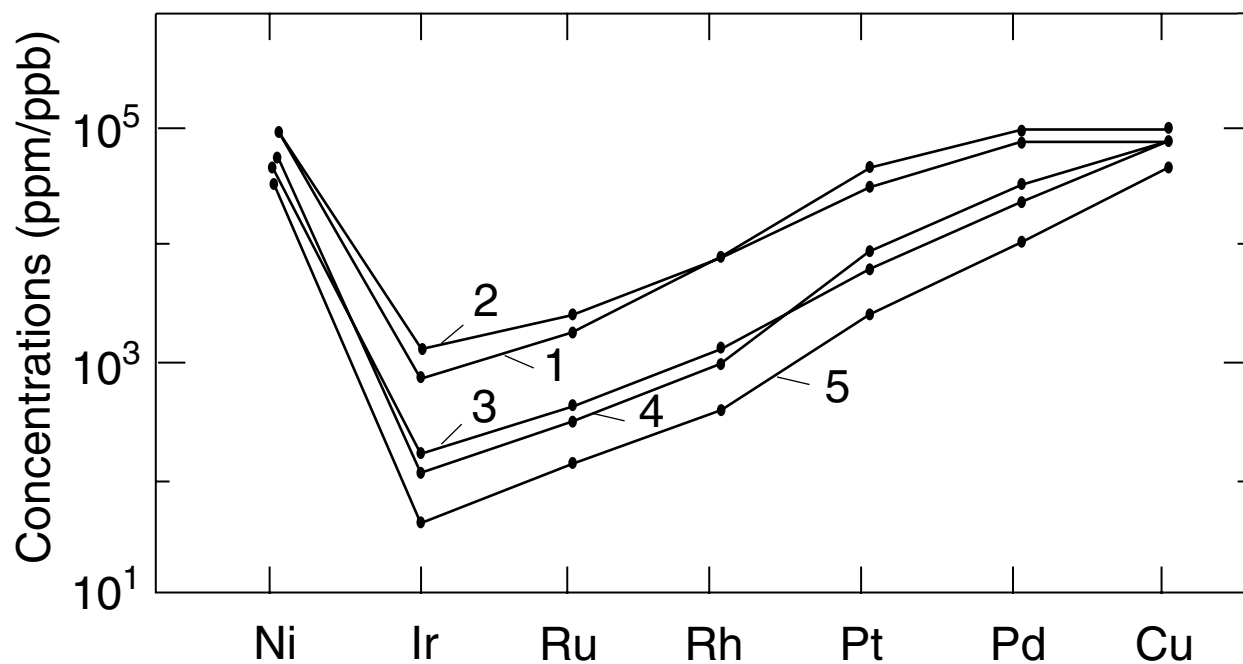


Fig. 19. Average concentrations of Ni, Cu, and PGE in disseminated ores, calculated for 35 wt% S (Ni and Cu, ppm; PGE, ppb). Ores are from the following intrusions: 1, Noril'sk I (4 samples); 2, Noril'sk II (3 samples); 3, Talnakh (5 samples); 4, Kharaelakh, Gluboky mine area (11 samples); 5, Kharaelakh, area of the Main Kharaelakh orebody (5 samples).

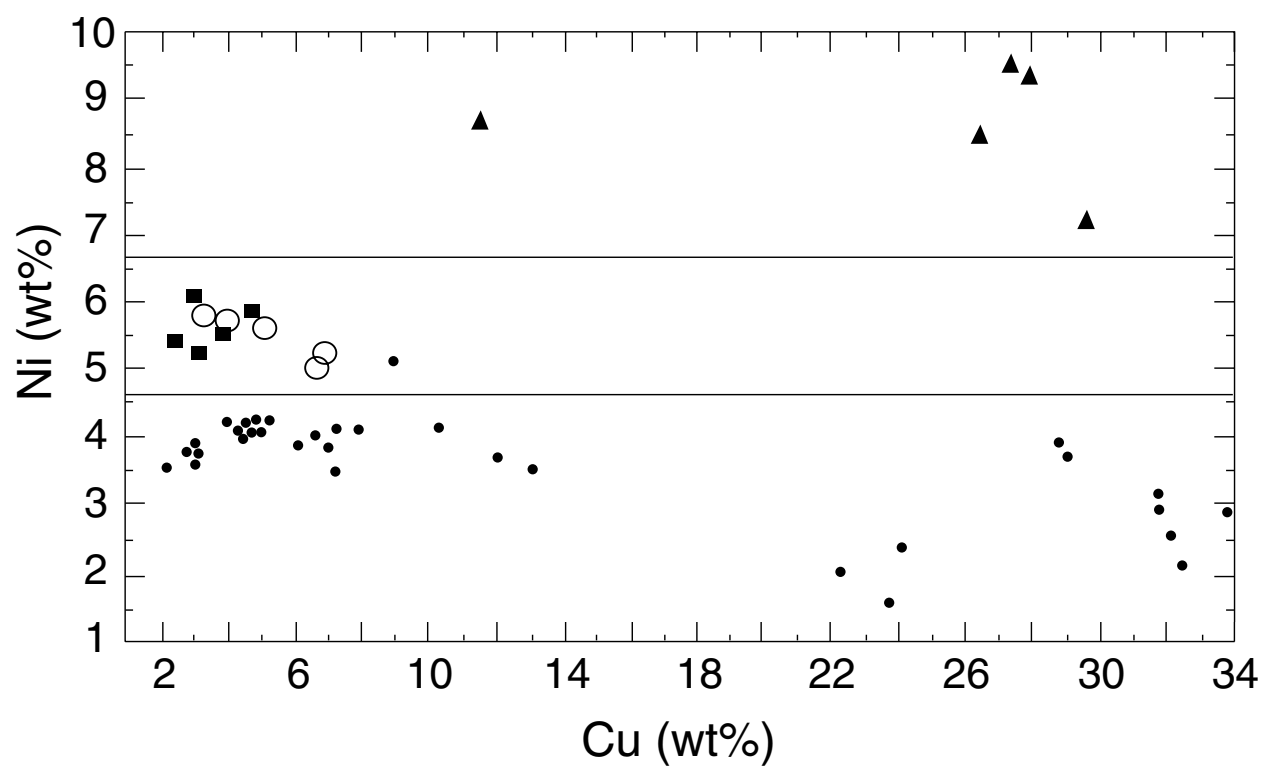


Fig. 20. Concentrations of Cu and Ni in massive ore, calculated for 35 wt% S. Triangles, Noril'sk I ores; squares, Talnakh ores; circles, ores from the Gluboky mine area of the Kharaelakh intrusion; dots, ores from the Main Kharaelakh orebody of the Kharaelakh intrusion.

## TABLES and APPENDIXES



**Table 1. Principal rock types of the Noril'sk-type intrusions and their petrographic characteristics.**

Rock type and examples*	Generations, morphologic types**, and modal abundances, and sizes of minerals	Notable features and textural characteristics
Leucocratic gabbro (leucogabbro) <b>KZ-1879-1689.5, -1704</b> <b>KZ-1818-1757.1</b>	$(Ol_2^3)_{0-3} [(Pl_1^{2,3})_{2-70} (Pl_2^4)_{10-75}]_{75-80} (Au^{2,4,6})_{7-15}$ $(Tm)_{0-5} (Sul)_{0-4} (Chl + Amf + Mus)_{3-7}$  (-) (d,2-4) (0.2x0.5 - 2x4) (d,0.5-8)+	The dominant feature is the content of as much as 80 modal % of large, tabular and xenomorphic, coalescing plagioclase crystals of relatively high An content. Augite is intergranular.  Anhedral texture (Fig. 41).++
Quartz diorite (Russian "quartz gabbro-diorite") <b>KZ-1799-1194, -1205.2, -1212</b>	$(Ol_2^3)_{0-one} [(Pl_1^{2,3})_{0-7} (Pl_2^4)_{50-70}]_{50-70} (Au^{1,2,6})_{7-15}$ $(Q \pm Mp)_{5-15} (Ap)_{2-3} (Tm)_{1-6} Sul_{0-8}$	Characteristics common to quartz diorite, magnetite gabbro, and prismatic gabbro are relatively coarse-grain size of plagioclase and other minerals; presence of quartz and micro-pegmatite; and general absence of $Ol_1^2$ , $Ol_2^2$ , and $Ol_2^6$ .  For quartz diorite--quartz+micropegmatite content is relatively high; augite content is relatively low; and apatite content is 2-3 modal %.  For magnetite gabbro--titanomagnetite content is high (5-11 modal %). Variety "A" contains more apatite; a relatively large proportion of secondary minerals; and less augite than variety "B." Both coarse and medium grained rocks are found in borehole KZ-1799.  For prismatic gabbro-- $Ol_2^2$ or $Ol_2^6$ are almost always present together with quartz+micropegmatite (each 0-5 modal %).
Magnetite gabbro "A" <b>NP-29-561.7, -563.8, -567, -584.6, -599.8</b>	$(Ol_1^2 \text{ or } Ol_2^6)_{0-one} [(Pl_1^{1,2,3})_{0-20} (Pl_2^4)_{30-60}]_{50-64}$ $(Au^{1,2,4,6})_{10-25} (Q)_{0-7} (Ap)_{0.5-2} (Bi)_{0-3} (Tm)_{5-10}$ $(Sul)_{0-1} (BowI + Bi + Amf + Carb + Chl + Mus)_{5-10}$	
Magnetite gabbro "B" <b>KZ-1799-1220, -1223.5, -1224.9, -1229, -1230.2, -1231.5</b>	$(Ol_2^3)_{0-4} [(Pl_1^{2,3})_{0-10} (Pl_2^4)_{45-60}]_{45-65} (Au^{1,2,6})_{20-35}$ $(Opx^4)_{0-3} (Q)_{0-5} (Bi)_{0-3} (Tm)_{5-11} Sul_{0-1}$ $(Bi + Amf + Sec)_{0-10}$	
Prismatic gabbro (Russian "gabbro-diorite") <b>KZ-1799-1233.6, -1240, -1243.8, -1249.8</b>	$(Ol_1^2 \text{ or } Ol_2^6 + Ol_2^3)_{0-5} [(Pl_1^2)_{0-10} (Pl_2^4)_{40-60}]_{45-65}$ $(Au^{1,2, \text{rarely } 6})_{25-30} (Q \pm Mp)_{0-5} (Bi)_{0-3}$ $(Tm \pm Mt)_{2-5} (Sul)_{0-1}$  (-) (d,0.1-7) (0.2x0.3 - 2x9) (d,0.3-4 to 1.5x6)	Textures range from euhedral granular, in which Pl and Au commonly have prismatic forms, to intergranular, with spaces between Pl occupied by one (rarely two) grains of Au (or Ol). (Fig. 61, but with random orientation of Pl grains that range from short prisms to laths. This type of intergranular texture is also found in olivine-bearing and taxitic gabbrodolerite). In magnetite gabbro "B," Au may form consertal intergrowths (Fig. 73). In prismatic gabbro, Au may contain pegmatoidal intergrowths of $Pl_2$ (as in Fig. 90, but not radially oriented).
Olivine-bearing gabbrodolerite <b>NP-29-588.3, -598.8</b> <b>KZ-1713-833, -837.5, -840.5, -844.5</b> <b>KZ-1799-1255, -1259, -1263.2, -1269, -1275</b>	$(Ol_2^{3,4,5 \text{ rarely } 6})_{3-7} [(Pl_1^{2,3})_{0-3} (Pl_2^4)_{50-60}]_{50-63}$ $(Au^2, \text{rarely } 1)_{20-30} (Opx)_{0-one} (Q \pm Mp)_{0-3}$ $(Bi)_{0-2} (Tm \pm Mt)_{3-5} (Cr?)_{0-one} (Sul)_{0-1}$	Laths of $Pl_2^4$ may be well oriented in a trachytic texture. Augite is almost always sub-prismatic and may contain pegmatoidal intergrowths of plagioclase. $Ol_2$ is always present, but orthopyroxene, quartz, and micropegmatite are seldom present.
Olivine-bearing to olivine gabbrodolerite <b>NP-29-610.8, -617.6, -628, -637.9, -652.3, -655.7</b>	$(Ol_2^{4,5,6})_{10-25} [(Pl_1^2)_{0-1} (Pl_2^{4,5})_{40-60}]_{40-60} (Au^2)_{20-30}$ $(Opx)_{0-one} (Bi)_{0-2} (Tm \pm Mt)_{2-4} (Sul)_{0-1}$  (-) (d,0.1-5) (0.1x0.3 - d,2 - 0.3x3) (d,0.2-4)	This transitional unit contains as much $Au^2$ as olivine-bearing gabbrodolerite and as much $Ol_2$ as olivine gabbrodolerite.  Intergranular texture. Predominately lath-shaped Pl may be well-oriented to form trachytic texture (Fig. 61). Au may contain pegmatoidal intergrowths of $Pl_2$ and may form consertal intergrowths.
Olivine gabbrodolerite <b>NP-29-658.7, -667</b> <b>KZ-1713-853, -860, -864, -866, -870.5, -876</b> <b>KZ-1799-1314</b> <b>KZ-1879-1718.4</b>	$[(Ol_1^2, \text{rarely } 1)_{0-10?} (Ol_2^{4,5,6, \text{rarely } 3})_{5-20}]_{10-27}$ $[(Pl_1^{1,2,3})_{0-8} (Pl_2^{4,5})_{47-60}]_{50-63} (Au^3)_{10-20, \text{rarely } 30} (Bi)_{0-3}$ $[(Tm)_{0-4} (Mt)_{0-3}]_{1-4} (Cr)_{0-1} (Sul)_{0-1}$	Plagioclase may form sparse phenocrysts and glomerocrysts of $Pl_1^{2,3} + Pl_2^4$ (<5 modal %). Augite is only present as oikocrysts. Olivine content increases toward the base of the unit and, on the basis of morphology and composition, $Ol_1^2$ is probably present. Chromite is often present near the base of the unit.
Picritic-like gabbrodolerite <b>NP-29-676.6, -678.2</b> <b>KZ-1713-879</b> <b>KZ-1799-1318.2</b> <b>KZ-1879-1720.2, -1731.8, -1734.7</b>	$[(Ol_1^{2,1}) (Ol_2^{4,5})]_{25-40} [(Pl_1^{2,3})_{0-2} (Pl_2^{5,4})_{30-50}]_{30-50}$ $(Au^3, \text{rarely } 2)_{15-23, \text{rarely } 30} (Bi)_{1-5} (Tm)_{0-3}$ $(Mt)_{0-2} (Cr)_{0-4} (Sul)_{0-1}$  (d,0.1-3) (d,0.1-4) (0.02x0.2 - d,2) (d,1-10)	Plagioclase may form sparse glomerocrysts of $Pl_1^{2,3} + Pl_2^4$ (<5 modal %; 1-2 cm across). Ol may be a significant component. Augite mainly forms oikocrysts. Chromite is commonly present and may reach 3-4 modal %; magnetite is rare.  Poikilophitic and subophitic varieties of ophitic texture, with lath-shaped Pl (Figs. 52, 53, 54, 55).

**Table 1, cont. Principal rock types of the Noril'sk-type intrusions and their petrographic characteristics.**

<p>Picritic gabbrodolerite  <b>NP-29-681.2, -683.6, -684.4</b>  <b>KZ-1713-880</b>  <b>KZ-1799-1319.8, -1324.9, -1330.8</b>  <b>KZ-1879-1746, -1767.9, -1772.1</b></p>	$\left(\text{Ol}_1^{1,2}\right)_{40-60} \left[ \left(\text{Pl}_1^{1,2,3}\right)_{0-7} \left(\text{Pl}_2^{4,5}\right)_{15-30} \right]_{15-35} \left(\text{Au}^3\right)_{10-25}$ $\left(\text{Bi}\right)_{1-4} \left(\text{Mt}\right)_{0-2} \left(\text{Cr}\right)_{0-5} \left(\text{Sul}\right)_{1-12}$	<p>The following characteristics are common to picritic and olivine-rich picritic gabbrodolerite. The dominant feature is the content of 40-80 modal % olivine, all of the first generation on the basis of morphology and composition. Augite is oikocrystic. Chromite is usually present and decreases downward in the unit. Sulfides are always present and often abundant. Typically, stratified sulfide droplets as much as 2 cm across are present. First-generation plagioclase is almost always present. Plagioclase may form sparse glomerocrysts of <math>\text{Pl}_1^{2,3} + \text{Pl}_2^4</math> (&lt;4 modal %; 1-2 cm across). Near the lower transition to taxitic gabbrodiorite, these glomerocrysts of <math>\text{Pl}_1 + \text{Pl}_2</math> may reach 3 cm across and compose 5-15 modal % of the rock. The middle and lower part of the unit may contain 1 to 3 cm long, rounded phenocrysts of <math>\text{Pl}_1</math>. Picritic gabbrodolerite commonly contains fine-grained fragments 2-6.5 mm across consisting of <math>\left(\text{Ol}_2\right)_{30-80} \left(\text{Pl}_2\right)_{0-40} \left(\text{Au}^3\right)_{0-70}</math> that may compose several modal % of the rock.</p>
<p>Olivine-rich, picritic gabbrodolerite  <b>KZ-1713-883.8, -888.3, -896.9, -902.8</b>  <b>KZ-1799-1321.5, -1324, -1326.8</b>  <b>KZ-1879-1752.5, -1757, -1761, -1763.1</b></p>	$\left(\text{Ol}_1^{1,2}\right)_{60-80} \left[ \left(\text{Pl}_1^{1,2,3}\right)_{0-10} \left(\text{Pl}_2^4\right)_{5-15} \right]_{10-20} \left(\text{Au}^3\right)_{5-15}$ $\left(\text{Bi}\right)_{0-4} \left(\text{Tm}\right)_{0-1} \left(\text{Mt}\right)_{0-2} \left(\text{Cr}\right)_{0-4} \left(\text{Sul}\right)_{1-7, \text{rarely } 18}$	<p>Hypidiomorphic (Fig. 40), poikilitic (Figs. 48, 51), and partly sideronitic+++ textures. Pl has tabular and xenomorphic forms.</p>
<p>Taxitic gabbrodolerite  <b>NP-29-689.6, -691.6, -693.5</b>  <b>KZ-1713-913.3, -922.9</b>  <b>KZ-1799-1331.5, -1332, -1335, -1336.5, -1337.5, -1339</b>  <b>KZ-1879-1791.6</b></p>	$\left[ \left(\text{Ol}_1^{1,2}\right)_{0-15} \left(\text{Ol}_2^{3,4,5,6}\right)_{3-15} \right]_{7-18}$ $\left[ \left(\text{Pl}_1^{2,3}\right)_{0-12} \left(\text{Pl}_2^4\right)_{40-60} \right]_{45-72} \left(\text{Au}^{2,3,4,6}\right)_{7-40} \left(\text{Opx}^{4,6}\right)_{0-1}$ $\left(\text{Bi}\right)_{0-3} \left(\text{Tm}\right)_{0-3} \left(\text{Mt}\right)_{0-2} \left(\text{Ilm}\right)_{0-1} \text{Sul}_{0-25}$	<p>The rock is of quite irregular grain-size and mode, and may contain almost all generations and morphologic types of all minerals. A typical feature is the presence of fine-grained fragments 4-30 mm across (2-10 modal %) consisting of <math>\left(\text{Ol}_2^8\right)_{40-85} \left(\text{Pl}_2^{5,4}\right)_{10-60} \left(\text{Au}^3\right)_{0-15}</math> <math>\left(\text{Bi} + \text{Amf} + \text{Chl}\right)_{0-7} \left(\text{Sul}\right)_{0-3}</math>. Plagioclase phenocrysts and glomerocrysts containing much <math>\text{Pl}_1</math> may be 3-8 mm across and reach 10 modal %. Second-generation olivine is common and may form oikocrysts. Sulfides are unevenly distributed (to as much as 25 modal %), typically as xenomorphic aggregates.</p> <p>Intergranular texture, combined with poikilophitic and subophitic textures. Au may contain pegmatoidal intergrowths of <math>\text{Pl}_2</math>.</p>
<p>Contact gabbrodolerite  <b>NP-29-697.2</b>  <b>KZ-1799-1340, -1341.9</b>  <b>KZ-1879-1798.1</b></p>	$\left(\text{Ol}_2^{3,6,8}\right)_{10-15} \left(\text{Pl}_2^{5,4}\right)_{60} \left[ \left(\text{Au}^3\right)_{10-20} \left(\text{Opx}^3\right)_{0-10} \right]$ $\left(\text{glass, replaced by Chl}\right)_{0-15} \left[ \left(\text{Bi}\right)_{15-30} \left(\text{Bi}\right)_{0-2} \right]$ $\left(\text{Tm}\right)_{1-3} \left(\text{Sul}\right)_{0-5}$	<p>The most fine grained of all rock types. <math>\text{Ol}_1</math> is never seen. Sparse phenocrysts of <math>\text{Pl}_1^1</math> may be present (&lt;3 modal %; 0.7-4 mm across) replacements of glass are sometimes present. Augite is usually strongly zoned, and each crystal contains parts (blocks) of slightly different optical orientation, resulting in extinction in blocks.</p> <p>A combination of intersertal (hyalophitic; Fig. 58), poikilophitic, and subophitic textures.</p>

Abbreviations: Ap, apatite; Amf, amphibole; Au, augite; Bi, biotite; Bowl, bowlingite; Carb, carbonate; Chl, chlorite; Cr, chromite; Ilm, ilmenite; Mp, micropegmatite; Mt, titanomagnetite; Mus, muscovite; Ol, olivine; Opx, orthopyroxene; Pl, plagioclase; Q, quartz; Sec, minor secondary minerals; Sul, sulfide; Tm, oxide networks after titanomagnetite.

\*Listed examples are those for which there is excellent correspondence between petrographic and geochemical characteristics. Last 3 to 5 digits of sample numbers represent depth in borehole, in meters. Italics indicate that no chemical analysis is available.

\*\*See Table 2 for explanation of the morphological types and generations of Au, Ol, and Pl. The modal percentage of a mineral type is given by a parenthetical subscript, e.g.,  $\left(\text{Ol}_2^3\right)_{10}$  indicates 10 modal percent of  $\left(\text{Ol}_2^3\right)$ . Often, two or more such estimates are bracketed to give an overall estimate of the modal abundance of plagioclase or olivine.

+Information regarding mineral grain size and dimensions of glomerocrysts (in mm) is summarized in the following order:  $\left(\text{Ol}_1\right) \left(\text{Ol}_2\right) \left(\text{Pl}_1 + \text{Pl}_2\right) \left(\text{Au}\right)$ . A small "d," is used if grains are commonly equidimensional and a "-" if the mineral (or morphological type) is absent. Occasionally, by listing an extra pair of dimensions, an effort is made to indicate the presence of a variety of grain shapes.

++Textural characteristics according to the terminology of MacKenzie et al. (1982) with references to figures in Part 1 of this reference.

+++In sideronitic texture, silicate minerals, typically olivine, are "suspended" in sulfide.

The subscript "o-one" is used to indicate the presence of a few solitary grains, i.e., <1 modal%

Augite in all rocks may be twinned and orthopyroxene in all rocks contains fine clinopyroxene exsolution lamellae.

**Table 2. Classification scheme for the morphological types and generations of the main rock-forming minerals.**

Olivine	Plagioclase	Augite
Ol <sub>1</sub> <sup>1</sup> - euhedral grains with no inclusions (0.5-4.0 mm)	Pl <sub>1</sub> <sup>1</sup> - large, prismatic grains with no inclusions and few twins (length >2 mm; width/length >1/3)	Au <sup>1</sup> - large prismatic grains with no inclusions (0.3 x 1 to 2 x 6 mm)
Ol <sub>1</sub> <sup>2</sup> - resorbed grains (rounded and ellipsoidal) with no inclusions (0.5-3.0 mm)	Pl <sub>1</sub> <sup>2</sup> - tabular grains with no inclusions and few twins (width >0.8 mm)	Au <sup>2</sup> - subprismatic grains--sometimes xenomorphic, often twined. The rims may be penetrated by laths and microlites of Pl <sub>2</sub> (Pl forms 15-20% of some grains) (0.5-1.5 mm)
Ol <sub>2</sub> <sup>3</sup> - large clutch (paw-like) grains (1.0-7.0 mm)	Pl <sub>1</sub> <sup>3</sup> - xenomorphic grains with few twins and no inclusions, or containing crystals of Ol <sub>1</sub> (diameter >0.8 mm)	Au <sup>3</sup> - oikocrysts of nearly isometric shape, with abundant chadacrysts (mainly small laths of Pl <sub>2</sub> that form 30-50% of some grains) (0.3-10.0 mm)
Ol <sub>2</sub> <sup>4</sup> - oikocrysts containing chadacrysts of Pl <sub>1</sub> or Pl <sub>2</sub> (0.5-1.0 mm)	Pl <sub>2</sub> <sup>4</sup> - laths, usually with abundant twins (length 0.8-9.0 mm; width/length <1/3, when length >2.0 mm)	Au <sup>4</sup> - oikocrysts whose shapes largely reflect several angular interstices between Pl <sub>1</sub> or Pl <sub>2</sub> grains (0.3-2.0 mm)
Ol <sub>2</sub> <sup>5</sup> - small xenomorphic grains - "hedgehogs" - penetrated by microlites and laths of Pl <sub>2</sub> (0.3-0.5 mm)	Pl <sub>2</sub> <sup>5</sup> - small laths with abundant twins (length <0.8 mm, width <0.2 mm)	Au <sup>5</sup> - small xenomorphic grains - "hedgehogs" - penetrated by microlites and laths of Pl <sub>2</sub> (0.3-0.6 mm)
Ol <sub>2</sub> <sup>6</sup> - small rounded grains with no inclusions (0.1-0.4 mm)		Au <sup>6</sup> - xenomorphic grains whose shapes correspond to those of interstices between Pl <sub>1</sub> or Pl <sub>2</sub> grains (0.1-3.0 mm)
Ol <sub>2</sub> <sup>7</sup> - small euhedral grains (phenocrysts) in quenched dolerites (0.1-0.5 mm)		
Ol <sub>2</sub> <sup>8</sup> - very small rounded grains usually found in the fine-grained fragments that are characteristic of taxitic gabbrodolerite (granular texture) (<0.1 mm)		

Notes: (1) The symbol Ol<sub>2</sub><sup>3</sup> indicates that the rock contains second-generation olivine of morphological type 3. In typical usage, the modal percentage of the mineral type is given by a parenthetical subscript, e.g., (Ol<sub>2</sub><sup>3</sup>)<sub>10</sub> indicates 10 modal percent of Ol<sub>2</sub><sup>3</sup>.

(2) Olivine and plagioclase grains of the first generation are considered to be intratelluric, i.e., to have crystallized in, and been transported from, a deeper chamber that was the source of magmas that fed the intrusions.

(3) Augite is entirely second generation, i.e., the product of crystallization *in situ*.

(4) Second-generation plagioclase is commonly twinned, whereas first-generation plagioclase is not.

**Table 3. Comparative chemical data for the most significant rock types of the ore-bearing intrusion sequence.**

	Leucogabbro	Quartz diorite	Magnetite gabbro		Prismatic gabbro		Olivine-bearing gabbrodolerite			Olivine gabbrodolerite			
	4 samples*	KZ-1799(3)**	KZ-1799(6)	NP-29(5)	KZ-1713(1)	KZ-1799(3)	KZ-1713(4)	KZ-1799(5)	NP-29(2)	KZ-1713(6)	KZ-1799(1)	KZ-1879(1)	NP-29(2)
SiO <sub>2</sub> , wt %	47.8-51.7	55.9-60.5	42.6-48.2	48.5-51.0	49.1	50.5-51.8	48.5-49.1	49.9-50.8	50.1-50.2	47.2-48.2	48.6	47.5	48.6
Al <sub>2</sub> O <sub>3</sub>	23.0-24.4	12.2-12.9	11.8-12.8	11.6-13.0	14.1	14.3-15.5	16.6-17.8	14.9-16.8	15.8-16.4	18.1-19.4	17.1	17.2	17.3-17.5
FeO <sup>T</sup>	5.60-6.91	12.3-13.9	18.6-22.6	16.3-18.1	11.4	10.6-11.8	8.27-8.74	9.39-10.7	10.1-10.9	7.85-9.27	9.91	9.71	9.46-9.74
MgO	3.92-6.42	1.23-1.70	4.39-7.21	4.48-5.78	7.33	6.17-6.62	7.23-8.01	6.20-8.37	6.15-7.00	9.53-11.6	9.25	11.2	8.65-8.91
CaO	8.13-13.3	3.97-6.54	9.36-11.1	8.78-9.85	12.0	10.8-12.2	13.1-13.8	11.7-13.1	11.4-11.8	11.1-11.8	11.6	11.2	11.7-12.3
Na <sub>2</sub> O	1.96-2.39	4.40-6.41	1.92-2.96	2.95-4.33	2.42	2.53-2.58	1.61-2.12	2.04-2.43	2.97-3.08	1.62-1.97	1.87	1.85	1.95-2.04
K <sub>2</sub> O	0.38-2.91	0.27-1.98	0.60-1.09	0.03-0.59	0.86	0.68-0.88	0.40-0.63	0.53-0.80	0.58-0.59	0.35-0.46	0.51	0.35	0.45-0.49
TiO <sub>2</sub>	0.35-0.74	1.37-2.18	2.22-3.14	2.40-2.54	0.99	1.15-1.34	0.72-0.77	0.98-1.16	1.10-1.20	0.61-0.75	0.91	0.71	0.85-0.88
P <sub>2</sub> O <sub>5</sub>	0.06-0.20	0.47-0.92	0.10-0.26	0.22-0.32	0.10	0.13-0.19	0.09-0.10	0.11-0.12	0.12	0.08-0.10	0.11	0.11	0.21-0.28
MnO	0.10-0.17	0.15-0.26	0.22-0.43	0.25-0.30	0.20	0.23-0.28	0.14-0.15	0.19-0.23	0.18	0.13-0.20	0.19	0.18	0.16
S	0.23-0.33	0.46-0.94	0.16-0.79	0.01-0.27	0.13	0.09-0.21	0.03-0.10	0.08-0.20	0.02-0.09	0.04-0.13	0.33	0.04	0.05-0.12
Pd, ppb	270-1200	<1	<2	<0.5	2.7	<0.5-0.7	<2-4.2	5.1-85	1.1-3.4	3-72	150	17	7.2-7.8
Cr, ppm	160-290	2.1-2.7	4.3-116	2.1-4.2	18	12-35	440-740	62-255	75-215	300-820	435	300	255-275
Cu	450-1150	25-124	108-870	10-186	192	134-245	66-78	95-174	106-132	65-190	650	76	110-118
Ta	1.23-3.69	0.930-1.83	0.171-0.386	0.424-0.534	0.187	0.226-0.377	0.133-0.185	0.200-0.263	0.215-0.238	0.118-0.166	0.18	0.161	0.173-0.177
Zr	48-104	290-370	66-120	142-174	78	81-122	52-69	71-87	91-93	45-68	64	61	62-68
La	3.10-13.2	27.8-38.5	5.77-15.0	12.2-15.9	7.03	7.76-11.6	4.27-5.02	6.00-8.42	6.82-6.98	3.79-4.82	5.3	5.1	5.02-5.24
Sm	1.44-3.58	10.3-17.9	2.19-5.66	5.27-5.87	2.62	3.05-3.66	1.79-2.16	2.71-3.05	2.72-2.99	1.54-1.96	2.33	1.94	4.07-5.27
Yb	0.909-2.08	7.01-10.7	1.76-3.70	3.93-4.43	2.04	2.28-2.69	1.51-2.00	1.96-2.31	2.10-2.35	1.23-1.51	1.80	1.46	1.68-1.75

	Picritic-like gabbrodolerite			Picritic gabbrodolerite				Taxitic gabbrodolerite				Contact gabbrodolerite		
	KZ-1713(1)	KZ-1879(3)	NP-29(1)	KZ-1713(1)	KZ-1799(3)	KZ-1879(3)	NP-29(3)	KZ-1713(1)	KZ-1799(5)	KZ-1879(1)	NP-29(1)	KZ-1799(2)	KZ-1879(1)	90MC7***
SiO <sub>2</sub> , wt %	46.2	45.5-46.7	46.6	43.9	44.5-49.1	44.5-44.6	44.6-46.5	47.6	45.9-51.0	48.3	47.5	49.6-51.0	50.1	48.9
Al <sub>2</sub> O <sub>3</sub>	14.3	14.1-16.1	12.3	8.98	8.60-10.6	7.87-10.3	9.33-12.2	17.4	15.9-18.3	15.2	19.6	15.7-16.2	15.6	16.6
FeO <sup>T</sup>	11.4	9.90-11.4	12.8	13.9	13.3-13.6	13.8-14.6	12.3-14.0	11.1	7.75-11.5	14.3	8.47	10.5-12.3	12.7	11.2
MgO	15.9	14.4-17.3	16.1	26.0	21.9-25.5	21.5-26.2	18.4-23.1	10.9	9.04-15.4	8.67	10.3	7.39-7.54	6.93	8.02
CaO	9.32	9.47-10.5	9.15	5.42	5.87-6.94	5.42-7.54	6.91-8.31	9.93	9.11-11.3	8.53	11.3	10.4-10.5	8.30	11.2
Na <sub>2</sub> O	1.57	1.34-1.51	1.41	0.78	0.91-1.09	1.01-1.14	0.86-1.29	1.30	1.16-2.27	2.89	1.63	1.97-2.00	3.34	2.18
K <sub>2</sub> O	0.34	0.21-0.44	0.35	0.25	0.22-0.28	0.19-0.23	0.20-0.35	0.67	0.29-0.91	0.72	0.33	0.89-0.92	1.09	0.50
TiO <sub>2</sub>	0.72	0.46-0.69	0.90	0.53	0.55-0.70	0.56-0.63	0.52-0.84	0.77	0.41-0.81	0.97	0.68	1.08-1.24	1.40	1.08
P <sub>2</sub> O <sub>5</sub>	0.08	0.05-0.08	0.12	0.09	0.09	0.07-0.08	0.08-0.11	0.10	0.05-0.11	0.11	0.08	0.14-0.15	0.16	0.12
MnO	0.19	0.16-0.21	0.23	0.23	0.22	0.22-0.23	0.21-0.23	0.24	0.17-0.28	0.40	0.15	0.22-0.23	0.31	0.21
S	0.12	0.04-0.06	0.05	1.27	1.52-2.12	0.05-0.95	0.05-1.68	4.66	1.48-6.52	4.49	3.09	0.32-1.14	0.04	0.27
Pd, ppb	46	8.9-11	43	2600	1100-2300	110-1100	400-5000	5200	1200-8500	3300	47000	66-810	60	430
Cr, ppm	2750	405-485	2700	4100	550-2300	230-4100	2550-3900	170	255-590	220	110	170-172	130	140
Cu	122	50-60	134	3700	3500-5100	94-3400	164-5300	16900	3500-21000	12800	9100	640-2700	355	1200
Ta	0.123	0.090-0.138	0.159	0.084	0.108-0.124	0.093-0.099	0.118-0.158	0.124	0.053-0.174	0.099	0.102	0.244-0.296	0.272	0.231
Zr	46	34-54	65	33	41-56	32-55	41-52	40	27-60	63	39	75-98	106	82
La	4.03	3.00-4.55	4.89	3.12	3.00-3.25	2.85-3.00	3.39-4.55	3.65	2.02-6.18	3.3	2.93	6.79-10.1	7.77	6.75
Sm	1.56	1.26-1.83	2.99	1.10	1.27-1.42	1.22-1.32	2.72-5.87	1.60	0.783-2.18	1.77	2.00	2.75-3.71	3.34	2.76
Yb	1.28	1.01-1.42	1.57	0.95	1.09-1.13	0.98-1.12	1.19-1.55	1.21	0.635-1.48	1.43	1.06	2.05-2.56	2.64	2.04

\*KZ-1879-1689.5; KZ-1879-1704; KZ-1818-1757.1, and KZ-1853K-1857.3. Throughout this report, the two initial letters and first set of numbers designate the borehole and the last digits represent the depth (in meters) in the borehole.

\*\*Borehole identification and number of samples included in range. Samples can be identified from Table 1.

\*\*\*From Medvezky Creek open-pit in the Noril'sk I intrusion.

All major-element data in this table have been averaged from the data in Appendixes 1 and 2, and in CZAMANSKE et al. (1994), which were recalculated to 100% anhydrous oxides by disregarding H<sub>2</sub>O<sup>+</sup> and H<sub>2</sub>O<sup>-</sup> and correcting CaO and FeO<sup>T</sup> for measured CO<sub>2</sub> and S concentrations. Correction for S based on analysis of the sulfide component of sample 90MC10 (CZAMANSKE et al., 1992). Total iron is given as FeO<sup>T</sup>.

**Table 4. Comparison of average Cu, Pd, Pt, and S concentrations for Upper Morongovsky and Mokulaevsky basalts, and rocks of the ore-bearing intrusions.**

	Cu, ppm	Pd, ppb	Pt, ppb	10 <sup>-3</sup> (Cu/Pd)	Pd/Pt	S, wt %
Upper Morongovsky - Mokulaevsky basalt (8)*	126 (64-151)**	10.9 (9.6-13.4)	11.6 (9.9-15.4)	11.6 (6.4-14.6)	0.90 (0.85-1.15)	~0.01
Noril'sk I intrusion olivine-bearing through olivine gabbrodolerite (7)	109 (80-132)	6.3 (3.4-7.8)	7.4 (3.7-9.1)	19.2 (12.2-38.8)	0.86 (0.75-1.01)	0.05 (0.03-0.12)
picritic gabbrodolerite (5)	2920 (900-5300)	2940 (1700-5000)	1100 (810-1500)	0.99 (0.53-1.18)	2.67 (1.93-3.33)	0.91 (0.44-1.68)
NE branch of Talnakh intrusion olivine-bearing through olivine gabbrodolerite (10)	95 (73-174)	4.6 (2.0-9.2)	9 (1-33)	22.6 (14.6-37.0)	0.70 (0.28-2.00)	0.07 (0.03-0.10)
picritic gabbrodolerite (11)	6350 (2600-13800)	2250 (970-3500)	695 (230-1100)	2.8 (1.42-4.08)	3.30 (2.78-4.22)	2.54 (0.98-5.60)
contact gabbrodolerite (2)	2700,640	810,66	280,28	3.33,9.70	2.89,2.36	1.14,0.32
Kharaelakh intrusion leucogabbro (2)	450,700	270,840	130,370	1.7,0.8	2.08,2.27	0.29,0.23
leucogabbro (1)***	1150	1200	570	0.96	2.11	0.25
olivine-bearing through olivine gabbrodolerite (8)	63 (50-76)	10.6 (7.7-17)	11.2 (8.2-21)	6.2 (4.47-8.57)	0.99 (0.75-1.56)	0.05 (0.03-0.06)
picritic gabbrodolerite (6)	4600 (3400-5600)	1780 (1100-2900)	470 (280-810)	2.69 (1.93-3.20)	3.89 (3.45-5.00)	1.57 (0.95-2.90)

\*Number of samples in average. \*\*Range of concentrations. \*\*\*Sample KZ-1818-1757.1. Averages and ranges based on data in this report, CZAMANSKE et al. (1994), and WOODEN et al. (1993).

**Table 5. Electron-microprobe analyses of clinopyroxene in magnetite gabbro and prismatic gabbro of the Talnakh intrusion, borehole KZ-1799.**

	Magnetite gabbro								Prismatic gabbro				
	1214.8* (2,7)**	1220 (2,8) (1,4)		1223.5 (2,6) (1,3)		1224.9 (2,8) (1,3)		1229 (3,9)	1231.5 (3,12)	1233.6 (2,5) (2,7)		1240 (3,9)	1249.8 (3,10)
SiO <sub>2</sub> , wt%	51.29	51.12	52.38	50.70	52.73	50.79	52.62	50.88	51.26	51.85	51.50	51.18	50.55
Al <sub>2</sub> O <sub>3</sub>	0.22	2.05	0.77	2.06	0.62	1.68	0.67	2.59	1.96	1.07	2.35	2.40	2.24
TiO <sub>2</sub>	0.05	0.68	0.12	0.62	0.09	0.51	0.11	0.68	0.60	0.49	0.63	0.58	0.49
MgO	9.85	14.47	13.90	14.13	14.35	13.46	14.18	14.57	14.13	13.51	15.27	15.16	15.57
FeO	16.31	11.29	8.81	11.85	8.53	13.06	8.55	10.29	10.67	12.93	9.68	8.90	8.01
CaO	20.28	18.83	22.19	18.67	22.38	18.46	22.55	19.66	19.87	18.96	19.61	19.86	19.63
Na <sub>2</sub> O	0.29	0.28	0.17	0.27	0.12	0.28	0.10	0.31	0.32	0.32	0.28	0.27	0.26
MnO	0.50	0.34	0.34	0.35	0.32	0.40	0.28	0.25	0.31	0.39	0.25	0.26	0.20
Cr <sub>2</sub> O <sub>3</sub>	0.00	0.00	0.01	0.01	0.01	0.01	0.00	0.00	0.00	0.00	0.02	0.02	0.04
Total	98.80	99.07	98.70	98.67	99.17	98.66	99.10	99.25	99.14	99.53	99.61	98.65	97.01
Cations per 6 oxygens													
Si	2.001	1.934	1.981	1.931	1.982	1.945	1.981	1.917	1.938	1.966	1.925	1.928	1.929
Al	0.010	0.091	0.034	0.092	0.027	0.076	0.03	0.115	0.087	0.048	0.104	0.107	0.101
Ti	0.001	0.019	0.003	0.018	0.003	0.015	0.003	0.019	0.017	0.014	0.018	0.016	0.014
Mg	0.573	0.816	0.784	0.802	0.804	0.768	0.796	0.818	0.796	0.764	0.851	0.851	0.886
Fe	0.532	0.357	0.279	0.377	0.268	0.418	0.269	0.324	0.337	0.410	0.303	0.280	0.256
Ca	0.848	0.763	0.899	0.762	0.901	0.757	0.91	0.794	0.805	0.770	0.786	0.801	0.803
Na	0.022	0.021	0.012	0.020	0.009	0.021	0.007	0.023	0.023	0.024	0.020	0.020	0.019
Mn	0.017	0.011	0.011	0.011	0.010	0.013	0.009	0.008	0.010	0.013	0.008	0.008	0.006
Cr	0.000	0.000	0.000	0.000	0.000	0.000	0.000	0.000	0.000	0.000	0.001	0.001	0.001
Mg	29.1	41.4	39.8	40.7	40.8	39.0	40.4	41.5	40.4	38.8	43.2	43.2	45.0
Fe+Mn	27.9	18.7	14.7	19.7	14.1	21.9	14.1	16.9	17.6	21.5	15.8	14.6	13.3
Ca	43.0	38.7	45.6	38.7	45.7	38.4	46.2	40.3	40.9	39.1	39.9	40.7	40.8

\*\*Values are last digits of sample numbers and depth in meters in borehole KZ-1799.

\*\* (2,7) indicates that the analysis represents an average for 7 spots on 2 grains. NiO contents in all analyzed pyroxenes are <0.03 wt%.

**Table 6. Electron-microprobe analyses of clinopyroxene and orthopyroxene in gabbrodolerites of the Noril'sk I intrusion, borehole NP-29.**

	Olivine-bearing to olivine				Olivine						Picritic-like and picritic		Taxitic	
	637.9*		655.7		658.7		667		669.7		678.2-684.4**	678.2+684.4	691.6	
	(4,29)***	Edge (3,3)	(2,10)	(1,8)	(2,13)	(1,8)	(1,4)	(2,12)	(1,11)	(2,14)	(6,49)	opx (2,19)	(1,8)	opx (1,9)
SiO <sub>2</sub> , wt%	51.33	50.67	51.42	51.39	51.22	50.75	52.18	52.02	51.09	50.77	51.74	54.08	51.07	52.77
Al <sub>2</sub> O <sub>3</sub>	2.66	2.10	2.92	2.11	2.93	2.22	2.34	2.13	2.12	1.95	2.80	1.19	2.55	0.90
TiO <sub>2</sub>	0.41	0.80	0.42	0.59	0.44	0.84	0.39	0.63	0.70	0.90	0.49	0.60	0.63	0.43
MgO	16.52	15.17	16.61	16.15	16.41	15.66	16.69	16.19	16.00	15.68	16.70	27.19	16.28	23.71
FeO	6.44	10.77	5.97	8.21	6.12	9.91	6.45	8.22	9.05	10.88	5.94	14.44	7.21	19.32
CaO	20.48	18.97	20.56	20.06	20.82	18.87	20.58	19.82	19.27	18.24	20.48	1.98	20.24	2.08
Na <sub>2</sub> O	0.23	0.27	0.24	0.25	0.26	0.28	0.22	0.24	0.24	0.27	0.25	0.04	0.22	0.06
MnO	0.18	0.31	0.17	0.22	0.17	0.26	0.18	0.23	0.24	0.30	0.17	0.35	0.19	0.46
Cr <sub>2</sub> O <sub>3</sub>	0.61	0.04	0.93	0.07	0.91	0.03	0.55	0.06	0.03	0.02	0.92	0.21	0.31	0.00
Total	98.86	99.10	99.21	99.06	99.27	98.81	99.58	99.51	98.74	98.98	99.50	100.07	98.68	99.72
Cations per 6 oxygens														
Si	1.913	1.915	1.906	1.923	1.901	1.914	1.928	1.933	1.922	1.917	1.911	1.949	1.911	1.955
Al	0.117	0.094	0.128	0.093	0.128	0.099	0.102	0.093	0.094	0.087	0.122	0.051	0.112	0.039
Ti	0.011	0.023	0.012	0.017	0.012	0.024	0.011	0.018	0.020	0.026	0.014	0.016	0.018	0.012
Mg	0.918	0.855	0.918	0.901	0.908	0.881	0.919	0.897	0.897	0.883	0.920	1.461	0.908	1.309
Fe	0.201	0.340	0.185	0.257	0.190	0.313	0.199	0.255	0.285	0.344	0.183	0.435	0.226	0.599
Ca	0.818	0.768	0.816	0.804	0.828	0.763	0.815	0.789	0.777	0.738	0.810	0.076	0.812	0.083
Na	0.017	0.020	0.017	0.018	0.019	0.020	0.016	0.017	0.018	0.020	0.018	0.003	0.016	0.004
Mn	0.006	0.010	0.005	0.007	0.005	0.008	0.006	0.007	0.008	0.010	0.005	0.011	0.006	0.014
Cr	0.018	0.001	0.027	0.002	0.027	0.001	0.016	0.002	0.001	0.001	0.027	0.006	0.009	0.000
Mg	47.2	43.3	47.7	45.8	47.0	44.8	47.4	46.0	45.6	44.7	48.0	73.7	46.5	65.3
Fe+Mn	10.7	17.7	9.9	13.4	10.1	16.3	10.6	13.4	14.9	17.9	9.8	22.5	11.9	30.6
Ca	42.1	38.9	42.4	40.8	42.9	38.8	42.0	40.5	39.5	37.4	42.2	3.8	41.6	4.1

\*Values are last digits of sample numbers and depth in meters in borehole NP-29.

\*\*Includes samples NP-29-678.2, -681.2, -683.6, and -684.4.

\*\*\* (4,29) indicates that the analysis represents an average for 29 spots on 4 grains.

**Table 7. Ranges in forsterite and NiO contents of olivine within individual rock types.**

Gabbrodolerite type	Borehole			
	KZ-1713	KZ-1799	KZ-1879	NP-29
Olivine-bearing	61.2-66.9(3)* 0.05-0.10	55.8-63.5(4) 0.03-0.08	--	--
Olivine-bearing to olivine	--	--	--	59.9-67.4(4) 0.05-0.11
Olivine	66.5-77.7(6) 0.10-0.18	62.6-70.7(1) 0.13-0.15	70.6-75.9(1) 0.11-0.15	61.5-75.2(2) 0.08-0.15
Picritic-like	73.2-75.7(1) 0.14-0.17	--	71.0-77.6(3) 0.12-0.16	--
Picritic to olivine- rich picritic	75.0-81.4(5) 0.17-0.28	73.7-81.5(5) 0.15-0.33	71.2-80.7(7) 0.16-0.31	74.4-79.1(3) 0.17-0.30
Taxitic	60.8-68.9(1) 0.17-0.21	62.3-77.0(4) 0.08-0.23	--	67.5-73.2(1) 0.20-0.28

\*Number in parenthesis indicates number of samples included in range.  
 Ranges of NiO contents listed beneath ranges of forsterite contents for the  
 same grains.

An average of ten olivine grains were analyzed in each sample.



**Table 8. Electron-microprobe analyses of biotite in gabbrodolerites of the Talnakh intrusion, borehole KZ-1713.**

	Olivine-bearing		Olivine		Olivine-rich picritic					Picritic		Taxitic		
	840.5* (4,13)**	844.5 (4,12)	860 (4,10)	876 (3,11)	880 (4,14)	883.8 (3,11)	888.3 (1,3)	896.9 (1,2) (1,2)		910.5 (1,2) (2,5)		922.9 (1,3) (1,4) (1,3)		
SiO <sub>2</sub> , wt%	39.12	39.15	42.07	38.30	38.38	40.68	41.34	41.96	38.97	39.89	38.80	39.98	38.14	37.19
Al <sub>2</sub> O <sub>3</sub>	12.17	11.94	11.64	13.52	13.53	12.22	13.43	12.12	12.83	13.01	13.28	13.34	13.12	12.26
TiO <sub>2</sub>	2.71	2.89	1.32	5.81	7.85	4.18	4.22	3.26	6.68	5.11	6.95	1.30	5.49	0.31
MgO	13.88	13.81	21.65	16.82	17.52	21.72	22.60	23.26	18.42	19.69	17.20	18.08	14.39	8.19
FeO	19.69	19.10	7.94	11.85	8.23	5.97	5.35	7.06	8.73	8.76	10.47	14.42	15.93	28.90
Na <sub>2</sub> O	0.01	0.19	0.01	0.05	0.77	0.24	0.18	0.02	0.54	0.01	0.02	0.01	0.02	0.02
MnO	0.17	0.06	0.28	0.36	0.04	0.91	0.83	0.49	0.96	0.74	0.88	0.35	0.35	0.12
Cr <sub>2</sub> O <sub>3</sub>	0.06	0.01	0.02	0.05	0.78	0.03	0.01	0.04	0.04	0.05	0.04	0.07	0.09	0.09
K <sub>2</sub> O	9.22	9.13	9.60	9.52	9.13	8.57	8.75	8.80	8.71	8.87	8.85	9.14	9.49	8.98
Cl	1.21	1.06	0.29	0.26	0.13	0.10	0.11	0.14	0.11	0.13	0.13	0.73	0.45	4.32
F	0.49	0.43	1.77	0.51	0.42	0.42	1.28	0.61	0.80	0.58	0.57	0.40	0.61	0.04
Total	98.26	97.37	95.78	96.77	96.58	94.84	97.54	97.46	96.42	96.57	96.92	97.47	97.72	99.44

\*Values are last digits of sample numbers and depth in meters in borehole KZ-1713.

\*\* (4,13) indicates that the analysis represents an average for 13 spots on 4 grains.

**Table 9. Electron-microprobe analyses of biotite in leucogabbro, magnetite gabbro, and picritic gabbrodolerite.**

	Leucogabbro		Magnetite gabbro				Picritic gabbrodolerite	
	KZ-1818 1757.1 (4,16)**	KZ-1853K 1857.5 (5,15)	KZ-1799 1214.8 (4,12)	KZ-1799 1229 (3,10) (1,3)		NP-29 603 (2,8) (2,6)		90MC22* (2,5)
SiO <sub>2</sub> , wt%	39.38	34.54	36.73	39.32	39.47	39.74	38.75	39.94
Al <sub>2</sub> O <sub>3</sub>	12.46	15.25	11.08	12.01	11.28	12.51	13.38	14.93
TiO <sub>2</sub>	1.68	3.46	0.54	3.68	2.05	4.32	4.96	1.61
MgO	16.34	5.36	7.80	14.74	13.34	18.61	16.88	21.04
FeO	14.60	28.54	30.13	18.03	20.95	11.43	13.59	8.69
Na <sub>2</sub> O	0.31	0.28	0.14	0.22	0.13	0.57	0.52	0.29
MnO	0.09	0.18	0.16	0.07	0.05	0.06	0.07	0.03
Cr <sub>2</sub> O <sub>3</sub>	0.01	0.08	0.00	0.01	0.01	0.01	0.00	0.31
K <sub>2</sub> O	9.29	8.97	8.35	9.53	9.20	9.42	9.36	9.31
Cl	0.33	1.70	2.59	0.81	1.73	0.18	0.38	0.40
F	0.63	0.28	0.12	0.46	0.31	1.48	1.07	0.41
Total	94.78	98.13	97.02	98.51	97.99	97.66	98.42	96.68

\*Booklets as thick as 2 mm, associated with sulfide aggregates.

\*\* (4,16) indicates that the analysis represents an average for 16 spots on 4 grains.

**Table 10. Representative electron-microprobe analyses for chromian spinel in olivine gabbrodolerite and picritic gabbrodolerite.**

	TiO <sub>2</sub>	Al <sub>2</sub> O <sub>3</sub>	Cr <sub>2</sub> O <sub>3</sub>	Fe <sub>2</sub> O <sub>3</sub> *	FeO*	MgO	V <sub>2</sub> O <sub>3</sub>	MnO	NiO	Total	Cr#**	Mg#**
Olivine gabbrodolerite												
KZ-1713-876 (2)+Int <sup>++</sup>	4.31	4.00	5.83	51.8	33.3	1.98	1.10	0.32	0.06	102.7	49.0	9.58
KZ-1713-876 (2) Cpx	2.44	12.7	34.7	18.6	25.5	6.96	0.44	0.37	0.04	101.8	64.8	32.7
KZ-1713-876 (2) Ol	5.16	4.80	10.2	43.7	34.7	1.46	1.11	0.36	0.07	101.6	58.5	6.99
Picritic gabbrodolerite												
KZ-1713-880 (1) Pl	1.60	17.0	36.2	14.8	22.7	8.78	0.34	0.39	0.06	101.9	58.8	40.8
KZ-1713-880 (1) Opx	7.63	5.85	26.0	25.7	29.9	6.56	0.78	0.42	0.11	103.0	74.9	28.1
KZ-1713-880 (2) Ol	3.95	6.75	32.2	23.5	29.0	4.73	0.60	0.47	0.10	101.3	76.4	22.5
NP-29-678.2 (2) Int	11.7	3.95	15.2	28.4	38.0	3.08	0.75	0.41	0.17	101.7	72.2	12.6
NP-29-678.2 (2) Pl	1.01	20.8	35.3	13.1	20.8	10.1	0.32	0.36	0.08	101.9	53.4	46.2
NP-29-678.2 (2) Ol	1.74	10.2	35.0	20.7	27.8	4.68	0.70	0.42	0.05	101.3	69.9	23.1

\*Fe<sub>2</sub>O<sub>3</sub> and FeO calculated by stoichiometry from FeO<sup>T</sup>.

\*\*Cr# is 100[Cr/(Cr+Al)]; Mg# is 100[Mg/(Mg+Fe<sup>2+</sup>)].

<sup>+</sup>Numbers of grains represented by analyses. In most cases, values reported are the average for two comparable grains.

<sup>++</sup>Host for Cr-spinel grains: Int, interstitial; Cpx, clinopyroxene; Ol, olivine; Opx, orthopyroxene; Pl, plagioclase.